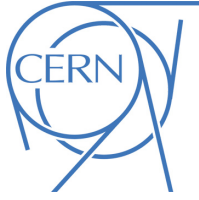


EUROPEAN ORGANISATION FOR NUCLEAR RESEARCH (CERN)



Submitted to: JHEP

CERN-EP-2018-171
14th December 2024

Search for new phenomena in events with same-charge leptons and b -jets in $p p$ collisions at $\sqrt{s} = 13$ TeV with the ATLAS detector

The ATLAS Collaboration

A search for new phenomena in events with two same-charge leptons or three leptons and jets identified as originating from b -quarks in a data sample of 36.1 fb^{-1} of $p p$ collisions at $\sqrt{s} = 13$ TeV recorded by the ATLAS detector at the Large Hadron Collider is reported. No significant excess is found and limits are set on vector-like quark, four-top-quark, and same-sign top-quark pair production. The observed (expected) 95% CL mass limits for a vector-like T - and B -quark singlet are $m_T > 0.98$ (0.99) TeV and $m_B > 1.00$ (1.01) TeV respectively. Limits on the production of the vector-like $T_{5/3}$ -quark are also derived considering both pair and single production; in the former case the lower limit on the mass of the $T_{5/3}$ -quark is (expected to be) 1.19 (1.21) TeV. The Standard Model four-top-quark production cross-section upper limit is (expected to be) 69 (29) fb. Constraints are also set on exotic four-top-quark production models. Finally, limits are set on same-sign top-quark pair production. The upper limit on $uu \rightarrow tt$ production is (expected to be) 89 (59) fb for a mediator mass of 1 TeV, and a dark-matter interpretation is also derived, excluding a mediator of 3 TeV with a dark-sector coupling of 1.0 and a coupling to ordinary matter above 0.31.

1 Introduction

One of the primary goals of the ATLAS experiment at the CERN Large Hadron Collider (LHC) is to search for physics beyond the Standard Model (BSM). The existence of dark matter, the matter–antimatter asymmetry of the universe, and the high degree of fine tuning required to stabilise the Higgs boson mass at 125 GeV are among the motivations for BSM physics. In this analysis, events with two leptons of the same electric charge or three leptons and at least one jet identified as originating from a b -hadron are considered. This is a promising final state to search for new phenomena, since the backgrounds from known processes are small. In addition to the lepton requirements, kinematic criteria are imposed to select events containing objects with large transverse momenta to further suppress the background. After applying these criteria, the largest background sources are $t\bar{t}W$, $t\bar{t}Z$, $t\bar{t}H$, and diboson production. There is also substantial background from events that appear to have the targeted final state only because one or more objects is misidentified. Three potential BSM sources of events in this final state are considered: production of vector-like quarks (VLQ), anomalous four-top-quark production ($t\bar{t}t\bar{t}$), and same-sign top-quark pair production (tt). Four-top-quark production in the context of the Standard Model (SM) is also studied, since this process has not yet been observed. Throughout this paper, ‘lepton’ is taken to mean electron or muon and is denoted by ℓ in formulae and tables, and a particular set of electrons and muons in the final state is referred to as a ‘lepton flavour combination’.

This final state represents one of the most sensitive channels for VLQ searches with a top quark involved in the decay, especially for masses below 1 TeV, and is also one of the most sensitive channels for four-top-quark production. An earlier ATLAS analysis using this signature at $\sqrt{s} = 8$ TeV [1] placed limits on the models considered in this paper, including $m_B > 0.62$ TeV and $m_T > 0.59$ TeV in the context of the singlet model of Ref. [2], where B and T indicate the VLQ with the same charges as the SM b - and t -quarks, respectively. That analysis also placed an upper limit of 70 fb on the cross-section of four-top-quark production with SM kinematics. Limits on same-sign top-quark pair production were also set; in the context of a flavour-changing neutral current (FCNC) model with a mediator similar to a Higgs boson of mass 125 GeV the cross-section for $uu \rightarrow tt$ was found to be < 35 fb. In addition, there have been prior searches for BSM effects in similar final states at $\sqrt{s} = 13$ TeV: Ref. [3] reports an ATLAS search in the context of supersymmetric (SUSY) models, and Ref. [4] reports a search by the CMS Collaboration where SUSY models and other BSM models are considered. The CMS Collaboration performed searches for pair production of the vector-like $T_{5/3}$ quark, which has charge 5/3, using events with either a single lepton or a same-charge lepton pair [5], resulting in limits of $m_{T_{5/3}} > 1.02$ TeV (0.99 TeV) for right-handed (left-handed) couplings. The CMS Collaboration reported on a search for SM four-top-quark production in Ref. [6], resulting in a measured cross-section of $16.9^{+13.8}_{-11.4}$ fb and a limit on the Yukawa coupling between the top quark and the Higgs boson of less than 2.1 times its expected SM value.

2 Signals considered

2.1 Vector-like T , B , and $T_{5/3}$ quarks

Vector-like quarks are fractionally charged, coloured fermions whose right- and left-handed components transform identically under weak isospin. Their existence is predicted in many BSM models that address the Higgs boson mass fine-tuning problem [7–16]. VLQ may come in several varieties, including the

aforementioned B -, T -, and $T_{5/3}$ -quarks and the $B_{-4/3}$ -quark that has charge $-4/3$.¹ They may appear as singlets, doublets, or triplets under $SU(2)$. In many models, the VLQ couple predominantly to third-generation SM quarks in order to address the naturalness problem, mostly driven by the couplings between the top quark and the Higgs boson [2]. Therefore, in this paper it is assumed that couplings to first- and second-generation SM quarks are negligible. Several production and decay scenarios could lead to an enhanced rate of multilepton events [2, 17, 18]. The B - and T -quarks could decay via both the charged and neutral current channels: $B \rightarrow Wt, Hb, Zb$, and $T \rightarrow Wb, Ht, Zt$, with model-dependent branching ratios. The most likely scenarios resulting in same-charge lepton pair or trilepton production are

- $B\bar{B} \rightarrow W^-tW^+\bar{t} \rightarrow W^-W^+bW^+W^-\bar{b}$
- $B\bar{B} \rightarrow W^-tZ\bar{b} \rightarrow W^-W^+bZ\bar{b}$
- $T\bar{T} \rightarrow ZtZ\bar{t} \rightarrow ZW^+bZW^-\bar{b}$
- $T\bar{T} \rightarrow ZtH\bar{t} \rightarrow ZW^+bHW^-\bar{b}$

where two or more of the vector bosons decay leptonically. Results are given for the $SU(2)$ singlet models of Ref. [2], as well as in a model-independent framework where all branching ratios are considered. The only decay mode of the $T_{5/3}$ quark is into $W^+t \rightarrow W^+W^+b$. If both W bosons decay leptonically, then a same-charge lepton pair is produced from a single $T_{5/3}$ decay. Therefore, results for the $T_{5/3}$ are presented for both pair and single production. The single production results depend on the assumed strength of the $T_{5/3}tW$ coupling. Figure 1 shows typical Feynman diagrams leading to the signature considered in this paper.

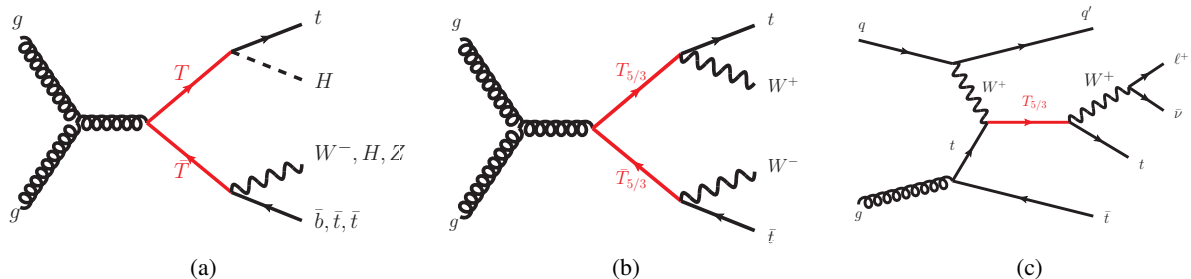


Figure 1: Three examples of VLQ production with (a) pair-produced T , (b) pair-produced $T_{5/3}$, and (c) singly produced $T_{5/3}$.

2.2 Four-top-quark production

Four-top-quark production is expected to occur in the SM with a next-to-leading-order cross-section of 9.2 fb at $\sqrt{s} = 13 \text{ TeV}$ [19] and leads to a same-charge lepton pair or a trilepton final state with a branching ratio of 12.1%, including leptonically decaying τ -leptons. In addition, the four-top-quark production rate could be enhanced in several BSM scenarios. Three benchmarks are considered in this paper. The first is based on an effective field theory (EFT) approach where the BSM contribution is represented via a contact

¹ The $B_{-4/3}$ quark can only decay into Wb , and therefore pair-production of these quarks does not result in same-charge prompt lepton pairs. Thus the $B_{-4/3}$ quark is not considered in this analysis.

interaction (CI) independently of the details of the underlying theory:

$$\mathcal{L}_{4t} = \frac{C_{4t}}{\Lambda^2} (\bar{t}_R \gamma^\mu t_R) (\bar{t}_R \gamma_\mu t_R)$$

where t_R is the right handed top spinor, γ_μ are the Dirac matrices, C_{4t} is a dimensionless constant and Λ is the new-physics energy scale. Only the contact interaction operator with right-handed top quarks is considered as left-handed top operators are already strongly constrained by electroweak precision data [20]. The four-top-quark production mechanism in this model is shown in Figure 2(a).

The second BSM four-top-quark production model is one with two universal extra dimensions (2UED) that are compactified in the real projective plane geometry (RPP), as described in Ref. [21]. The compactification of the two extra dimensions, characterised by the radii R_4 and R_5 , leads to the discretisation of the momenta along these directions with the allowed values labelled by the integers i and j . Each momentum state appears as a particle called a Kaluza–Klein (KK) excitation with a mass m , defined by (i, j) values and later referenced as a ‘tier’. At leading order, the mass of a KK excitation of a particle with a mass m_0 is

$$m^2 = \frac{i^2}{R_4^2} + \frac{j^2}{R_5^2} + m_0^2. \quad (1)$$

The additional mass differences within a given tier (i, j) are due to next-to-leading-order corrections and are small compared with the masses [21]. By using the notations $m_{\text{KK}} = 1/R_4$ and $\xi = R_4/R_5$, Eq. (1) reads as

$$m^2 = m_{\text{KK}}^2 \left(i^2 + j^2 \xi^2 \right) + m_0^2.$$

The four-top-quark signal of the model considered in this paper arises from pair-produced particles of tier $(1, 1)$, which then chain-decay into the lightest particle of this tier, the KK excitation of the photon, $A^{(1,1)}$, by emitting SM particles [22], as shown in Figure 2(b). This heavy photon $A^{(1,1)}$ decays into $t\bar{t}$ with a branching ratio assumed to be 100%. Therefore, additional quarks and leptons are expected to be produced in association with the four-top-quark system, which makes this signature quite different from the other considered benchmarks, as shown in Figure 2. In addition, cosmological observations constrain m_{KK} between 600 GeV and 1000 GeV [22, 23], leading to typical resonance masses between 0.6 TeV and 2 TeV depending on the ratio ξ of the two compactification radii. This analysis probes different scenarios varying both m_{KK} and ξ , where the four-top-quark signal arises from particles of tier $(1, 1)$ [22].

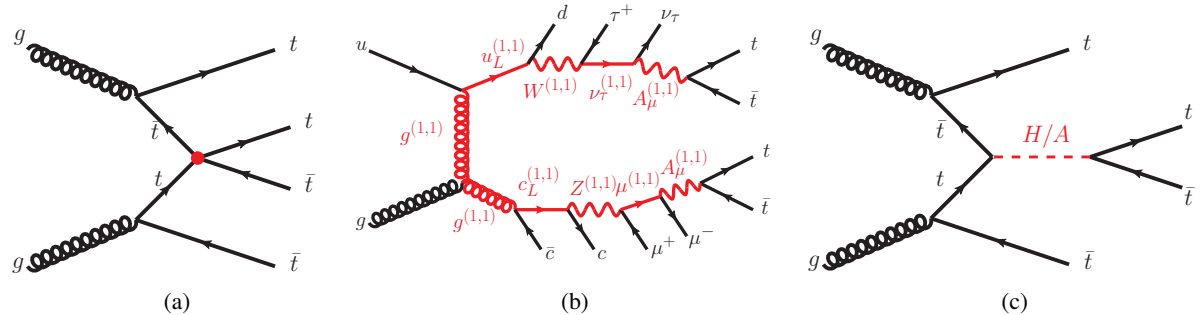


Figure 2: Three examples of four-top-quark production in the context of (a) a four-fermion contact interaction (CI), (b) two compactified universal extra-dimensions (2UED), and (c) two-Higgs-doublet model (2HDM).

The third BSM four-top-quark production model is one with two Higgs doublets Φ_1 and Φ_2 (2HDM), which spontaneously break the electroweak symmetry $SU(2)_L \times U(1)_Y$ [24]. In this model, Φ_1 couples only to down-type quarks and leptons, and Φ_2 couples only to up-type quarks and neutrinos [25]. The parameter space is constrained to avoid large FCNC at tree level, resulting in four different sets of Yukawa couplings between the Higgs doublets and SM fermions. Among these, the Type-II 2HDM is considered. Measurements of the properties of the SM Higgs boson constrain all 2HDM types to be in the so-called alignment limit [25], where the mass eigenstates are aligned with the gauge eigenstates in the new scalar sector. In this model, the $t\bar{t}t\bar{t}$ final state arises from the production of heavy neutral Higgs bosons H (scalar) and A (pseudo-scalar) in association with a $t\bar{t}$ pair, with the H or A boson decaying into $t\bar{t}$ as shown in Figure 2(c):

$$gg \rightarrow t\bar{t}H/A \rightarrow t\bar{t}t\bar{t}.$$

In the alignment limit, the scalar and the pseudo-scalar Higgs boson have the same mass $m_{H/A}$ and both contribute to the four-top-quark production with similar kinematics. The cross-section predicted by this model depends on $m_{H/A}$ and the ratio $\tan\beta$ of vacuum expectation values of the two Higgs doublets. This benchmark is particularly interesting since the four-top-quark kinematics are rather soft compared with the CI signature, especially at low masses where the direct search for $H/A \rightarrow t\bar{t}$ loses sensitivity due to interference effects with the SM $t\bar{t}$ production [26].

2.3 Same-sign top-quark pair production

Same-sign top-quark pair production (tt) is suppressed to a negligible level in the SM but allowed in BSM models. This signature is distinct from VLQ or $t\bar{t}t\bar{t}$ production, and is treated separately in the analysis. In particular, only positively charged lepton pairs are considered for this signal (since tt production has a cross-section higher by a typical factor 100 than $t\bar{t}$ production at the LHC). The kinematic criteria also differ from those applied in the VLQ and four-top-quark searches. The considered benchmark is a generic dark-matter model relying on an effective theory invariant under $SU(2)_L \times U(1)_Y$ [27]. In this model, a top quark is produced in association with an FCNC mediator V which could then decay into dark-matter χ or SM particles $t\bar{u}/\bar{t}u$:

$$\mathcal{L}_{\text{DM}} = \mathcal{L}_{\text{kin}}[\chi, V_\mu] + g_{\text{SM}} V_\mu \bar{t}_R \gamma^\mu u_R + g_{\text{DM}} V_\mu \bar{\chi} \gamma^\mu \chi$$

where g_{SM} and g_{DM} represent the coupling strengths of the mediator to SM and dark-matter particles, respectively, and $\mathcal{L}_{\text{kin}}[\chi, V_\mu]$ represents the kinetic term of the mediator and the dark-matter fields. The tt final state could arise if V couples to the top quark, in both the t - and s -channels, leading to the three processes shown in Figure 3, with a relative contribution which depends on the total width of the mediator.

The results are interpreted for each process in Figure 3 independently, allowing constraints to be placed on generic FCNC via the process $uu \rightarrow tt$ as well as specific resonances decaying into $t\bar{u}$. The results are also interpreted for different values of the mass of the mediator m_V , g_{SM} , and g_{DM} , taking into account width effects. This provides additional sensitivity to dark-matter mediators when its branching ratio into SM particles is sizeable,² where a direct search based on final states with missing transverse energy and a top quark [28] might lose sensitivity.

² This is a realistic scenario since the mediator must have visible partial width in order to be produced in proton–proton collisions.

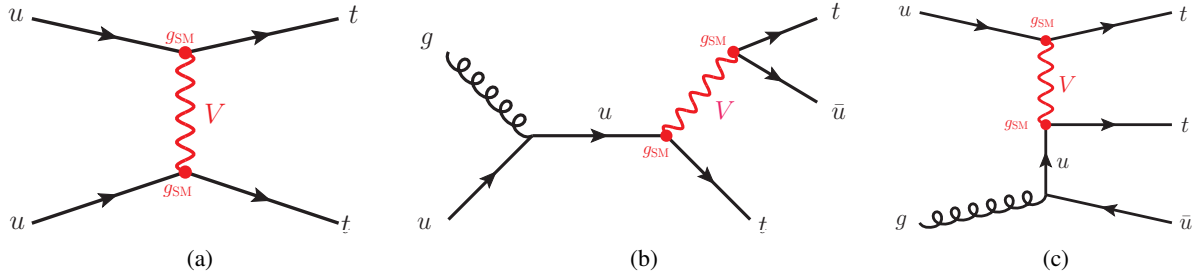


Figure 3: Three examples of same-sign top quark pair signatures in the context of the dark-matter mediator model: (a) prompt tt production, (b) via an on-shell mediator, (c) via an off-shell mediator. The mediator is denoted by V and its coupling to SM particles is denoted by g_{SM} .

3 ATLAS detector

The ATLAS detector [29] at the LHC covers nearly the entire solid angle around the collision point.³ It consists of an inner tracking detector surrounded by a thin superconducting solenoid, electromagnetic and hadronic calorimeters, and a muon spectrometer incorporating three large superconducting toroidal magnets. The inner-detector system is immersed in a 2 T axial magnetic field and provides charged-particle tracking in the range $|\eta| < 2.5$.

A high-granularity silicon pixel detector covers the vertex region and typically provides four three-dimensional measurements per track, the innermost being in the insertable B-layer [30]. It is followed by a silicon microstrip tracker, which provides four two-dimensional measurement points per track. These silicon detectors are complemented by a transition radiation tracker, which enables radially extended track reconstruction up to $|\eta| = 2.0$. The transition radiation tracker also provides electron identification information based on the fraction of hits (typically 30 in total) above a higher energy-deposit threshold corresponding to transition radiation.

The calorimeter system covers the pseudorapidity range $|\eta| < 4.9$. Within the region $|\eta| < 3.2$, electromagnetic calorimetry is provided by barrel and endcap high-granularity lead/liquid-argon (LAr) sampling calorimeters, with an additional thin LAr presampler covering $|\eta| < 1.8$ to correct for energy loss in material upstream of the calorimeters. Hadronic calorimetry is provided by a steel/scintillator-tile calorimeter, segmented into three barrel structures within $|\eta| < 1.7$, and two copper/LAr hadronic endcap calorimeters. The solid angle coverage is completed with forward copper/LAr and tungsten/LAr calorimeter modules optimised for electromagnetic and hadronic measurements, respectively.

The muon spectrometer comprises separate trigger and high-precision tracking chambers measuring the deflection of muons in a magnetic field generated by the superconducting air-core toroidal magnets. The field integral of the toroidal magnets ranges between 2.0 and 6.0 T m across most of the acceptance. A set of precision chambers covers the region $|\eta| < 2.7$ with three layers of monitored drift tubes, complemented by cathode strip chambers in the forward region, where the background is highest. The muon trigger

³ ATLAS uses a right-handed coordinate system with its origin at the nominal interaction point (IP) in the centre of the detector and the z -axis along the beam pipe. The x -axis points from the IP to the centre of the LHC ring, and the y -axis points upward. Cylindrical coordinates (r, ϕ) are used in the transverse plane, ϕ being the azimuthal angle around the z -axis. The pseudorapidity is defined in terms of the polar angle θ as $\eta = -\ln \tan(\theta/2)$, and the rapidity y is defined as $y = \frac{1}{2} \ln \frac{E+p_z}{E-p_z}$.

system covers the range $|\eta| < 2.4$ with resistive plate chambers in the barrel, and thin gap chambers in the endcap regions.

The ATLAS detector has a two-level trigger system to select events for offline analysis [31]. The first-level trigger is implemented in hardware and uses a subset of detector information to reduce the event rate to a design value of 100 kHz. This is followed by a software-based high-level trigger which reduces the event rate to about 1 kHz.

4 Data sample and trigger requirements

The data were recorded in LHC proton–proton (pp) collisions at $\sqrt{s} = 13$ TeV in 2015 and 2016, corresponding to an integrated luminosity of 36.1 ± 0.8 fb^{-1} . The luminosity and its uncertainty are derived, following a methodology similar to that detailed in Ref. [32], from a calibration of the luminosity scale using $x - y$ beam-separation scans. In this dataset the average number of simultaneous pp interactions per bunch crossing in addition to the triggered hard-scatter interaction, pile-up, was approximately 24. Data-quality requirements were applied to ensure that events were selected only from periods where all subdetectors were operating at nominal conditions, and where the LHC beams were in stable-collision mode. The events used in the analysis were required to have at least one primary vertex formed from at least two charged-particle tracks with transverse momentum $p_T > 0.4$ GeV, and to have been triggered either by two leptons or a single high- p_T lepton. Only triggers with loose lepton quality and isolation requirements were used, since tight requirements at the trigger level would complicate the estimation of the background originating from fake or non-prompt leptons. The dilepton triggers provide sensitivity at low lepton p_T values, and the single-lepton triggers provide additional efficiency for high- p_T leptons. The p_T thresholds for the dilepton triggers varied from 8 to 24 GeV depending on the lepton flavours and the year in which the event was recorded. The single-muon trigger had a p_T threshold of 50 GeV; the corresponding single-electron trigger had a p_T threshold of 24 GeV for data recorded in 2015 and 60 GeV for data recorded in 2016. The trigger efficiency depends on the lepton flavour combination, but in all cases is $> 95\%$ for events of interest in this analysis.

5 Object selection criteria

This analysis makes use of reconstructed electrons, muons, jets, b -tagged jets, and missing transverse momentum. Their selection is described in this section and summarised in Table 1.

Electrons are reconstructed from clusters of energy deposits in electromagnetic calorimeter cells with a matching inner detector track [33]. The candidate electrons are required to have $p_T > 28$ GeV and be in the $|\eta| < 2.47$ region, excluding the transition region between the barrel and endcap calorimeters ($1.37 < |\eta| < 1.52$). For events with two electrons or one electron and one muon, electrons with $|\eta| > 1.37$ are not considered since such events are subject to backgrounds from electron charge misidentification, which has a substantially higher probability of occurring for electrons at high $|\eta|$, as detailed in Section 7. Muons are reconstructed from tracks in the muon spectrometer and inner detector [34]. They must have $p_T > 28$ GeV and $|\eta| < 2.5$.

Electrons and muons are required to be consistent with originating from the primary event vertex, using the quantities $|d_0/\sigma_{d_0}|$, where d_0 is the impact parameter relative to the primary vertex in the x – y plane and

σ_{d_0} is its uncertainty, and $|z_0 \sin \theta|$, where z_0 is the r - ϕ projection of the impact point onto the beamline. Electrons are required to satisfy $|d_0/\sigma_{d_0}| < 5$ and $|z_0 \sin \theta| < 0.5$ mm, while muons are required to satisfy $|d_0/\sigma_{d_0}| < 3$ and $|z_0 \sin \theta| < 0.5$ mm.

All leptons are required to satisfy either relaxed or nominal identification criteria. The nominal sample, which is a subset of the relaxed sample, is used in the final analysis, and the relaxed sample is used to estimate one component of the reducible background as described in Section 7. For electrons, the relaxed (nominal) selection requires that the electron satisfies the likelihood medium (tight) requirements defined in Ref. [33], while for muons both the relaxed and nominal selections require that the muon satisfies the medium criteria defined in Ref. [34]. Nominal leptons are required to be isolated from other activity in the detector: the scalar sum of the p_T of tracks within a variable-size cone around the lepton (excluding its own track), must be less than 6% of the lepton p_T . The track isolation cone size for electrons (muons) $\Delta R = \sqrt{(\Delta\eta)^2 + (\Delta\phi)^2}$ is given by the smaller of $\Delta R = 10 \text{ GeV}/p_T$ and $\Delta R = 0.2$ (0.3). In addition, in the case of electrons the sum of the transverse energy of the calorimeter energy clusters in a cone of $\Delta R = 0.2$ around the electron (excluding the energy from the electron itself) must be less than 6% of the electron p_T .

Jets are reconstructed from clusters of energy in the calorimeter using the anti- k_t algorithm [35] with a radius parameter of 0.4. Jets are considered if $p_T > 25 \text{ GeV}$ and $|\eta| < 2.5$. Quality criteria are applied to jets to ensure that they are not reconstructed from detector noise, beam losses, or cosmic rays [36]. If any jet fails to satisfy these criteria, the event is vetoed. To reject jets from pile-up, an observable called the jet vertex tagger (JVT) is formed by combining variables that discriminate pile-up jets from hard-scattering jets [37]. Jets with $p_T < 60 \text{ GeV}$ and $|\eta| < 2.4$ that have associated tracks are subject to a requirement on JVT that is 92% efficient for hard-scattering jets while rejecting 98% of pile-up jets. If such jets have no associated tracks they are removed. Jets containing a b -hadron are identified using a multivariate technique [38]. An operating point is defined by a threshold in the range of discriminant output values, and is chosen to provide specific b -, c -, and light-jet efficiencies in simulated $t\bar{t}$ events. The operating point used in this analysis has a 77% b -jet efficiency with rejection factors of 6 and 134 for c - and light-jets, respectively.

The missing transverse momentum is calculated as the negative vectorial sum of the transverse momenta of reconstructed calibrated objects in the event. Its magnitude is denoted E_T^{miss} , and is computed using electrons, photons, hadronically decaying τ -leptons, jets and muons as well as a soft term calculated with tracks matched to the primary vertex which are not associated with any of these objects [39].

A set of requirements are applied to resolve overlaps between reconstructed objects. This procedure is applied to the leptons satisfying the relaxed selection criteria. In the first step, electrons which share a track with a muon are removed, to avoid cases where muon radiation would mimic an electron. Next, the jet closest to an electron within $\Delta R_y \equiv \sqrt{(\Delta y)^2 + (\Delta\phi)^2} = 0.2$ is removed to avoid double counting. Then, to reduce the contributions from non-prompt electrons originating from heavy-flavour decays, electrons within $\Delta R_y = 0.4$ of any remaining jets are removed. Finally, the overlap between muons and jets is considered: jets with less than three tracks and within $\Delta R_y = 0.4$ of a muon are removed. Muons are then removed if they are within $\Delta R_y = 0.04 + 10 \text{ GeV}/p_{T,\mu}$ of remaining jets.

The events are preselected if they contain at least one jet, and at least two leptons that satisfy the nominal selection criteria. If exactly two of the three highest- p_T leptons satisfy the nominal criteria, they must have the same electric charge, and if these two leptons are electrons, a quarkonia/Z-veto is applied to their invariant mass: $m_{ee} > 15 \text{ GeV}$ and $|m_{ee} - 91 \text{ GeV}| > 10 \text{ GeV}$. Events that satisfy these criteria are called ‘same-charge lepton’ events. If the three highest- p_T leptons satisfy the nominal criteria, no requirement

is imposed on their charge or on the invariant mass of any pair. These events are called ‘trilepton’ events. Same-charge lepton and trilepton events are treated separately in the analysis.

Table 1: Summary of object identification and definition. ‘ID quality’ refers to the identification criteria used for each object type. For electrons, ‘mediumLH’ and ‘tightLH’ refer to the likelihood medium and tight requirements defined in Ref. [33]; for muons the criteria for ‘medium’ ID quality are defined in Ref. [34]. For jets, ‘cleaning’ means applying a procedure to reduce contamination from spurious jets [36], and ‘JVT’ means applying criteria to select jets that are consistent with being produced at the primary vertex rather than from pile-up [37]. For b -jets, ‘MVA77’ refers to placing a requirement on the multivariate discriminant defined in Ref. [38] that is 77% efficient for b -jets in simulated $t\bar{t}$ events.

	Electrons		Muons		Jets	b -jets
	relaxed	nominal	relaxed	nominal		
p_T [GeV]		> 28		> 28	> 25	> 25
$ \eta $		< 1.37 or $1.52 - 2.47$ (< 1.37 for ee and $e\mu$)		< 2.5	< 2.5	< 2.5
ID quality	mediumLH	tightLH		medium	cleaning + JVT	MVA77
Isolation	none	track- and calorimeter-based	none	track-based		
Track vertex :						
– $ d_0/\sigma_{d_0} $		< 5		< 3		
– $ z_0 \sin \theta $ [mm]		< 0.5		< 0.5		

6 Simulation

Monte Carlo (MC) simulation was used to model the signals and the irreducible backgrounds. EvtGen v1.2 [40] was used to model charm and bottom hadron decays for all samples, except those generated with SHERPA [41], and the A14 set of tuned parameters [42] was used for all samples unless stated otherwise.

The production of $T\bar{T}$, $B\bar{B}$ and $T_{5/3}\bar{T}_{5/3}$ pairs was modelled by PROTOS v2.2 [2], with PYTHIA v8.186 [43] for showering and hadronisation,⁴ using the NNPDF2.3LO set [45] of parton distribution functions (PDF). VLQ masses from 0.50 to 1.40 TeV were simulated. Standard Model production of four top quarks was simulated using MG5_AMC@NLO v2.2.2 [19] with PYTHIA v8.186, using the NNPDF2.3LO PDF set. In the 2UED/RPP scenario, four-top-quark production was modelled with PYTHIA v8.186, using the NNPDF2.3LO PDF set. For the contact interaction model, four-top-quark production was modelled with MG5_AMC@NLO v2.2.3 and PYTHIA v8.205 using the NNPDF2.3LO PDF set. Same-sign top-quark pair production was modelled by MG5_AMC@NLO v2.3.3 and PYTHIA v8.210 using the NNPDF2.3LO PDF set.

The main sources of irreducible backgrounds are $t\bar{t}V$ production (where V represents either a W or Z boson), $t\bar{t}H$ production, and diboson production. Smaller contributions from triboson, VH , $t\bar{t}t$,

⁴ Throughout this analysis it is assumed that pair production of vector-like quarks occurs only via QCD. There are models, such as the model in Ref. [44], that allow additional production mechanisms.

$t\bar{t}WW$, tZW , and tZ production are shown in the tables and figures as ‘Other bkg’. The SM four-top-quark production is included as a background for all BSM searches, but is considered as the signal in the search for SM four-top-quark production. The matrix elements for $t\bar{t}V$, $t\bar{t}H$, $t\bar{t}\bar{t}$, $t\bar{t}\bar{t}\bar{t}$, $t\bar{t}WW$, and tZW production processes were modelled with MG5_AMC@NLO v2.2.2 and PYTHIA v8.186 for hadronisation and showering, using the NNPDF3.0NLO PDF set. Next-to-leading-order (NLO) matrix-element calculation was used for $t\bar{t}V$, $t\bar{t}H$ and tZW while leading-order (LO) calculation was used for $t\bar{t}\bar{t}$, $t\bar{t}\bar{t}\bar{t}$ and $t\bar{t}WW$. The tZ process was modelled by MG5_AMC@NLO v2.2.2 based on LO matrix-element calculation with PYTHIA v6.428 [46] for showering and hadronisation. The CTEQ6L1 PDF set [47] and Perugia2012 set of tuned parameters [48] were used. Diboson and triboson production was modelled with the SHERPA v2.2.1 generator, which uses the Comix [49] and OpenLoops [50] matrix-element generators merged with the SHERPA parton shower [51] using the ME+PS@NLO prescription [52]. The VH production process was modelled using PYTHIA v8.186, with the NNPDF2.3LO PDF set. The cross-sections for all processes are calculated at NLO in QCD, except for tZ where the leading-order calculation is used.

Simulated PYTHIA v8.186 minimum-bias events were overlaid on each simulated event to model the effects of pile-up; the generated events were then reweighted so that the distribution of the number of interactions per bunch crossing matched the distribution observed in the data. The response of the ATLAS detector for most samples was modelled using GEANT4 [53] within the ATLAS simulation infrastructure [54]. The $t\bar{t}\bar{t}$, single $T_{5/3}$, and same-sign top-quark pair production samples were processed with a fast simulation that relies on a parameterisation of the calorimeter response [55]. Events were reconstructed using the same algorithms as used for the collider data. Corrections were applied to the simulated events to account for differences observed in trigger efficiencies, object identification efficiencies and resolutions when comparing the simulation with data.

7 Estimation of reducible backgrounds

In addition to the irreducible backgrounds described above, there are reducible backgrounds where a jet or lepton from heavy-flavour hadron decay mimics a prompt lepton⁵ (called ‘fake/non-prompt lepton background’ in the following), or the charge of a lepton is misidentified. These backgrounds are estimated using data-driven techniques.

The fake/non-prompt lepton background yield is estimated with the matrix method [56, 57], which uses the relaxed and nominal lepton categories defined in Table 1. The fraction of prompt leptons satisfying the relaxed criteria that also satisfy the nominal criteria is referred to as r . Similarly, the fraction of fake/non-prompt leptons satisfying the relaxed requirements that also satisfy the nominal requirements is referred to as f . Using the measured values of r and f , the number of events with at least one non-prompt/fake lepton in the nominal sample can be inferred from the numbers of relaxed and nominal leptons in the relaxed sample, and this number is taken as the fake/non-prompt yield. A Poisson likelihood approach is used to estimate the final fake/non-prompt yield and its statistical uncertainty. This approach guarantees that the estimated yield is not negative, and provides a more reliable estimate of the statistical uncertainty in regions with a small number of selected events.

Single-lepton control regions enriched in prompt and fake/non-prompt leptons are used to measure r and f . The criteria used to select the single-lepton events are different for electrons and muons due to the

⁵ Prompt leptons are leptons which do not originate from hadron decays or conversion processes.

different sources of fake/non-prompt leptons for each flavour. For electrons, r is measured using events with $E_T^{\text{miss}} > 150 \text{ GeV}$, where the dominant contribution is from $W \rightarrow e\nu$, and f is measured using events with the transverse mass of the E_T^{miss} -lepton system⁶ $m_T(W) < 20 \text{ GeV}$ and $E_T^{\text{miss}} + m_T(W) < 60 \text{ GeV}$, where the dominant contribution is from multijet production (including heavy-flavour production) where one or more jets are misidentified as electrons. For muons, r is measured using events with $m_T(W) > 100 \text{ GeV}$, a sample dominated by $W \rightarrow \mu\nu$, and f is measured using events where the transverse impact parameter of the muon relative to the primary vertex is more than five standard deviations away from zero, consistent with muons originating from heavy-flavour hadron decays. The small contribution of prompt leptons in the control samples used to measure f is estimated from simulation and this contribution is subtracted from the sample. The values of r and f are parameterised in terms of variables of the leptons ($|\eta|$, p_T , and the angular distance to the nearest jet) and the number of b -tagged jets. For muons, r ranges from 55% to 97% while f ranges from 7% to 30%. For electrons, r ranges from 70% to 95% while f ranges from 8% to 30%. In general, the values of r and f are smaller for leptons near a jet, and larger for high- p_T leptons.

The second reducible background, corresponding to events where the charge of a lepton is misidentified, is considered only for electrons since the probability of muon charge misidentification is negligibly small. There are two primary mechanisms by which the electron charge can be misidentified: the first is the ‘trident’ process in which an electron emits an energetic bremsstrahlung photon, which subsequently produces an e^+e^- pair. This can result in a track of the incorrect charge being associated with the electron. The second is the mismeasurement of the curvature of the electron track. The probability for an electron to have its charge incorrectly reconstructed is measured using a sample of dielectron events with invariant mass consistent with the Z boson. The trident process can result in misidentified charge for an electron that is also likely to be considered fake/non-prompt due to the presence of nearby charged tracks. To avoid double-counting the background contribution from such electrons, the matrix method is used to subtract the fake/non-prompt electron yield from the Z sample. The charge misidentification probability is calculated in bins of electron $|\eta|$ and p_T , using a likelihood fit that adjusts these binned probabilities to find the best agreement with the observed numbers of same-charge and opposite-charge electron pairs. The charge misidentification probability varies from 2×10^{-5} (for electrons at low p_T and small $|\eta|$) to 10^{-2} for electrons at high p_T and $|\eta|$ near the edge of the barrel calorimeter; for electrons with larger values of $|\eta|$ the probability can reach 10%.

Since charge misidentification is negligible for muons and not relevant for trilepton events (for which no lepton charge requirements are imposed), the background from charge misidentification (called charge mis-ID hereafter) only appears in ee or $e\mu$ events. To estimate its yield, ee and $e\mu$ events are selected using all the criteria applied in the analysis, with the exception that the leptons are required to have opposite charge. Then the charge misidentification probabilities are applied to this sample to determine the background yield.

8 Signal and validation regions

Several signal regions (SR) are defined to represent the broad range of BSM signals considered. The selection criteria are designed to maximise the sensitivity to the signals. The signal regions are separated

⁶ The transverse mass of the E_T^{miss} -lepton system is defined as $m_T(W) \equiv \sqrt{2p_{T\ell}E_T^{\text{miss}}(1 - \cos \Delta\phi)}$ where $p_{T\ell}$ is the lepton transverse momentum and $\Delta\phi$ is the azimuthal angle between the lepton and the missing transverse momentum.

into two categories: one category is designed for maximal sensitivity to VLQ and four-top-quark production, while the second category is optimised for the same-sign top-quark pair production searches. For the VLQ and four-top-quark searches, the preselected sample is first split according to the numbers of leptons (two or three) and b -tagged jets (one, two, or greater than two). Within each of the resulting subsamples, requirements are placed on H_T and E_T^{miss} , where H_T is the scalar sum of the p_T of all selected jets and leptons, to maximise the average sensitivity for the signal models considered. In addition, to fully exploit specific features of VLQ and four-top-quark signatures, the signal regions with at least three b -tagged jets are further split. Relaxed H_T and high jet multiplicity requirements are sensitive to the four-top-quark signature, while high H_T and low jet multiplicity requirements enhance sensitivity to the VLQ signature. For all the signal regions described above, lepton flavours are considered inclusively to increase the number of data events in the loosely selected samples used to estimate the reducible backgrounds. The values of r and f appropriate to each lepton's flavour are used to estimate the fake/non-prompt lepton background. The selection criteria are summarised in Table 2, and the selection efficiencies for some signal models are shown in Table 3.

The same-sign top-quark selection requires exactly two leptons with positive charge, reflecting the preponderance of $t\bar{t}$ over $t\bar{t}$ production in pp collisions by a typical factor of 100. Additional criteria are imposed to maximise the sensitivity of the search: at least one b -tagged jet, H_T greater than 750 GeV, E_T^{miss} greater than 40 GeV, and the azimuthal separation between the two leptons $|\Delta\phi_{ee}|$ greater than 2.5. Since the optimal kinematic selection is looser than for VLQ and four-top-quark signal regions, more statistics are available for estimating the reducible backgrounds, so the lepton flavours (ee , $e\mu$, and $\mu\mu$) are treated separately in the search for same-sign top-quark pair production. These selection criteria are summarised in Table 4 and the selection efficiencies for the three same-sign top-quark pair signal processes are shown in Table 5.

In addition to the signal regions, a set of validation regions (VR) with criteria similar to those used for the SR, in which the expected signal yield is small, are defined. The VR are used to verify that the background is correctly modelled in regions that are kinematically similar to the signal regions. The definitions of the validation regions are presented in Tables 2 and 4, and the corresponding expected and observed yields are shown in Tables 6 and 7. These tables also report the probability for the expected background to fluctuate to equal or exceed the observed yield in each validation region; the smallest such probability is 0.10, which occurs in VR2 $b2\ell$. The distributions of E_T^{miss} and H_T in each validation region are shown in Figures 4–6. The χ^2 probabilities for compatibility of the observed and expected distributions are reasonable when all systematic uncertainties, including their bin-to-bin correlations, are considered. The smallest probability is 2%, which occurs for the E_T^{miss} distribution in VR1 $b2\ell$. The systematic uncertainties are described in Section 9.

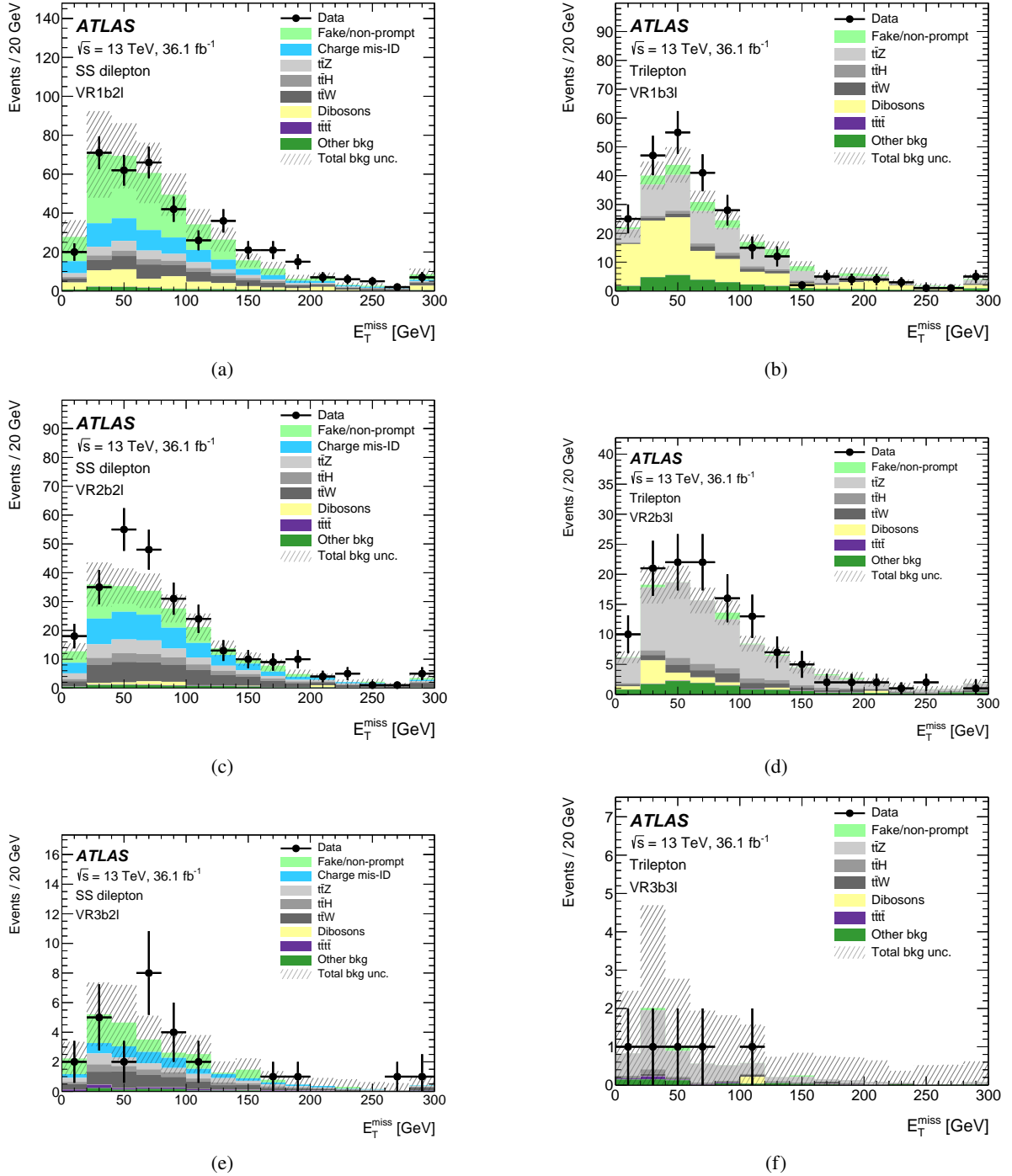


Figure 4: Distributions of E_T^{miss} in each of the validation regions used for the four-top-quark and VLQ searches. The first (second) column shows distributions of dilepton (trilepton) events while each row corresponds to a given b -tagged jet multiplicity. The uncertainty, shown as the hashed region, includes both the statistical and systematic uncertainties from each background source.

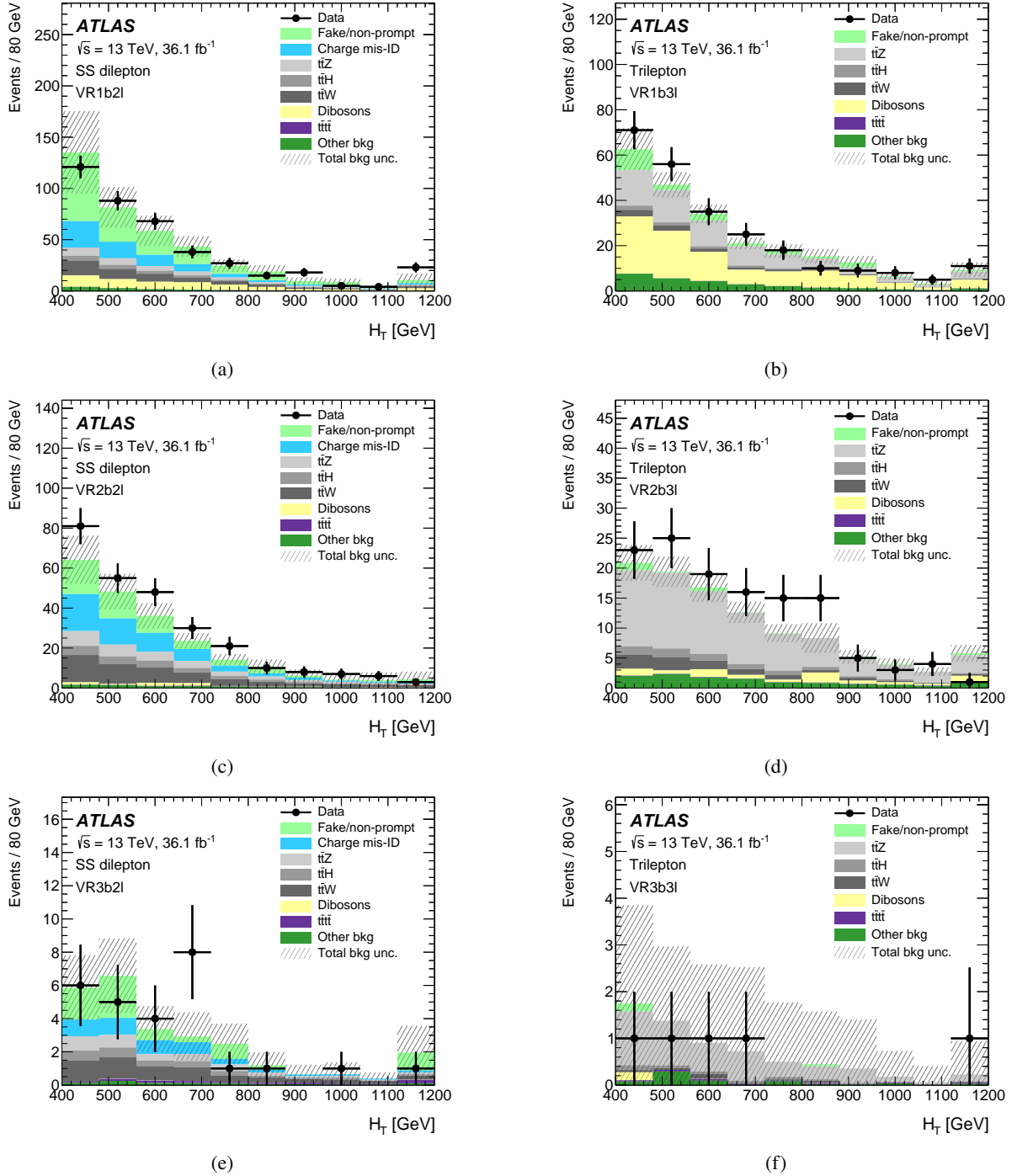


Figure 5: Distributions of H_T in each of the validation regions used for the four-top-quark and VLQ searches. The first (second) column shows distributions of dilepton (trilepton) events while each row corresponds to a given b -tagged jet multiplicity. The uncertainty, shown as the hashed region, includes both the statistical and systematic uncertainties from each background source.

Table 2: Definitions of the validation and corresponding signal regions for the four-top-quark and VLQ searches, where N_j is the number of jets, N_b is the number of b -tagged jets, and N_ℓ is the number of leptons. The name of each signal (validation) region begins with “SR” (“VR”), with the rest of the name indicating the number of leptons and number of b -tagged jets required. The suffix “_L” denotes the signal regions with relaxed H_T but stricter N_j requirements. For regions that require two leptons, the leptons must have the same charge. Events that appear in any of the signal regions are vetoed in the validation regions.

Region name	N_j	N_b	N_ℓ	Lepton charges	Kinematic criteria
VR1 $b2\ell$	≥ 1	1	2	++ or ---	$400 < H_T < 2400 \text{ GeV}$ or $E_T^{\text{miss}} < 40 \text{ GeV}$
SR1 $b2\ell$	≥ 1	1	2	++ or ---	$H_T > 1000 \text{ GeV}$ and $E_T^{\text{miss}} > 180 \text{ GeV}$
VR2 $b2\ell$	≥ 2	2	2	++ or ---	$H_T > 400 \text{ GeV}$
SR2 $b2\ell$	≥ 2	2	2	++ or ---	$H_T > 1200 \text{ GeV}$ and $E_T^{\text{miss}} > 40 \text{ GeV}$
VR3 $b2\ell$	≥ 3	≥ 3	2	++ or ---	$400 < H_T < 1400 \text{ GeV}$ or $E_T^{\text{miss}} < 40 \text{ GeV}$
SR3 $b2\ell$ _L	≥ 7	≥ 3	2	++ or ---	$500 < H_T < 1200 \text{ GeV}$ and $E_T^{\text{miss}} > 40 \text{ GeV}$
SR3 $b2\ell$	≥ 3	≥ 3	2	++ or ---	$H_T > 1200 \text{ GeV}$ and $E_T^{\text{miss}} > 100 \text{ GeV}$
VR1 $b3\ell$	≥ 1	1	3	any	$400 < H_T < 2000 \text{ GeV}$ or $E_T^{\text{miss}} < 40 \text{ GeV}$
SR1 $b3\ell$	≥ 1	1	3	any	$H_T > 1000 \text{ GeV}$ and $E_T^{\text{miss}} > 140 \text{ GeV}$
VR2 $b3\ell$	≥ 2	2	3	any	$400 < H_T < 2400 \text{ GeV}$ or $E_T^{\text{miss}} < 40 \text{ GeV}$
SR2 $b3\ell$	≥ 2	2	3	any	$H_T > 1200 \text{ GeV}$ and $E_T^{\text{miss}} > 100 \text{ GeV}$
VR3 $b3\ell$	≥ 3	≥ 3	3	any	$H_T > 400 \text{ GeV}$
SR3 $b3\ell$ _L	≥ 5	≥ 3	3	any	$500 < H_T < 1000 \text{ GeV}$ and $E_T^{\text{miss}} > 40 \text{ GeV}$
SR3 $b3\ell$	≥ 3	≥ 3	3	any	$H_T > 1000 \text{ GeV}$ and $E_T^{\text{miss}} > 40 \text{ GeV}$

Table 3: Signal selection and preselection efficiencies for events in various signal models, as estimated from MC simulation. VLQs are assumed to decay with the branching ratios expected in the singlet model of Ref. [2].

Signal	Preselection efficiency [%]	Signal region efficiencies [%]			
		SR1 $b2\ell / 3\ell$	SR2 $b2\ell / 3\ell$	SR3 $b2\ell$ _L / 3 ℓ _L	SR3 $b2\ell / 3\ell$
$B\bar{B}$, $m_B = 800 \text{ GeV}$	1.7	0.12 / 0.16	0.19 / 0.14	0.007 / 0.002	0.05 / 0.04
$B\bar{B}$, $m_B = 1200 \text{ GeV}$	1.9	0.27 / 0.28	0.31 / 0.24	$4 \times 10^{-4} / 4 \times 10^{-4}$	0.07 / 0.05
$T\bar{T}$, $m_T = 800 \text{ GeV}$	1.2	0.06 / 0.02	0.09 / 0.02	0.008 / 0.006	0.04 / 0.06
$T\bar{T}$, $m_T = 1200 \text{ GeV}$	1.3	0.10 / 0.25	0.13 / 0.22	$0.002 / 9 \times 10^{-4}$	0.06 / 0.11
$t\bar{t}t\bar{t}$ (SM)	2.7	0.02 / 0.02	0.11 / 0.04	0.37 / 0.17	0.20 / 0.18
$t\bar{t}t\bar{t}$ (CI)	3.0	0.06 / 0.05	0.23 / 0.08	0.30 / 0.16	0.33 / 0.27
$t\bar{t}t\bar{t}$ (2HDM, $m_H = 700 \text{ GeV}$)	3.1	0.02 / 0.03	0.11 / 0.03	0.62 / 0.24	0.19 / 0.17
$t\bar{t}t\bar{t}$ (2UED/RPP, $m_{KK} = 1400 \text{ GeV}$)	3.3	0.27 / 0.16	0.62 / 0.31	$8 \times 10^{-4} / 0.0$	0.89 / 0.51

Table 4: Definitions of the validation and signal regions for the same-sign top-quark pair production search, where N_b is the number of b -tagged jets, N_ℓ is the number of leptons, and $|\Delta\phi_{\ell\ell}|$ is the azimuthal angle between the leptons. The name of each signal (validation) region begins with “SR” (“VR”). The validation region is inclusive in lepton flavour.

Region name	N_b	N_ℓ	H_T [GeV]	E_T^{miss} [GeV]	$ \Delta\phi_{\ell\ell} $ [radians]	Lepton flavour/charge
VRtt	≥ 1	2	> 750	> 40	> 2.5	$e^-e^- + e^-\mu^- + \mu^-\mu^-$
SRttee						e^+e^+
SRtte μ	≥ 1	2	> 750	> 40	> 2.5	$e^+\mu^+$
SRtt $\mu\mu$						$\mu^+\mu^+$

Table 5: Signal selection and preselection efficiencies for events in the three same-sign top-quark pair production processes, as estimated from MC simulation.

Signal	Preselection efficiency [%]	Signal region efficiencies [%]		
		SRttee	SRtte μ	SRtt $\mu\mu$
$t\bar{t}$, $m_V = 2000$ GeV	2.0	0.1	0.3	0.3
$t\bar{t}u$ off-shell, $m_V = 2000$ GeV	1.7	0.1	0.2	0.2
$tV(\rightarrow t\bar{t})$ on-shell, $m_V = 2000$ GeV	1.8	0.04	0.2	0.1

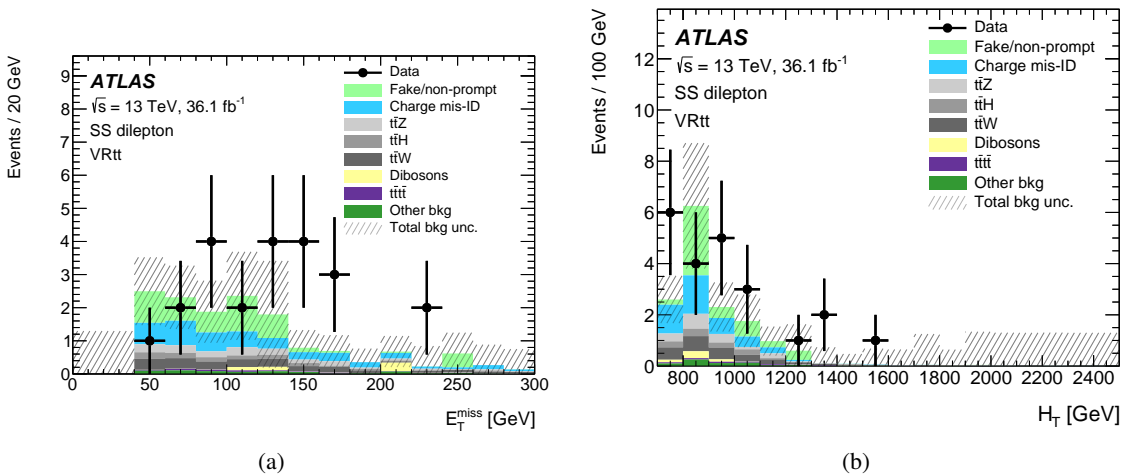


Figure 6: Distributions of (a) E_T^{miss} and (b) H_T in the validation region used for the same-sign top-quark pair production search. The uncertainty, shown as the hashed region, includes both the statistical and systematic uncertainties from each background source.

Table 6: Expected background and observed event yields in the validation regions used in the VLQ and four-top-quark searches. The ‘Other bkg’ category includes contributions from all rare SM processes listed in Section 6. The first uncertainty is statistical and the second is systematic. The p -values are the probabilities for the expected background to fluctuate to equal or exceed the observed yield in each region.

Source	VR1b2 ℓ			VR2b2 ℓ			VR3b2 ℓ									
$t\bar{t}W$	49	\pm	1	\pm	14		48	\pm	1	\pm	13	5.8	\pm	0.3	\pm	2.8
$t\bar{t}Z$	28.7	\pm	0.5	\pm	4.6		27.6	\pm	0.4	\pm	5.3	3.4	\pm	0.2	$\pm^{+4.2}_{-3.4}$	
Dibosons	48	\pm	4	\pm	35		4.9	\pm	1.3	\pm	3.5	< 0.5				
$t\bar{t}H$	17.7	\pm	0.4	\pm	2.4		18.3	\pm	0.4	\pm	2.6	2.6	\pm	0.2	\pm	1.9
$t\bar{t}t\bar{t}$	0.59	\pm	0.04	\pm	0.39		1.3	\pm	0.1	\pm	1.2	1.0	\pm	0.1	$\pm^{+2.5}_{-1.0}$	
Other bkg	12.3	\pm	0.5	\pm	6.4		7.3	\pm	0.3	\pm	4.0	1.1	\pm	0.2	\pm	1.1
Fake/non-prompt	170	\pm	8	\pm	87		53	\pm	5	\pm	28	7.8	\pm	1.6	\pm	3.8
Charge mis-ID	70	\pm	1	\pm	17		54	\pm	1	\pm	15	4.4	\pm	0.2	\pm	1.3
Total bkg	395	\pm	9	\pm	98		216	\pm	5	\pm	38	26	\pm	2	\pm	11
Data yield	407			269			27									
p -value	0.45			0.10			0.46									
Source	VR1b3 ℓ			VR2b3 ℓ			VR3b3 ℓ									
$t\bar{t}W$	10.4	\pm	0.3	\pm	3.3		9.4	\pm	0.3	\pm	2.4	0.31	\pm	0.09	$\pm^{+0.57}_{-0.30}$	
$t\bar{t}Z$	70	\pm	1	\pm	11		66	\pm	1	\pm	15	4.6	\pm	0.2	$\pm^{+7.4}_{-4.6}$	
Dibosons	93	\pm	7	\pm	66		7.7	\pm	2.1	\pm	6.2	0.17	\pm	0.17	$\pm^{+0.26}_{-0.00}$	
$t\bar{t}H$	6.5	\pm	0.2	\pm	0.8		6.8	\pm	0.2	\pm	0.8	0.41	\pm	0.05	$\pm^{+0.78}_{-0.41}$	
$t\bar{t}t\bar{t}$	0.21	\pm	0.02	\pm	0.14		0.64	\pm	0.03	\pm	0.37	0.21	\pm	0.02	$\pm^{+1.20}_{-0.21}$	
Other bkg	27	\pm	1	\pm	14		12.0	\pm	0.5	\pm	6.1	0.7	\pm	0.2	$\pm^{+0.9}_{-0.7}$	
Fake/non-prompt	22	\pm	4	\pm	13		2.7	\pm	1.5	\pm	2.1	0.21	$\pm^{+0.31}_{-0.18}$	\pm	0.12	
Total bkg	229	\pm	8	\pm	70		105	\pm	3	\pm	19	6.5	\pm	0.4	$\pm^{+10.8}_{-6.5}$	
Data yield	248			126			5									
p -value	0.40			0.17			0.56									

Table 7: Expected background and observed event yields in the validation region for the same-sign top-quark pair production search. The ‘Other bkg’ category includes contributions from all rare SM processes listed in Section 6. The first uncertainty is statistical and the second is systematic. The p -value is the probability for the expected background to fluctuate to equal or exceed the observed yield.

Source	VRtt
$t\bar{t}W$	2.3 \pm 0.1 \pm 1.1
$t\bar{t}Z$	1.6 \pm 0.1 \pm 0.6
Dibosons	0.5 \pm 0.4 \pm 0.3
$t\bar{t}H$	1.0 \pm 0.1 \pm 0.4
$t\bar{t}t\bar{t}$	0.30 \pm 0.03 $^{+0.59}_{-0.30}$
Other bkg	0.7 \pm 0.1 \pm 0.6
Charge mis-ID	4.0 \pm 0.2 \pm 1.4
Fake/non-prompt	4.7 $^{+1.5}_{-1.3} \pm$ 2.5
Total bkg.	15.1 $^{+1.6}_{-1.4} \pm$ 4.2
Data yield	22
p -value	0.14

9 Systematic uncertainties

The expected background yields are subject to several sources of systematic uncertainty. For the irreducible backgrounds, the uncertainties include those from the background model and from the simulation of the response of the detector. The background model uncertainties arise from the uncertainty of both the cross-section for a given process and of the acceptance of the signal regions for that process. For $t\bar{t}W$ and $t\bar{t}Z$ production, these uncertainties are estimated by varying the renormalisation and factorisation scales up and down by a factor of two from their nominal values, and comparing the nominal MG5_AMC@NLO v2.2.2 with a sample generated with SHERPA v2.2.1. For diboson production these uncertainties are estimated by varying the renormalisation, factorisation, and resummation scales up and down by a factor of two from their nominal values, and setting the CKKW merging scale to 15 and 30 GeV (where the nominal value is 20 GeV) [52]. The cross-section uncertainties for $t\bar{t}W$ and $t\bar{t}Z$ are 13% and 12%, respectively, 6% for diboson production, and $^{+6\%}_{-9\%}$ for $t\bar{t}H$ production [19]. For other irreducible backgrounds, this uncertainty is set to 50% of the nominal yield. The most important detector-related uncertainties are those of the efficiency for identifying b -jets (or misidentifying c - or light-jets as b -jets) [38], the jet energy calibration [58], and the efficiencies for jets and leptons to satisfy the identification criteria [33, 34]. In addition, there is a global 2.1% uncertainty of the irreducible background yields due to the uncertainty of the integrated luminosity of the data sample.

Uncertainties of the fake/non-prompt lepton background arise from: *i*) possible differences between the values of r and f in the regions used to measure the efficiencies and in the signal regions, *ii*) statistical uncertainty of the control samples used to measure r and f , and *iii*) uncertainties of the normalisation of the MC sample used to subtract the prompt-lepton contribution in the fake control sample used to measure f . The first uncertainty is estimated by modifying the selection criteria for the control samples. The modified sample for measuring r for electrons requires $E_T^{\text{miss}} > 175$ GeV, the modified sample for measuring f for electrons requires $E_T^{\text{miss}} < 20$ GeV, the modified sample for measuring r for muons requires $m_{\text{T}}(W) > 110$ GeV, and the modified sample for measuring f for muons requires $E_T^{\text{miss}} < 20$ GeV and $E_T^{\text{miss}} + m_{\text{T}}(W) < 60$ GeV. The second uncertainty is estimated by dividing the control samples randomly into four subsamples, computing the efficiencies in each of them, and observing the variation in the fake/non-prompt lepton yield. This variation is then divided by two since each of the subsamples has only one fourth of the statistics of the full sample. This procedure accounts for any correlations in the efficiencies. The third uncertainty is estimated by varying the normalisation of the MC subtraction in the fake control sample by 10%. The resulting uncertainty depends on the region the fake/non-prompt lepton background is estimated in, since the fake sample can vary kinematically, but is generally around 40–50% of the expected fake/non-prompt lepton yield for the dominant uncertainty in the signal regions. The first is the dominant uncertainty, particularly from variations in the fake-lepton efficiency when the selection criteria for the control samples are changed.

The uncertainties of the charge mis-ID background arise from uncertainties of the measured rates for electron charge misidentification and uncertainties of the fake/non-prompt lepton background. The uncertainties of the charge misidentification rates include the following contributions: the statistical uncertainty of the likelihood fit to determine the rates ($\approx 15\%$), the changes in rates observed when the mass windows used to define the $Z \rightarrow ee$ and sideband regions are varied from 0 GeV to 20 GeV ($\approx 6\%$), and the differences observed between the results of the likelihood fit and the true rates when the method is applied to simulation ($\approx 5\%$). These uncertainties sum in quadrature to about 20% of the expected charge mis-ID yield in the signal regions. The systematic uncertainty of the fake/non-prompt component is estimated as described above, and impacts the charge mis-ID background through a variation

in the fake/non-prompt background that is subtracted when calculating the charge misidentification rates ($\approx 10\%$). This component of the uncertainty is anti-correlated between the fake/non-prompt and charge mis-ID backgrounds.

Since the optimised selection criteria result in small expected background yields in the signal regions, the dominant uncertainty in the analysis is statistical. Among the systematic uncertainties, the leading contributors are from uncertainties of the fake/non-prompt lepton background estimate, the modelling of the irreducible backgrounds (in terms of both their production cross-sections and acceptance) and uncertainties of the efficiency for identifying b -jets. Summaries of the leading sources of systematic uncertainty in each signal region are provided in Tables 8 and 10 for the total background yield, and in Tables 9 and 11 for representative signal models (a T vector-like quark with $m_T = 1$ TeV, and exclusive $t\bar{t}$ production with $m_V = 2$ TeV, respectively).

Table 8: Uncertainty of the total background yields in the signal regions for the four-top-quark and VLQ searches due to the leading sources of systematic uncertainty.

Uncertainty source	SR1 $b2\ell$ [%]	SR2 $b2\ell$ [%]	SR3 $b2\ell_L$ [%]	SR3 $b2\ell$ [%]	SR1 $b3\ell$ [%]	SR2 $b3\ell$ [%]	SR3 $b3\ell_L$ [%]	SR3 $b3\ell$ [%]
Jet energy resolution	3	1	5	6	3	5	3	4
Jet energy scale	3	3	9	6	3	5	11	6
b -tagging efficiency	5	3	6	7	3	4	9	9
Lepton ID efficiency	2	1	1	1	3	3	2	3
Pile-up reweighting	5	2	3	3	3	5	1	6
Luminosity	1	1	2	2	2	2	2	2
Fake/non-prompt	20	12	13	8	7	2	3	1
Charge mis-ID	2	3	1	2	-	-	-	-
Cross-section \times acceptance	25	13	22	32	32	26	21	24

Table 9: Uncertainty of the event yields in the signal regions for a representative signal (vector-like T quark, $m_T = 1$ TeV) due to the leading sources of experimental systematic uncertainty. The expected yield for this signal in each region is also given.

Uncertainty source	SR1 $b2\ell$ [%]	SR2 $b2\ell$ [%]	SR3 $b2\ell_L$ [%]	SR3 $b2\ell$ [%]	SR1 $b3\ell$ [%]	SR2 $b3\ell$ [%]	SR3 $b3\ell_L$ [%]	SR3 $b3\ell$ [%]
Jet energy resolution	< 1	1	6	4	< 1	< 1	24	< 1
Jet energy scale	2	1	23	3	1	1	12	< 1
b -tagging efficiency	6	3	9	8	5	4	7	8
Lepton ID efficiency	2	2	1	2	3	3	2	3
Luminosity	2	2	2	2	2	2	2	2
Pile-up reweighting	3	3	7	3	< 1	< 1	3	2
Expected yield	1.7	2.1	0.08	1.0	3.0	3.2	0.03	1.8

Table 10: Uncertainty of the total background yields in the signal regions for the same-sign top-quark pair production search due to the leading sources of systematic uncertainty.

Source	SR $ttee$ [%]	SR $tte\mu$ [%]	SR $tt\mu\mu$ [%]
Jet energy resolution	3	< 1	13
Jet energy scale	2	2	9
b -tagging efficiency	1	2	3
Lepton ID efficiency	< 1	1	4
Pile-up reweighting	2	2	4
Luminosity	< 1	1	2
Fake/non-prompt	36	17	5
Charge mis-ID	12	5	-
Cross-section \times acceptance	10	15	25

Table 11: Uncertainty of the event yields in the signal regions for a representative signal of the same-sign top-quark pair production search (exclusive $t\bar{t}$ production, $m_V = 2$ TeV normalised to 100 fb) due to the leading sources of experimental systematic uncertainty. In all three channels, the uncertainty due to jet energy resolution is compatible with the statistical uncertainty of the simulated samples.

Source	SR $ttee$ [%]	SR $tte\mu$ [%]	SR $tt\mu\mu$ [%]
Jet energy resolution	7	< 1	< 1
Jet energy scale	1	1	< 1
b -tagging efficiency	3	2	< 1
Lepton ID efficiency	5	3	4
Luminosity	2	2	2
Pile-up reweighting	3	< 1	1
Expected yield	3.4	13	12

10 Results

To test for the presence of a BSM signal, the observed numbers of events in a set of signal regions are compared with the expected background yields in those regions. The searches for VLQ and four-top-quark production use the combination of the signal regions defined in Table 2, while the searches for $t\bar{t}$ production use the combination of the signal regions defined in Table 4. In the case where the SM four-top-quark production is probed, this process is removed from the background contribution. In all other cases, the quoted significances refer to BSM benchmarks.

A Poisson likelihood ratio test is used to assess the probability that the observed yields are compatible with the sum of the expected background and signal, with the nominal signal cross-section scaled by a value μ . Systematic uncertainties are introduced as nuisance parameters that have Gaussian or log-normal constraints corresponding to their uncertainty values. For any given choice of μ the likelihood ratio q_μ is compared with the distribution of values that would be expected under the background-only and signal plus background hypotheses. The probabilities $p_b(\mu)$ of the background fluctuating to be more signal-like than the data, and $p_{s+b}(\mu)$ of the signal plus background fluctuating to be more background-like than the data are both by comparing q_μ with these distributions. The values of $p_b(\mu)$ and $p_{s+b}(\mu)$ are derived using the asymptotic approximation described in Ref. [59]. The quantity R_{CL_s} [60] is then defined as

$$R_{\text{CL}_s}(\mu) \equiv \frac{p_{s+b}(\mu)}{1 - p_b(\mu)}.$$

If the data are statistically consistent with the background expectation, $R_{\text{CL}_s}(\mu)$ will tend to decrease as μ increases. All values of μ for which $R_{\text{CL}_s}(\mu)$ is less than 0.05 are considered as being excluded at 95% confidence level (CL). If, for a particular signal model, $R_{\text{CL}_s}(\mu = 1)$ is less than 0.05, that model is excluded.

The observed yields in each of the signal regions, along with the expected yields from background sources and some representative BSM physics models are shown in Tables 12 and 13 and in Figure 7. There are no statistically significant differences between the event yields and the expected background, although in two of the signal regions, SR3 $b2\ell_L$ and SR3 $b3\ell_L$, the event yield exceeds the background by 1.7 and 1.8 standard deviations, respectively. The resulting combined significance depends on the signal being considered, reaching 3.0 standard deviations for SM four-top-quark production (where this contribution is not included among the backgrounds), while a significance of 0.9 standard deviations is expected. More than half of the excess is observed in events with two muons, three b -tagged jets and H_T around 700 GeV. The largest significance for any of the BSM models considered is 2.3 standard deviations, which is obtained for the 2HDM model. Therefore no evidence of BSM signals is found, and limits are set as detailed below.

Several studies were done to validate the background estimate. One potential issue was noted when applying the matrix method for muons to the same sample of events used to calculate the fake/non-prompt muon efficiency, where the predicted yield was observed to deviate from data at the level of 1.2 standard deviations near $\Delta R(\mu, \text{jet}) = 1.0$. Applying a two-dimensional parameterisation of the efficiencies in $p_{T,\mu} \times \Delta R(\mu, \text{jet})$ substantially improves the level of agreement, and the background in the signal regions was recomputed with this parameterisation. In addition, the prompt- and fake-lepton efficiencies used in the estimation of the fake/non-prompt lepton background were recomputed using different requirements for the number of b -tagged jets in the control regions (this test is especially important for electrons, where the fraction of candidates arising from photon conversion versus heavy-flavour decay varies strongly with the

presence or absence of a b -tagged jet), and also using a completely different set of control regions (dilepton events where a tag-and-probe procedure was applied). The fake/non-prompt lepton background was also estimated using the fake-factor method [61] instead of the matrix method. The level of compatibility between the expected background and observed data yields was similar in all of these variations.

Further, the events in the signal regions were scrutinised to determine if some of them might have arisen from detector defects or other anomalies. The distribution of objects in η , ϕ , and p_T was found to be consistent with expectations, as was the temporal distribution of the events across the data-taking period. The reconstructed muon candidates in these events were inspected, and their features (such as the χ^2 of their fitted tracks, and compatibility of the momenta measured in the inner detector and the muon spectrometer) were found to be unremarkable. The three-lepton samples were split between those with and without a lepton pair that formed a Z -boson candidate. In the subsample with a Z -boson candidate, four events are observed with an expected background of 2.4 ± 0.6 , while in the subsample without a Z -boson candidate, five events are observed with an expected background of 1.7 ± 0.6 . The composition of b -tagged jets (the fractions of such jets that arise from b -, c -, or light-quarks or gluons) was studied in simulated background events. It was found that the dominant source of b -tagged jets in both the signal and validation regions was in fact b -jets, which accounted for 76 – 95% of the b -tagged jets in each region. In addition, the kinematic properties of the events were compared with the expectations from the BSM four-top-quark production benchmark models, and found to agree poorly with all of them, particularly in the b -tagged jet multiplicity.

Table 12: Expected background and observed event yields in the signal regions for the vector-like quark and four-top-quark searches. The ‘Other bkg’ category contains contributions from all rare SM processes listed in Section 6. The first uncertainty is statistical and the second is systematic. The BSM significance is the number of standard deviations by which a BSM signal plus background hypothesis is preferred to the background-only hypothesis. Since this significance depends only on the event yield and expected background in the given signal region, it is independent of the BSM model. When computing the SM $t\bar{t}t\bar{t}$ significance, the expected SM $t\bar{t}t\bar{t}$ yield is not included in the expected background. Both significances are calculated using the same procedure used to calculate the reported limits.

Source	SR1b2 ℓ	SR2b2 ℓ	SR3b2 ℓ _L	SR3b2 ℓ
$t\bar{t}W$	$2.04 \pm 0.14 \pm 0.49$	$2.68 \pm 0.15 \pm 0.55$	$0.95 \pm 0.11 \pm 0.31$	$0.40 \pm 0.06 \pm 0.10$
$t\bar{t}Z$	$0.58 \pm 0.08 \pm 0.10$	$0.95 \pm 0.11 \pm 0.17$	$0.72 \pm 0.11 \pm 0.19$	$0.11 \pm 0.05 \pm^{+0.13}_{-0.10}$
Dibosons	$3.2 \pm 1.5 \pm 2.4$	< 0.5	$0.13 \pm 0.13 \pm^{+0.27}_{-0.00}$	< 0.5
$t\bar{t}H$	$0.56 \pm 0.07 \pm 0.07$	$0.57 \pm 0.10 \pm 0.09$	$0.91 \pm 0.11 \pm 0.22$	$0.19 \pm 0.05 \pm 0.07$
$t\bar{t}t\bar{t}$	$0.10 \pm 0.01 \pm 0.05$	$0.44 \pm 0.03 \pm 0.23$	$1.46 \pm 0.05 \pm 0.74$	$0.75 \pm 0.04 \pm 0.38$
Other bkg	$0.52 \pm 0.07 \pm 0.14$	$0.68 \pm 0.09 \pm 0.24$	$0.47 \pm 0.08 \pm 0.18$	$0.20 \pm 0.04 \pm 0.06$
Fake/non-prompt	$4.1 \pm^{+1.6}_{-1.4} \pm 2.4$	$2.5 \pm^{+1.0}_{-0.9} \pm 1.1$	$1.2 \pm^{+0.9}_{-0.7} \pm 0.6$	$0.20 \pm^{+0.46}_{-0.20} \pm 0.16$
Charge mis-ID	$1.17 \pm 0.10 \pm 0.27$	$1.29 \pm 0.10 \pm 0.28$	$0.32 \pm 0.04 \pm 0.09$	$0.21 \pm 0.04 \pm 0.04$
Total bkg	$12.3 \pm^{+2.2}_{-2.1} \pm 3.4$	$9.1 \pm^{+1.2}_{-1.1} \pm 1.2$	$6.2 \pm^{+1.0}_{-0.8} \pm 1.2$	$2.0 \pm^{+0.5}_{-0.2} \pm 0.3$
Data yield	14	10	12	4
BSM significance	0.31	0.25	1.7	1.1
SM $t\bar{t}t\bar{t}$ significance	0.33	0.38	2.1	1.6
Source	SR1b3 ℓ	SR2b3 ℓ	SR3b3 ℓ _L	SR3b3 ℓ
$t\bar{t}W$	$0.66 \pm 0.08 \pm 0.20$	$0.38 \pm 0.05 \pm 0.11$	$0.21 \pm 0.05 \pm 0.09$	$0.15 \pm 0.04 \pm 0.05$
$t\bar{t}Z$	$2.66 \pm 0.15 \pm 0.43$	$1.90 \pm 0.14 \pm 0.42$	$2.80 \pm 0.17 \pm 0.58$	$1.47 \pm 0.14 \pm 0.28$
Dibosons	$2.3 \pm 0.7 \pm 1.7$	$0.22 \pm 0.16 \pm 0.27$	< 0.5	< 0.5
$t\bar{t}H$	$0.30 \pm 0.04 \pm 0.04$	$0.28 \pm 0.05 \pm 0.05$	$0.38 \pm 0.06 \pm 0.07$	$0.10 \pm 0.03 \pm 0.02$
$t\bar{t}t\bar{t}$	$0.06 \pm 0.01 \pm 0.03$	$0.13 \pm 0.02 \pm 0.06$	$0.58 \pm 0.04 \pm 0.29$	$0.59 \pm 0.03 \pm 0.30$
Other bkg.	$1.37 \pm 0.13 \pm 0.45$	$0.65 \pm 0.10 \pm 0.27$	$0.17 \pm 0.09 \pm 0.10$	$0.31 \pm 0.07 \pm 0.11$
Fake/non-prompt	$1.0 \pm^{+0.6}_{-0.5} \pm 0.6$	$0.14 \pm^{+0.31}_{-0.12} \pm 0.09$	$0.00 \pm^{+0.38}_{-0.00} \pm^{+0.09}_{-0.00}$	$0.03 \pm^{+0.15}_{-0.02} \pm 0.00$
Total bkg	$8.3 \pm^{+0.9}_{-0.8} \pm 1.8$	$3.7 \pm^{+0.6}_{-0.3} \pm 0.4$	$4.2 \pm^{+0.4}_{-0.2} \pm 0.7$	$2.7 \pm 0.2 \pm 0.5$
Data yield	8	4	9	3
BSM significance	-0.09	0.14	1.8	0.19
SM $t\bar{t}t\bar{t}$ significance	-0.07	0.21	2.1	0.6

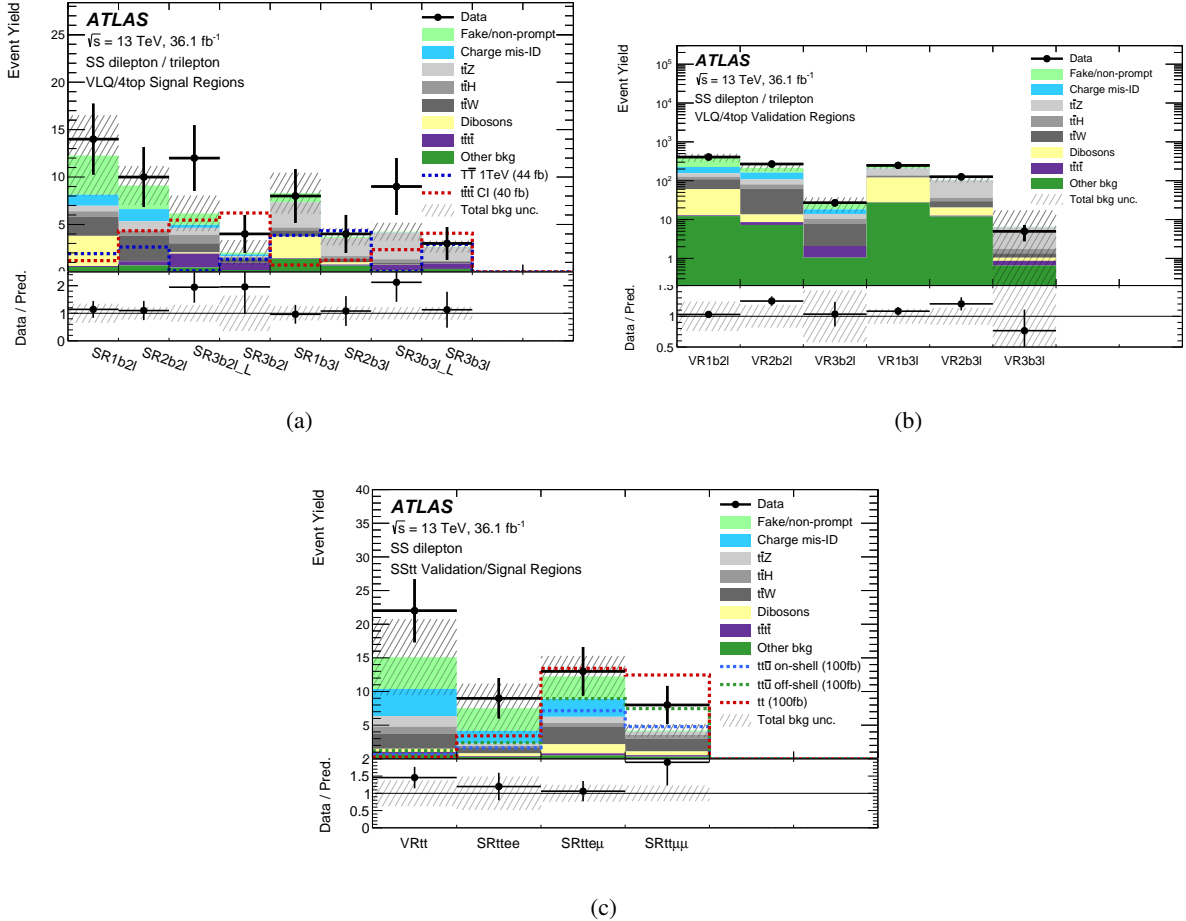


Figure 7: Predicted background and observed data in (a) the signal regions and (b) validation regions for the vector-like quark and SM four-top-quark searches, and (c) in the signal and validation regions for the same-sign top-quark pair production search, along with the predicted yields for typical signals. The uncertainty, shown as the hashed region, includes both the statistical and systematic uncertainties from each background source.

Table 13: Expected background and observed event yields in the signal regions for the same-sign top-quark pair production search. The ‘Other bkg’ category includes contributions from all rare SM processes listed in Section 6. The first uncertainty is statistical and the second is systematic. The significance is the number of standard deviations by which the $t\bar{t}$ signal plus background hypothesis is preferred to the background-only hypothesis. It is calculated using the same procedure used to calculate the reported limits.

Source	SR $ttee$	SR $tte\mu$	SR $tt\mu\mu$
$t\bar{t}W$	$0.91 \pm 0.09 \pm 0.19$	$2.64 \pm 0.15 \pm 0.48$	$1.86 \pm 0.13 \pm 0.37$
$t\bar{t}Z$	$0.35 \pm 0.07 \pm 0.09$	$0.91 \pm 0.09 \pm 0.12$	$0.47 \pm 0.08 \pm 0.09$
Dibosons	$0.40 \pm 0.45 \pm 0.09$	$1.4 \pm 0.6 \pm 0.9$	$0.5 \pm 0.5 \pm 0.5$
$t\bar{t}H$	$0.19 \pm 0.06 \pm 0.02$	$0.53 \pm 0.08 \pm 0.08$	$0.58 \pm 0.07 \pm 0.05$
$t\bar{t}t\bar{t}$	$0.12 \pm 0.02 \pm 0.06$	$0.30 \pm 0.02 \pm 0.15$	$0.22 \pm 0.03 \pm 0.11$
Other bkg	$0.29 \pm 0.06 \pm 0.13$	$0.51 \pm 0.08 \pm 0.16$	$0.33 \pm 0.08 \pm 0.12$
Fake/non-prompt	$3.4 \begin{array}{l} +2.1 \\ -1.7 \end{array} \pm 2.5$	$3.3 \begin{array}{l} +1.2 \\ -1.1 \end{array} \pm 2.1$	$0.20 \begin{array}{l} +0.24 \\ -0.20 \end{array} \pm 0.18$
Charge mis-ID	$1.90 \pm 0.11 \pm 0.91$	$2.69 \pm 0.14 \pm 0.59$	N/A
Total bkg.	$7.5 \begin{array}{l} +2.2 \\ -1.8 \end{array} \pm 2.7$	$12.2 \pm 1.3 \pm 2.5$	$4.2 \begin{array}{l} +0.6 \\ -0.6 \end{array} \pm 0.7$
Data yield	9	13	8
Significance	0.31	0.16	1.44

Limits on B - and T -quark pair production are set in two scenarios. In the first, it is assumed that the branching ratios are given by the singlet model of Ref. [2]. These branching ratios vary slightly with the VLQ mass; they are approximately $(0.48, 0.27, 0.25)$ for $B \rightarrow (Wt, Zb, Hb)$ and $(0.49, 0.22, 0.27)$ for $T \rightarrow (Wb, Zt, Ht)$. The resulting 95% CL upper limits on the production cross-section as a function of the VLQ mass are shown in Figure 8. Lower limits on the B - and T -quark masses are extracted from these cross-section limits, resulting in observed (expected) excluded mass $m_B < 1.00$ TeV (1.01 TeV) and $m_T < 0.98$ TeV (0.99 TeV). The expected and observed limits agree well in spite of the observed excesses in some signal regions because the expected yield of VLQ in those regions is small. In the second scenario, no assumptions are made about the branching ratio, and lower limits on the masses are determined for any possible set of branching ratios, as shown in Figure 9.

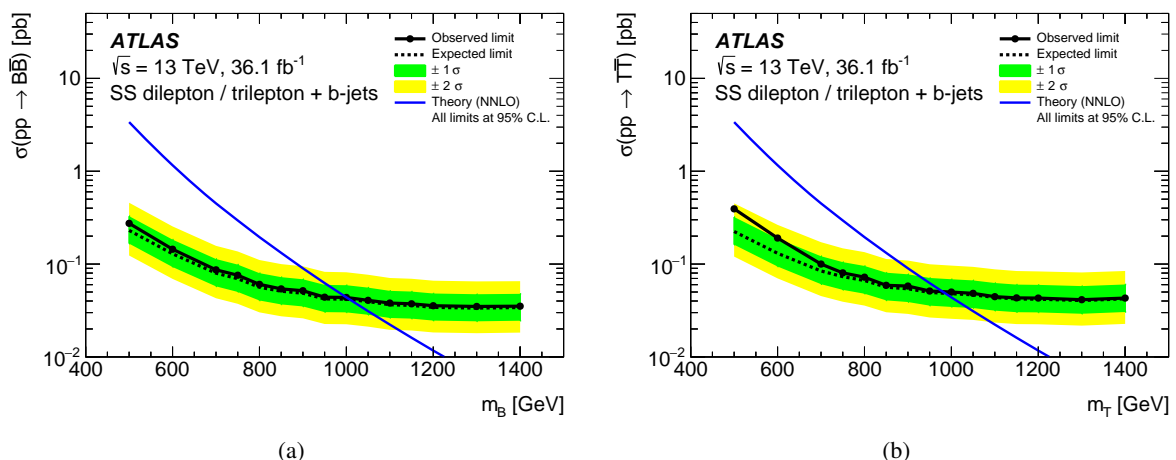


Figure 8: Expected and observed limits on (a) vector-like B - and (b) T -quark pair production as a function of mass, assuming the branching ratios expected in the singlet model. The expected 95% CL limits are shown as a continuous line with their ± 1 and ± 2 standard deviation bands, and the NNLO theory prediction is shown as a continuous line.

Since a single $T_{5/3}$ quark could decay into a same-charge lepton pair, limits on both single and pair production of $T_{5/3}$ quarks are set. If only pair production is considered, then the cross-section limit as a function of mass is unambiguous since the only allowed decay channel is $T_{5/3} \rightarrow Wt$, as shown in Figure 10(a). The corresponding lower observed (expected) limit on the $T_{5/3}$ -quark mass is 1.19 TeV (1.21 TeV). If single production is considered in addition to pair production, the limit depends on the assumed strength of the $T_{5/3}tW$ coupling, as shown in Figure 10(b).

Limits on four-top-quark production are set in a variety of models. The observed (expected) limit on the cross-section assuming SM kinematics is 69 fb (29 fb), and the observed (expected) limit assuming kinematics from the EFT model is 39 fb (21 fb). These results are summarised in Table 14, along with the limits on the ratio of the contact interaction strength to the cut-off scale in the EFT model. The latter limit can also be expressed in the plane of the interaction strength $|C_{4t}|$ versus cut-off scale Λ , as shown in Figure 11(a). Limits on the 2UED/RPP model are shown in Figures 11(b) and 11(c). The 2UED/RPP limits corresponds to an observed lower limit on the parameter m_{KK} of 1.45 TeV, where a limit of 1.48 TeV is expected in the background-only model. Limits on four-top-quark production in the 2HDM interpretation are shown in Figure 12. Two scenarios are considered: one where only the heavy scalar Higgs boson contributes to the process $pp \rightarrow t\bar{t}H$ and $H \rightarrow t\bar{t}$, and one where the heavy scalar

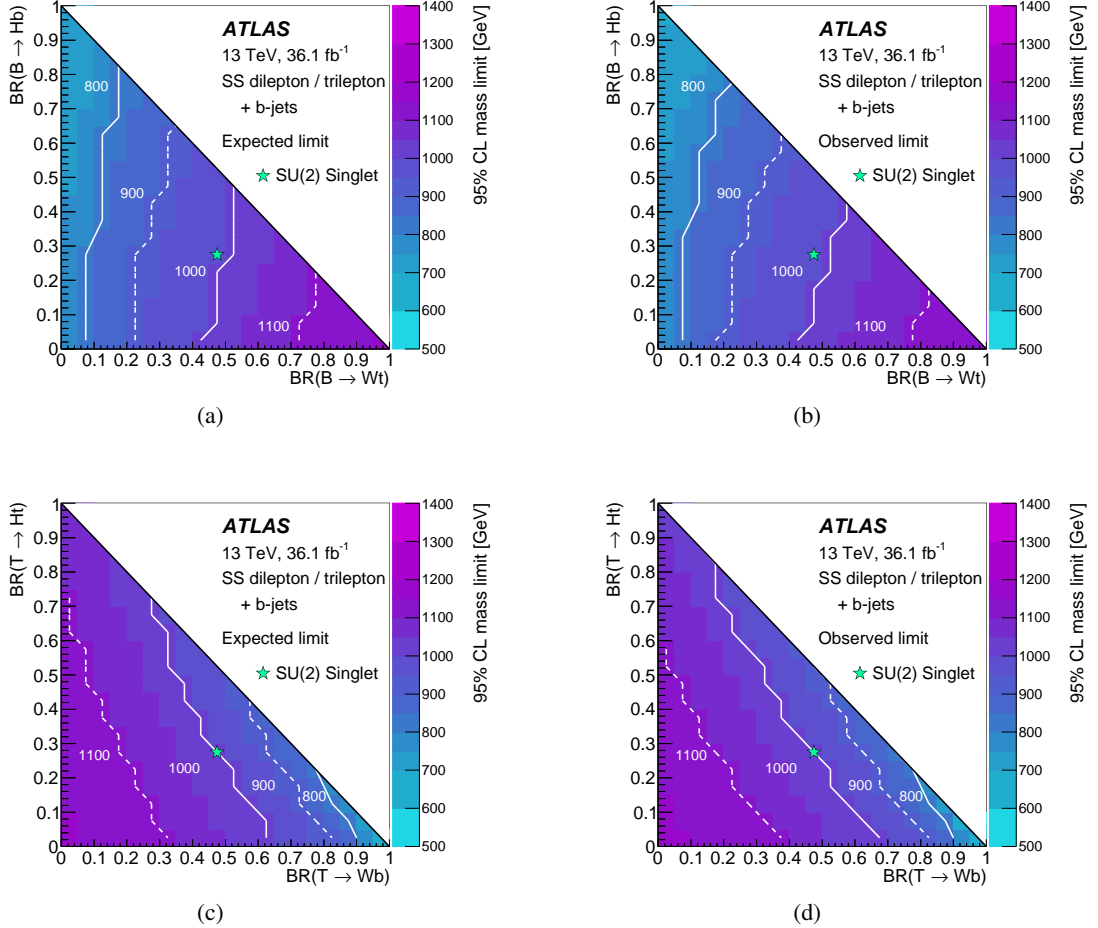


Figure 9: Mass hypotheses excluded at 95% CL as a function of the branching ratio: (a) expected and (b) observed limits for a vector-like B -quark, (c) expected and (d) observed limits for a vector-like T -quark. Contours of constant 95% CL lower mass limits are shown in white in each plot, and labelled with the mass limit in GeV. The star represents the branching ratios for the SU(2) singlet models of Ref. [2].

and pseudo-scalar Higgs bosons have equal masses and both contribute to the four-top-quark production. Limits are computed and compared with theoretical predictions at partial NNLO in QCD [62–64].

Table 14: Expected and observed 95% CL upper limits on the four-top-quark production cross-section in various models.

Observable	Expected median with 1σ range	Observed
SM cross-section [fb]	$29.0^{+12.2}_{-8.1}$	69.2
CI cross-section [fb]	$20.8^{+12.2}_{-8.1}$	38.6
CI coupling $ C_{4t} /\Lambda^2$ (TeV $^{-2}$)	$1.9^{+1.2}_{-0.7}$	2.6

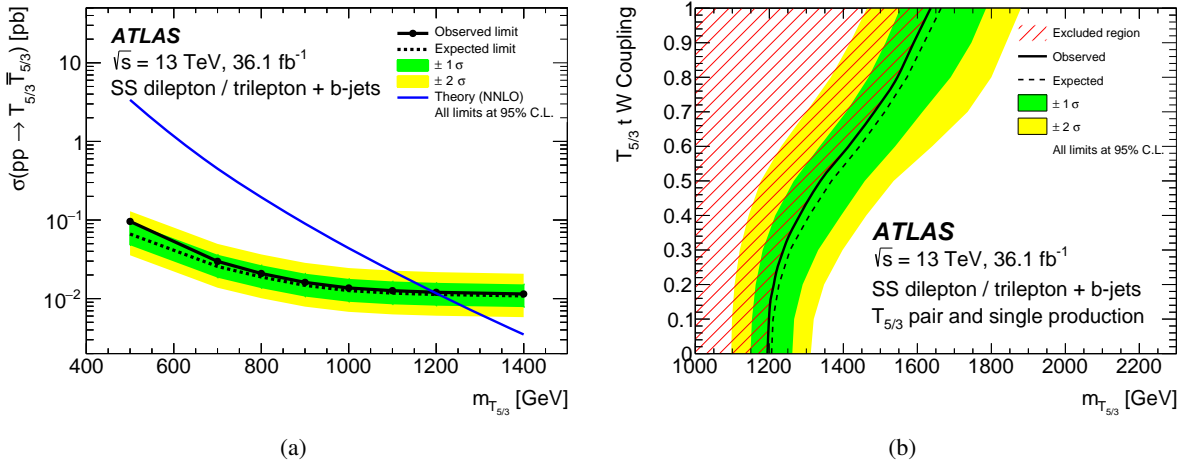


Figure 10: (a) Expected and observed limits on vector-like $T_{5/3}$ pair production as a function of mass. The NNLO theory prediction is shown as the continuous line. (b) Expected and observed limits on vector-like $T_{5/3}$ single- plus pair-production as a function of mass and $T_{5/3}tW$ coupling. In both plots, the expected 95% CL limits are shown with their ± 1 and ± 2 standard deviation bands and it is assumed that the branching ratio $\mathcal{B}(T_{5/3} \rightarrow Wt) = 100\%$.

Limits on same-sign top-quark pair production are set using the signal regions dedicated to this signature (SR $ttee$, SR $tt\mu\mu$, and SR $t\tau\mu\mu$). These are interpreted in the context of a dark-matter model with three parameters: the mass of the exotic FCNC mediator particle m_V , and the couplings g_{DM} and g_{SM} of the mediator to dark-matter and SM particles, respectively. In the context of this model, three different same-sign top-quark pair production processes are considered: *i*) production via a t -channel mediator, *ii*) production via an on-shell s -channel mediator, and *iii*) production via an off-shell s -channel mediator. Limits on the production cross-section for each mechanism as a function of m_V are shown in Figure 13. They are independent of the model parameter values and constrain generic processes such as $uu \rightarrow tt$ to a cross-section of less than 89 fb, where a limit of 59 fb is expected in the background-only model. More generally, the total signal includes the three contributions with a relative importance which depends on the mediator's total width, and thus on the model parameters. Limits in the plane of g_{SM} versus m_V for three values of g_{DM} are shown in Figure 14 where the width effects are taken into account. As a reference, the observed upper limit on g_{SM} is 0.31 when m_V is taken to be 3 TeV and g_{DM} is taken to be one, where a limit of 0.28 is expected in the background-only hypothesis. Assuming that $m_V = 1$ TeV and $g_{\text{DM}} = 1$, the observed (expected) upper limit on g_{SM} is 0.14 (0.13).

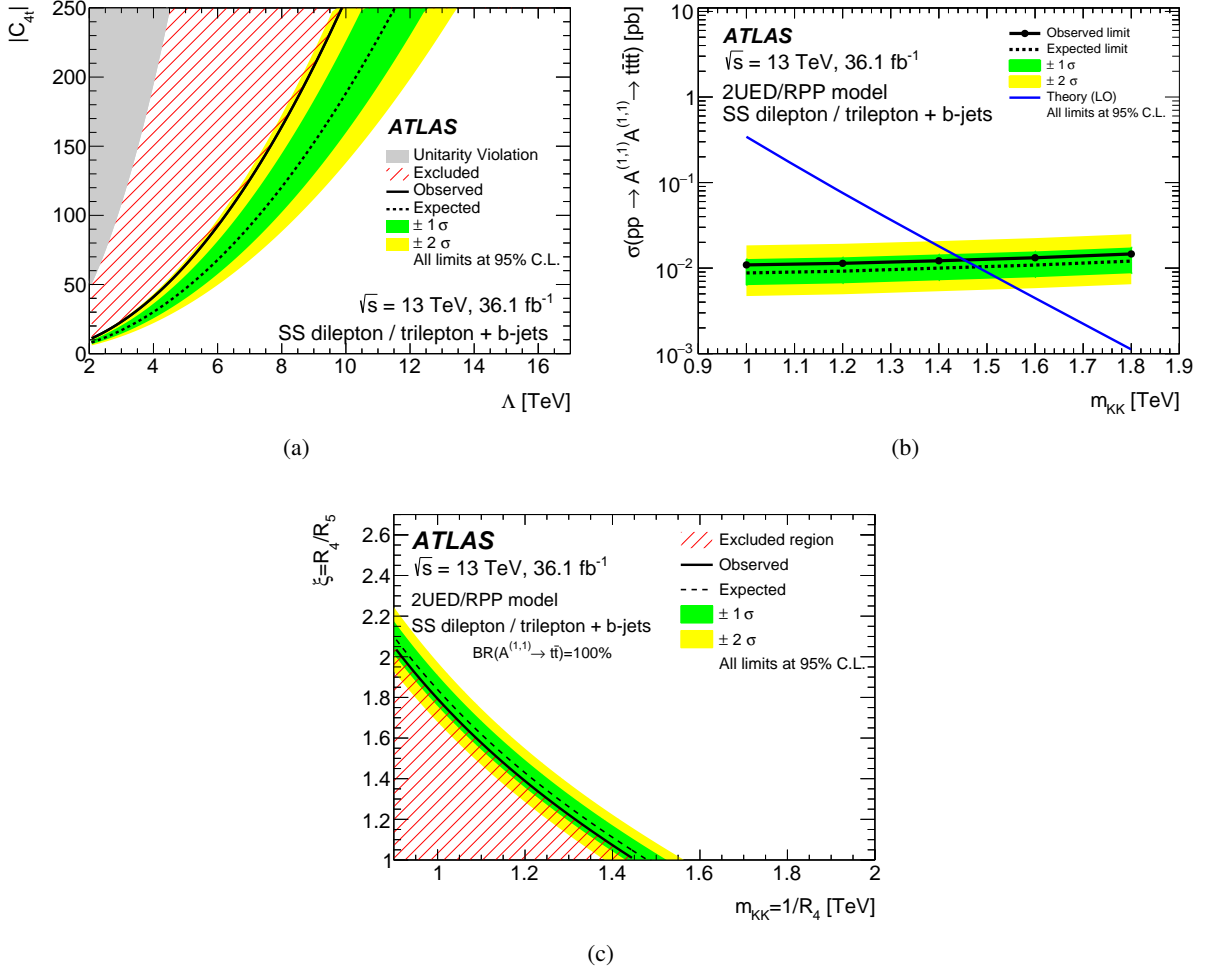


Figure 11: (a) Constraints in the $(|C_{4t}|, \Lambda)$ plane (black line), and (b) expected and observed limits on m_{KK} in the symmetric case. The theory line corresponds to the production of four top quarks by tier (1, 1) assuming the branching ratio $\mathcal{B}(A^{(1,1)} \rightarrow t\bar{t}) = 100\%$. (c) Expected and observed limit in the $(m_{KK} = 1/R_4, \xi = R_4/R_5)$ plane for the 2UED/RPP model. In all plots, the expected 95% CL limits are shown with their ± 1 and ± 2 standard deviation bands.

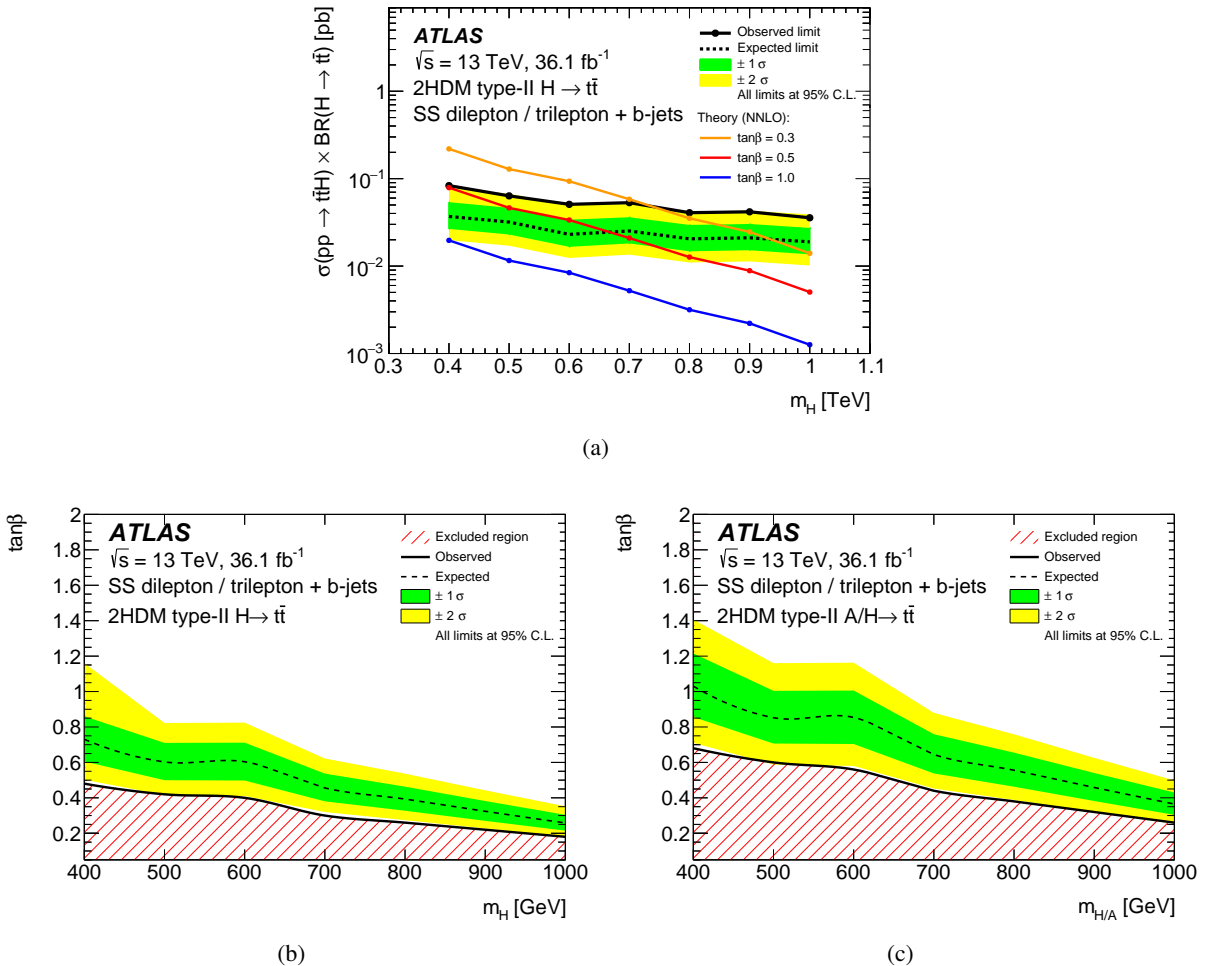


Figure 12: Limits on the two-Higgs-doublet model interpretation. (a) Limits on the cross-section of the four-top-quark production through a heavy scalar Higgs boson times the branching ratio for the Higgs boson to decay into $t\bar{t}$. Theoretical predictions for three values of $\tan\beta$ are shown. (b) Limits on four-top-quark production through a heavy scalar Higgs boson in the plane (m_H , $\tan\beta$). (c) Limits on four-top-quark production considering both a heavy pseudo-scalar and a scalar Higgs boson having the same mass $m_{H/A}$ in the plane ($m_{H/A}$, $\tan\beta$). In all plots, the expected 95% CL limits are shown with their ± 1 and ± 2 standard deviation bands. In the context of the two-Higgs-doublet model, the Higgs boson width can be large for low $\tan\beta$. In spite of that, it was checked that the signal efficiency has a negligible dependence on $\tan\beta$ in the region of interest.

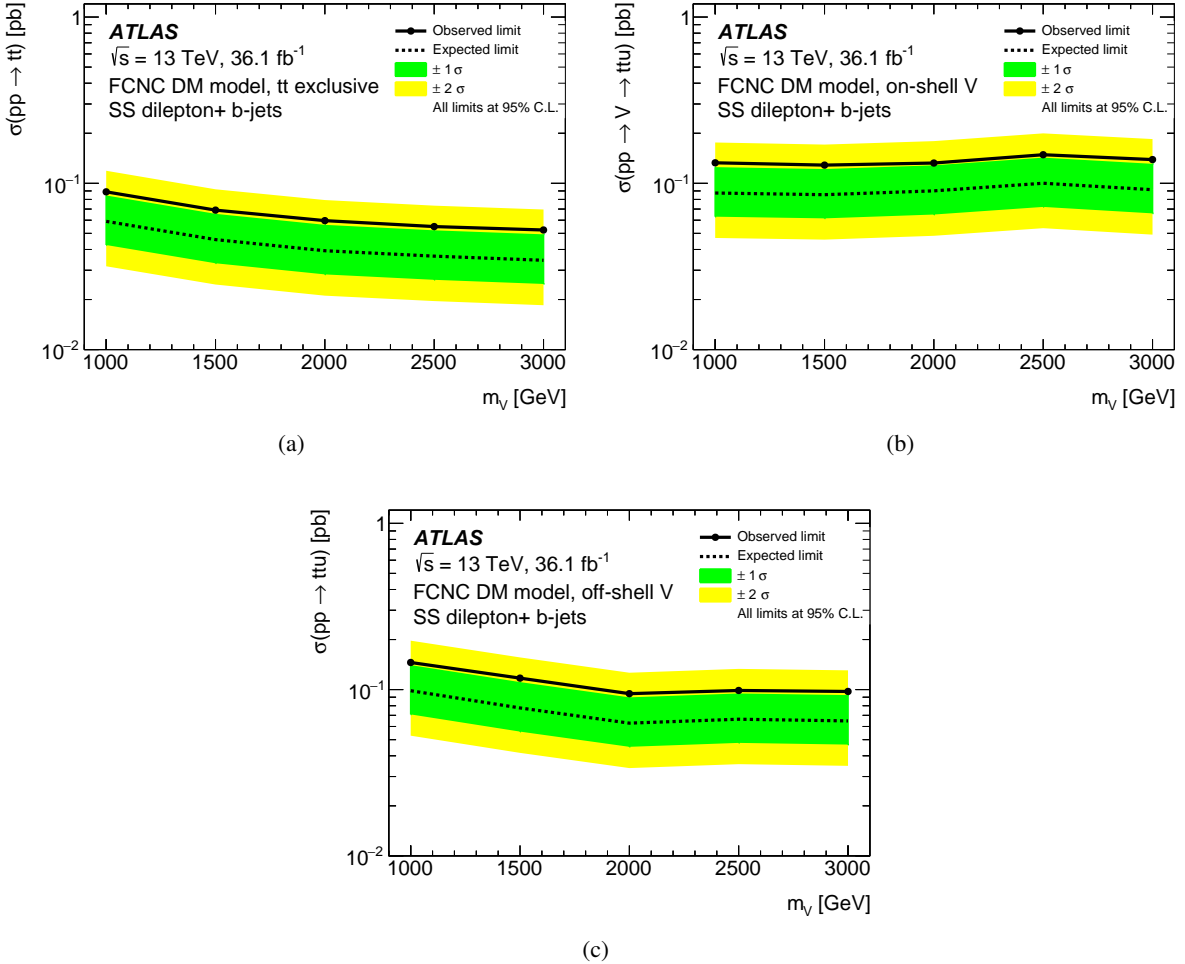


Figure 13: Expected and observed 95% CL upper limits on the cross-section for (a) prompt $t\bar{t}$ production, (b) on-shell mediator, (c) off-shell mediator subprocesses of the same-sign top-quark pair production. In all plots, the expected 95% CL limits are shown with their ± 1 and ± 2 standard deviation bands. Each subprocess is considered as a generic BSM signature and therefore no theory prediction is shown.

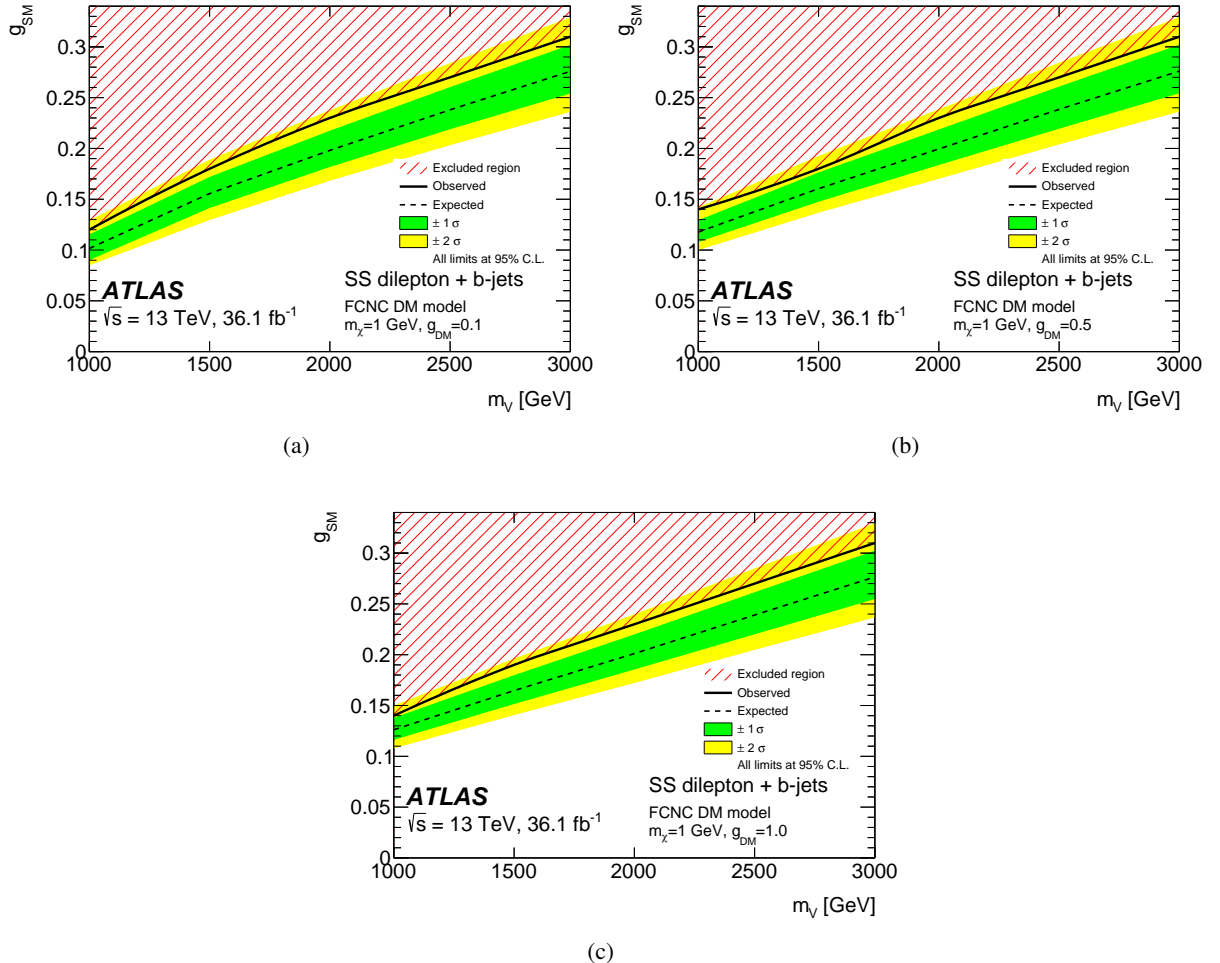


Figure 14: Expected and observed constraints in the (g_{SM}, m_V) plane for the combined visible same-sign top-quark pair production, (a) $g_{\text{DM}} = 0.1$, (b) $g_{\text{DM}} = 0.5$, (c) $g_{\text{DM}} = 1$. In all plots, the expected 95% CL limits are shown with their ± 1 and ± 2 standard deviation bands. The mediator width effects are taken into account for every value of the model parameters.

11 Conclusion

A search for processes beyond the Standard Model is performed using 36.1 fb^{-1} of proton–proton collisions at $\sqrt{s} = 13 \text{ TeV}$ recorded by the ATLAS detector at the LHC, based on events with at least two leptons, including a pair of the same electric charge, at least one b -tagged jet, sizeable missing transverse momentum, and large H_T . Several BSM processes are considered that could enhance the yield of such events over the small expected background. The search is performed in the context of BSM models, with signal regions defined for different models. No significant excess over the expected background is observed. The regions of parameter space excluded by the data are quantified by setting limits at 95% confidence level. The masses of vector-like T - and B -quarks are (expected to be) constrained to $m_T > 0.98 \text{ TeV}$ (0.99 TeV), $m_B > 1.00 \text{ TeV}$ (1.01 TeV) assuming branching ratios of the W , Z , and H decay modes as predicted by a singlet model, and the mass of the vector-like $T_{5/3}$ quark is (expected to be) constrained to $m_{T_{5/3}} > 1.19 \text{ TeV}$ (1.21 TeV) based only on pair production and assuming a branching ratio $\mathcal{B}(T_{5/3} \rightarrow Wt) = 100\%$. With single $T_{5/3}$ production included, the observed (expected) lower mass limit is 1.6 TeV (1.7 TeV) for a $T_{5/3}tW$ coupling of 1.0 . The four-top-quark production cross-section is (expected to be) less than 69 fb (29 fb) assuming SM kinematics and less than 39 fb (21 fb) assuming kinematics from EFT model. The lower limit on the Kaluza–Klein mass in the context of models with two universal extra dimensions, is (expected to be) 1.45 TeV (1.48 TeV). Finally, limits are set on a dark-matter model based on a flavour changing neutral current producing a pair of top quarks with the same electric charge. The $uu \rightarrow tt$ cross-section is (expected to be) lower than 89 fb (59 fb) for a FCNC mediator mass of 1 TeV . Considering a full dark-matter model with a dark-sector coupling $g_{\text{DM}} = 1$, the observed (expected) excluded values for the coupling to SM particles are $g_{\text{SM}} > 0.31$ (0.28) for a mediator mass of $m_V = 3 \text{ TeV}$, and $g_{\text{SM}} > 0.14$ (0.13) for $m_V = 1 \text{ TeV}$.

Acknowledgements

We thank CERN for the very successful operation of the LHC, as well as the support staff from our institutions without whom ATLAS could not be operated efficiently.

We acknowledge the support of ANPCyT, Argentina; YerPhI, Armenia; ARC, Australia; BMWFW and FWF, Austria; ANAS, Azerbaijan; SSTC, Belarus; CNPq and FAPESP, Brazil; NSERC, NRC and CFI, Canada; CERN; CONICYT, Chile; CAS, MOST and NSFC, China; COLCIENCIAS, Colombia; MSMT CR, MPO CR and VSC CR, Czech Republic; DNRF and DNSRC, Denmark; IN2P3-CNRS, CEA-DRF/IRFU, France; SRNSFG, Georgia; BMBF, HGF, and MPG, Germany; GSRT, Greece; RGC, Hong Kong SAR, China; ISF, I-CORE and Benoziyo Center, Israel; INFN, Italy; MEXT and JSPS, Japan; CNRST, Morocco; NWO, Netherlands; RCN, Norway; MNiSW and NCN, Poland; FCT, Portugal; MNE/IFA, Romania; MES of Russia and NRC KI, Russian Federation; JINR; MESTD, Serbia; MSSR, Slovakia; ARRS and MIZŠ, Slovenia; DST/NRF, South Africa; MINECO, Spain; SRC and Wallenberg Foundation, Sweden; SERI, SNSF and Cantons of Bern and Geneva, Switzerland; MOST, Taiwan; TAEK, Turkey; STFC, United Kingdom; DOE and NSF, United States of America. In addition, individual groups and members have received support from BCKDF, the Canada Council, CANARIE, CRC, Compute Canada, FQRNT, and the Ontario Innovation Trust, Canada; EPLANET, ERC, ERDF, FP7, Horizon 2020 and Marie Skłodowska-Curie Actions, European Union; Investissements d’Avenir Labex and Idex, ANR, Région Auvergne and Fondation Partager le Savoir, France; DFG and AvH Foundation, Germany; Herakleitos, Thales and Aristeia programmes co-financed by EU-ESF and the Greek NSRF; BSF, GIF and

Minerva, Israel; BRF, Norway; CERCA Programme Generalitat de Catalunya, Generalitat Valenciana, Spain; the Royal Society and Leverhulme Trust, United Kingdom.

The crucial computing support from all WLCG partners is acknowledged gratefully, in particular from CERN, the ATLAS Tier-1 facilities at TRIUMF (Canada), NDGF (Denmark, Norway, Sweden), CC-IN2P3 (France), KIT/GridKA (Germany), INFN-CNAF (Italy), NL-T1 (Netherlands), PIC (Spain), ASGC (Taiwan), RAL (UK) and BNL (USA), the Tier-2 facilities worldwide and large non-WLCG resource providers. Major contributors of computing resources are listed in Ref. [65].

References

- [1] ATLAS Collaboration, *Analysis of events with b -jets and a pair of leptons of the same charge in pp collisions at $\sqrt{s} = 8$ TeV with the ATLAS detector*, *JHEP* **10** (2015) 150, arXiv: [1504.04605 \[hep-ex\]](#).
- [2] J. A. Aguilar-Saavedra, *Identifying top partners at LHC*, *JHEP* **11** (2009) 030, arXiv: [0907.3155 \[hep-ph\]](#).
- [3] ATLAS Collaboration, *Search for supersymmetry in final states with two same-sign or three leptons and jets using 36 fb^{-1} of $\sqrt{s} = 13$ TeV pp collision data with the ATLAS detector*, *JHEP* **09** (2017) 084, arXiv: [1706.03731 \[hep-ex\]](#).
- [4] CMS Collaboration, *Search for physics beyond the standard model in events with two leptons of same sign, missing transverse momentum, and jets in proton-proton collisions at $\sqrt{s} = 13$ TeV*, *Eur. Phys. J. C* **77** (2017) 578, arXiv: [1704.07323 \[hep-ex\]](#).
- [5] CMS Collaboration, *Search for top quark partners with charge $5/3$ in proton-proton collisions at $\sqrt{s} = 13$ TeV*, *JHEP* **08** (2017) 073, arXiv: [1705.10967 \[hep-ex\]](#).
- [6] CMS Collaboration, *Search for standard model production of four top quarks with same-sign and multilepton final states in proton-proton collisions at $\sqrt{s} = 13$ TeV*, *Eur. Phys. J. C* **78** (2018) 140, arXiv: [1710.10614 \[hep-ex\]](#).
- [7] F. del Aguila and M. J. Bowick, *The possibility of new fermions with $\Delta I = 0$ mass*, *Nucl. Phys. V* **224** (1983) 107.
- [8] B. A. Dobrescu and C. T. Hill, *Electroweak Symmetry Breaking via a Top Condensation Seesaw Mechanism*, *Phys. Rev. Lett.* **81** (1998) 2634, arXiv: [hep-ph/9712319](#).
- [9] C. T. Hill and E. H. Simmons, *Strong dynamics and electroweak symmetry breaking*, *Phys. Rept.* **381** (2003) 235, arXiv: [hep-ph/0203079](#).
- [10] K. Agashe, R. Contino and A. Pomarol, *The minimal composite Higgs model*, *Nucl. Phys. B* **719** (2005) 165, arXiv: [hep-ph/0412089](#).
- [11] C. Anastasiou, E. Furlan and J. Santiago, *Realistic composite Higgs models*, *Phys. Rev. D* **79** (2009) 075003, arXiv: [0901.2117](#).
- [12] A. Davidson and K. C. Wali, *Family mass hierarchy from universal seesaw mechanism*, *Phys. Rev. Lett.* **60** (1988) 1813.
- [13] K. S. Babu and R. N. Mohapatra, *Solution to the strong CP problem without an axion*, *Phys. Rev. D* **41** (1990) 1286.
- [14] N. Arkani-Hamed, A. Cohen, E. Katz and A. Nelson, *The Littlest Higgs*, *JHEP* **07** (2002) 034, arXiv: [hep-ph/0206021](#).
- [15] M. Schmaltz and D. Tucker-Smith, *Little Higgs Theories*, *Ann. Rev. Nucl. Part. Sci.* **55** (2005) 229, arXiv: [hep-ph/0502182](#).
- [16] S. Matsumoto, T. Moroi and K. Tobe, *Testing the littlest Higgs model with T parity at the CERN Large Hadron Collider*, *Phys. Rev. D* **78** (2008) 055018, arXiv: [0806.3837 \[hep-ph\]](#).

- [17] R. Contino and G. Servant,
Discovering the top partners at the LHC using same-sign dilepton final states,
JHEP **06** (2008) 026, arXiv: [0801.1679 \[hep-ph\]](#).
- [18] K. Kong, M. McCaskey and G. W. Wilson,
Multi-lepton signals from the top-prime quark at the LHC, **JHEP** **04** (2012) 079,
arXiv: [1112.3041 \[hep-ph\]](#).
- [19] J. Alwall et al., *The automated computation of tree-level and next-to-leading order differential cross sections, and their matching to parton shower simulations*, **JHEP** **07** (2014) 079,
arXiv: [1405.0301 \[hep-ph\]](#).
- [20] H. Georgi, L. Kaplan, D. Morin and A. Schenk, *Effects of top quark compositeness*,
Phys. Rev. D **51** (7 1995) 3888.
- [21] G. Cacciapaglia, A. Deandrea and J. Llodra-Perez,
A dark matter candidate from Lorentz invariance in 6D, **JHEP** **03** (2010) 083,
arXiv: [0907.4993 \[hep-ph\]](#).
- [22] G. Cacciapaglia et al., *Four tops on the real projective plane at LHC*, **JHEP** **10** (2011) 042,
arXiv: [1107.4616 \[hep-ph\]](#).
- [23] A. Arbey, G. Cacciapaglia, A. Deandrea and B. Kubik, *Dark Matter in a twisted bottle*,
JHEP **01** (2013) 147, arXiv: [1210.0384 \[hep-ph\]](#).
- [24] G. C. Branco et al., *Theory and phenomenology of two-Higgs-doublet models*,
Phys. Rept. **516** (2012) 1, arXiv: [1106.0034 \[hep-ph\]](#).
- [25] P. S. Bhupal Dev and A. Pilaftsis,
Maximally symmetric two Higgs doublet model with natural standard model alignment,
JHEP **12** (2014) 024, [Erratum: **JHEP**11,147(2015)], arXiv: [1408.3405 \[hep-ph\]](#).
- [26] ATLAS Collaboration, *Search for heavy Higgs bosons A/H decaying to a top quark pair in pp collisions at $\sqrt{s} = 8$ TeV with the ATLAS detector*, **Phys. Rev. Lett.** **119** (2017) 191803,
arXiv: [1707.06025 \[hep-ex\]](#).
- [27] I. Boucheneb, G. Cacciapaglia, A. Deandrea and B. Fuks,
Revisiting monotop production at the LHC, **JHEP** **01** (2015) 017.
- [28] CMS Collaboration, *Search for dark matter in events with energetic, hadronically decaying top quarks and missing transverse momentum at $\sqrt{s} = 13$ TeV*, **JHEP** **06** (2018) 027,
arXiv: [1801.08427 \[hep-ex\]](#).
- [29] ATLAS Collaboration, *The ATLAS Experiment at the CERN Large Hadron Collider*,
JINST **3** (2008) S08003.
- [30] ATLAS Collaboration, *ATLAS Insertable B-Layer Technical Design Report*,
CERN-LHCC-2010-013. ATLAS-TDR-19 (2010),
URL: <https://cds.cern.ch/record/1291633>.
- [31] ATLAS Collaboration, *Performance of the ATLAS trigger system in 2015*,
Eur. Phys. J. C **77** (2017) 317, arXiv: [1611.09661 \[hep-ex\]](#).
- [32] ATLAS Collaboration,
Luminosity determination in pp collisions at $\sqrt{s} = 8$ TeV using the ATLAS detector at the LHC,
Eur. Phys. J. C **76** (2016) 653, arXiv: [1608.03953 \[hep-ex\]](#).

- [33] ATLAS Collaboration, *Electron identification measurements in ATLAS using $\sqrt{s} = 13$ TeV data with 50 ns bunch spacing*, ATL-PHYS-PUB-2015-041 (2015), URL: <https://cds.cern.ch/record/2048202>.
- [34] ATLAS Collaboration, *Muon reconstruction performance of the ATLAS detector in proton–proton collision data at $\sqrt{s} = 13$ TeV*, *Eur. Phys. J. C* **76** (2016) 292, arXiv: [1603.05598 \[hep-ex\]](#).
- [35] M. Cacciari, G. P. Salam and G. Soyez, *The anti- k_t jet clustering algorithm*, *JHEP* **04** (2008) 063, arXiv: [0802.1189 \[hep-ph\]](#).
- [36] ATLAS Collaboration, *Selection of jets produced in 13 TeV proton–proton collisions with the ATLAS detector*, ATLAS-CONF-2015-029, 2015, URL: <https://cds.cern.ch/record/2037702>.
- [37] ATLAS Collaboration, *Tagging and suppression of pileup jets with the ATLAS detector*, ATLAS-CONF-2014-018, 2014, URL: <https://cds.cern.ch/record/1700870>.
- [38] ATLAS Collaboration, *Performance of b-jet identification in the ATLAS experiment*, *JINST* **11** (2016) P04008, arXiv: [1512.01094 \[hep-ex\]](#).
- [39] ATLAS Collaboration, *Performance of missing transverse momentum reconstruction with the ATLAS detector using proton-proton collisions at $\sqrt{s} = 13$ TeV*, (2018), arXiv: [1802.08168 \[hep-ex\]](#).
- [40] D. J. Lange, *The EvtGen particle decay simulation package*, *Nucl. Instrum. Meth. A* **462** (2001) 152.
- [41] T. Gleisberg, S. Höche, F. Krauss, M. Schönher, S. Schumann et al., *Event generation with SHERPA 1.1*, *JHEP* **02** (2009) 007, arXiv: [0811.4622 \[hep-ph\]](#).
- [42] ATLAS Collaboration, *ATLAS Pythia 8 tunes to 7 TeV data*, ATL-PHYS-PUB-2014-021, 2014, URL: <https://cds.cern.ch/record/1966419>.
- [43] T. Sjöstrand et al., *An introduction to PYTHIA 8.2*, *Comput. Phys. Commun.* **191** (2015) 159, arXiv: [1410.3012 \[hep-ph\]](#).
- [44] M. Chala, J. Juknevich, G. Perez and J. Santiago, *The elusive gluon*, *JHEP* **01** (2015) 092, arXiv: [1411.1771 \[hep-ph\]](#).
- [45] R. D. Ball et al., *Parton distributions with LHC data*, *Nucl. Phys. B* **867** (2013) 244, arXiv: [1207.1303 \[hep-ph\]](#).
- [46] T. Sjostrand, S. Mrenna and P. Z. Skands, *PYTHIA 6.4 physics and manual*, *JHEP* **05** (2006) 026, arXiv: [hep-ph/0603175](#).
- [47] J. Pumplin et al., *New Generation of Parton Distributions with Uncertainties from Global QCD Analysis*, *JHEP* **07** (2002) 012, arXiv: [hep-ph/0201195](#).
- [48] P. Z. Skands, *Tuning Monte Carlo generators: The Perugia tunes*, *Phys. Rev. D* **82** (2010) 074018, arXiv: [1005.3457](#).
- [49] T. Gleisberg and S. Höche, *Comix, a new matrix element generator*, *JHEP* **12** (2008) 039, arXiv: [0808.3674 \[hep-ph\]](#).
- [50] S. Schumann and F. Krauss, *A Parton shower algorithm based on Catani-Seymour dipole factorisation*, *JHEP* **03** (2008) 038, arXiv: [0709.1027 \[hep-ph\]](#).

- [51] S. Höche, F. Krauss, M. Schönherr and F. Siegert, *QCD matrix elements + parton showers. The NLO case*, JHEP **04** (2013) 027, arXiv: [1207.5030 \[hep-ph\]](#).
- [52] S. Höche, F. Krauss, S. Schumann and F. Siegert, *QCD matrix elements and truncated showers*, JHEP **05** (2009) 053, arXiv: [0903.1219 \[hep-ph\]](#).
- [53] S. Agostinelli et al., *GEANT4 – A simulation toolkit*, Nucl. Instrum. Meth. A **506** (2003) 250.
- [54] ATLAS Collaboration, *The ATLAS Simulation Infrastructure*, Eur. Phys. J. C **70** (2010) 823, arXiv: [1005.4568 \[physics.ins-det\]](#).
- [55] ATLAS Collaboration, *The simulation principle and performance of the ATLAS fast calorimeter simulation FastCaloSim*, ATL-PHYS-PUB-2010-013, 2010, URL: <https://cds.cern.ch/record/1300517>.
- [56] D0 Collaboration, *Extraction of the width of the W boson from measurements of $\sigma(p\bar{p} \rightarrow W + X) \times B(W \rightarrow e\nu)$ and $\sigma(p\bar{p} \rightarrow Z + X) \times B(Z \rightarrow ee)$ and their ratio*, Phys. Rev. D **61** (2000) 072001, arXiv: [hep-ex/9906025](#).
- [57] ATLAS Collaboration, *Estimation of non-prompt and fake lepton backgrounds in final states with top quarks produced in proton–proton collisions at $\sqrt{s} = 8$ TeV with the ATLAS Detector*, ATLAS-CONF-2014-058, 2014, URL: <https://cds.cern.ch/record/1951336>.
- [58] ATLAS Collaboration, *Jet Calibration and Systematic Uncertainties for Jets Reconstructed in the ATLAS Detector at $\sqrt{s} = 13$ TeV*, ATL-PHYS-PUB-2015-015, 2015, URL: <https://cds.cern.ch/record/2037613>.
- [59] G. Cowan, K. Cranmer, E. Gross and O. Vitells, *Asymptotic formulae for likelihood-based tests of new physics*, Eur. Phys. J. C **71** (2011) 1554, [Erratum: Eur. Phys. J. C **73** (2013) 2501], arXiv: [1007.1727 \[physics.data-an\]](#).
- [60] A. L. Read, *Presentation of search results: The CL_s technique*, J. Phys. G **28** (2002) 2693.
- [61] ATLAS Collaboration, *Search for anomalous production of prompt same-sign lepton pairs and pair-produced doubly charged Higgs bosons with $\sqrt{s} = 8$ TeV pp collisions using the ATLAS detector*, JHEP **03** (2015) 041, arXiv: [1412.0237 \[hep-ex\]](#).
- [62] D. Eriksson, J. Rathsman and O. Stal, *2HDMC: two-Higgs-doublet model calculator*, Comput. Phys. Commun. **181** (2010) 189, arXiv: [0902.0851 \[hep-ph\]](#).
- [63] R. V. Harlander, S. Liebler and H. Mantler, *SusHi: A program for the calculation of Higgs production in gluon fusion and bottom-quark annihilation in the Standard Model and the MSSM*, Comput. Phys. Commun. **184** (2013) 1605, arXiv: [1212.3249 \[hep-ph\]](#).
- [64] R. V. Harlander, S. Liebler and H. Mantler, *SusHi Bento: Beyond NNLO and the heavy-top limit*, Comput. Phys. Commun. **212** (2017) 239, arXiv: [1605.03190 \[hep-ph\]](#).
- [65] ATLAS Collaboration, *ATLAS Computing Acknowledgements*, ATL-GEN-PUB-2016-002, URL: <https://cds.cern.ch/record/2202407>.

The ATLAS Collaboration

M. Aaboud^{34d}, G. Aad⁹⁹, B. Abbott¹²⁴, O. Abdinov^{13,*}, B. Abelos¹²⁸, D.K. Abhayasinghe⁹¹, S.H. Abidi¹⁶⁴, O.S. AbouZeid³⁹, N.L. Abraham¹⁵³, H. Abramowicz¹⁵⁸, H. Abreu¹⁵⁷, Y. Abulaiti⁶, B.S. Acharya^{64a,64b,n}, S. Adachi¹⁶⁰, L. Adamczyk^{81a}, J. Adelman¹¹⁹, M. Adersberger¹¹², A. Adiguzel^{12c,ag}, T. Adye¹⁴¹, A.A. Affolder¹⁴³, Y. Afik¹⁵⁷, C. Agheorghiesei^{27c}, J.A. Aguilar-Saavedra^{136f,136a}, F. Ahmadov^{77,ae}, G. Aielli^{71a,71b}, S. Akatsuka⁸³, T.P.A. Åkesson⁹⁴, E. Akilli⁵², A.V. Akimov¹⁰⁸, G.L. Alberghi^{23b,23a}, J. Albert¹⁷³, P. Albicocco⁴⁹, M.J. Alconada Verzini⁸⁶, S. Alderweireldt¹¹⁷, M. Aleksa³⁵, I.N. Aleksandrov⁷⁷, C. Alexa^{27b}, T. Alexopoulos¹⁰, M. Alhoob¹²⁴, B. Ali¹³⁸, G. Alimonti^{66a}, J. Alison³⁶, S.P. Alkire¹⁴⁵, C. Allaire¹²⁸, B.M.M. Allbrooke¹⁵³, B.W. Allen¹²⁷, P.P. Allport²¹, A. Aloisio^{67a,67b}, A. Alonso³⁹, F. Alonso⁸⁶, C. Alpigiani¹⁴⁵, A.A. Alshehri⁵⁵, M.I. Alstaty⁹⁹, B. Alvarez Gonzalez³⁵, D. Álvarez Piqueras¹⁷¹, M.G. Alvaggi^{67a,67b}, B.T. Amadio¹⁸, Y. Amaral Coutinho^{78b}, L. Ambroz¹³¹, C. Amelung²⁶, D. Amidei¹⁰³, S.P. Amor Dos Santos^{136a,136c}, S. Amoroso⁴⁴, C.S. Amrouche⁵², C. Anastopoulos¹⁴⁶, L.S. Ancu⁵², N. Andari²¹, T. Andeen¹¹, C.F. Anders^{59b}, J.K. Anders²⁰, K.J. Anderson³⁶, A. Andreazza^{66a,66b}, V. Andrei^{59a}, C.R. Anelli¹⁷³, S. Angelidakis³⁷, I. Angelozzi¹¹⁸, A. Angerami³⁸, A.V. Anisenkov^{120b,120a}, A. Annovi^{69a}, C. Antel^{59a}, M.T. Anthony¹⁴⁶, M. Antonelli⁴⁹, D.J.A. Antrim¹⁶⁸, F. Anulli^{70a}, M. Aoki⁷⁹, J.A. Aparisi Pozo¹⁷¹, L. Aperio Bella³⁵, G. Arabidze¹⁰⁴, J.P. Araque^{136a}, V. Araujo Ferraz^{78b}, R. Araujo Pereira^{78b}, A.T.H. Arce⁴⁷, R.E. Ardell⁹¹, F.A. Arduh⁸⁶, J-F. Arguin¹⁰⁷, S. Argyropoulos⁷⁵, A.J. Armbruster³⁵, L.J. Armitage⁹⁰, A. Armstrong¹⁶⁸, O. Arnaez¹⁶⁴, H. Arnold¹¹⁸, M. Arratia³¹, O. Arslan²⁴, A. Artamonov^{109,*}, G. Artoni¹³¹, S. Artz⁹⁷, S. Asai¹⁶⁰, N. Asbah⁴⁴, A. Ashkenazi¹⁵⁸, E.M. Asimakopoulou¹⁶⁹, L. Asquith¹⁵³, K. Assamagan²⁹, R. Astalos^{28a}, R.J. Atkin^{32a}, M. Atkinson¹⁷⁰, N.B. Atlay¹⁴⁸, K. Augsten¹³⁸, G. Avolio³⁵, R. Avramidou^{58a}, M.K. Ayoub^{15a}, G. Azuelos^{107,as}, A.E. Baas^{59a}, M.J. Baca²¹, H. Bachacou¹⁴², K. Bachas^{65a,65b}, M. Backes¹³¹, P. Bagnaia^{70a,70b}, M. Bahmani⁸², H. Bahrasemani¹⁴⁹, A.J. Bailey¹⁷¹, J.T. Baines¹⁴¹, M. Bajic³⁹, C. Bakalis¹⁰, O.K. Baker¹⁸⁰, P.J. Bakker¹¹⁸, D. Bakshi Gupta⁹³, E.M. Baldin^{120b,120a}, P. Balek¹⁷⁷, F. Balli¹⁴², W.K. Balunas¹³³, J. Balz⁹⁷, E. Banas⁸², A. Bandyopadhyay²⁴, S. Banerjee^{178,j}, A.A.E. Bannoura¹⁷⁹, L. Barak¹⁵⁸, W.M. Barbe³⁷, E.L. Barberio¹⁰², D. Barberis^{53b,53a}, M. Barbero⁹⁹, T. Barillari¹¹³, M-S. Barisits³⁵, J. Barkeloo¹²⁷, T. Barklow¹⁵⁰, N. Barlow³¹, R. Barnea¹⁵⁷, S.L. Barnes^{58c}, B.M. Barnett¹⁴¹, R.M. Barnett¹⁸, Z. Barnovska-Blenessy^{58a}, A. Baroncelli^{72a}, G. Barone²⁶, A.J. Barr¹³¹, L. Barranco Navarro¹⁷¹, F. Barreiro⁹⁶, J. Barreiro Guimaraes da Costa^{15a}, R. Bartoldus¹⁵⁰, A.E. Barton⁸⁷, P. Bartos^{28a}, A. Basalaev¹³⁴, A. Bassalat¹²⁸, R.L. Bates⁵⁵, S.J. Batista¹⁶⁴, S. Batlamous^{34e}, J.R. Batley³¹, M. Battaglia¹⁴³, M. Bauce^{70a,70b}, F. Bauer¹⁴², K.T. Bauer¹⁶⁸, H.S. Bawa^{150,1}, J.B. Beacham¹²², M.D. Beattie⁸⁷, T. Beau¹³², P.H. Beauchemin¹⁶⁷, P. Bechtle²⁴, H.C. Beck⁵¹, H.P. Beck^{20,q}, K. Becker⁵⁰, M. Becker⁹⁷, C. Becot⁴⁴, A. Beddall^{12d}, A.J. Beddall^{12a}, V.A. Bednyakov⁷⁷, M. Bedognetti¹¹⁸, C.P. Bee¹⁵², T.A. Beermann³⁵, M. Begalli^{78b}, M. Begel²⁹, A. Behera¹⁵², J.K. Behr⁴⁴, A.S. Bell⁹², G. Bella¹⁵⁸, L. Bellagamba^{23b}, A. Bellerive³³, M. Bellomo¹⁵⁷, P. Bellos⁹, K. Belotskiy¹¹⁰, N.L. Belyaev¹¹⁰, O. Benary^{158,*}, D. Benchekroun^{34a}, M. Bender¹¹², N. Benekos¹⁰, Y. Benhammou¹⁵⁸, E. Benhar Noccioli¹⁸⁰, J. Benitez⁷⁵, D.P. Benjamin⁴⁷, M. Benoit⁵², J.R. Bensinger²⁶, S. Bentvelsen¹¹⁸, L. Beresford¹³¹, M. Beretta⁴⁹, D. Berge⁴⁴, E. Bergeaas Kuutmann¹⁶⁹, N. Berger⁵, L.J. Bergsten²⁶, J. Beringer¹⁸, S. Berlendis⁷, N.R. Bernard¹⁰⁰, G. Bernardi¹³², C. Bernius¹⁵⁰, F.U. Bernlochner²⁴, T. Berry⁹¹, P. Berta⁹⁷, C. Bertella^{15a}, G. Bertoli^{43a,43b}, I.A. Bertram⁸⁷, G.J. Besjes³⁹, O. Bessidskaia Bylund^{43a,43b}, M. Bessner⁴⁴, N. Besson¹⁴², A. Bethani⁹⁸, S. Bethke¹¹³, A. Betti²⁴, A.J. Bevan⁹⁰, J. Beyer¹¹³, R.M.B. Bianchi¹³⁵, O. Biebel¹¹², D. Biedermann¹⁹, R. Bielski⁹⁸, K. Bierwagen⁹⁷, N.V. Biesuz^{69a,69b}, M. Biglietti^{72a}, T.R.V. Billoud¹⁰⁷, M. Bindi⁵¹, A. Bingul^{12d}, C. Bini^{70a,70b}, S. Biondi^{23b,23a}, M. Birman¹⁷⁷, T. Bisanz⁵¹, J.P. Biswal¹⁵⁸, C. Bittrich⁴⁶,

D.M. Bjergaard⁴⁷, J.E. Black¹⁵⁰, K.M. Black²⁵, T. Blazek^{28a}, I. Bloch⁴⁴, C. Blocker²⁶, A. Blue⁵⁵, U. Blumenschein⁹⁰, Dr. Blunier^{144a}, G.J. Bobbink¹¹⁸, V.S. Bobrovnikov^{120b,120a}, S.S. Bocchetta⁹⁴, A. Bocci⁴⁷, D. Boerner¹⁷⁹, D. Bogavac¹¹², A.G. Bogdanchikov^{120b,120a}, C. Bohm^{43a}, V. Boisvert⁹¹, P. Bokan^{169,x}, T. Bold^{81a}, A.S. Boldyrev¹¹¹, A.E. Bolz^{59b}, M. Bomben¹³², M. Bona⁹⁰, J.S. Bonilla¹²⁷, M. Boonekamp¹⁴², A. Borisov¹⁴⁰, G. Borissov⁸⁷, J. Bortfeldt³⁵, D. Bortoletto¹³¹, V. Bortolotto^{71a,61b,61c,71b}, D. Boscherini^{23b}, M. Bosman¹⁴, J.D. Bossio Sola³⁰, K. Bouaouda^{34a}, J. Boudreau¹³⁵, E.V. Bouhova-Thacker⁸⁷, D. Boumediene³⁷, C. Bourdarios¹²⁸, S.K. Boutle⁵⁵, A. Boveia¹²², J. Boyd³⁵, I.R. Boyko⁷⁷, A.J. Bozson⁹¹, J. Bracinik²¹, N. Brahimi⁹⁹, A. Brandt⁸, G. Brandt¹⁷⁹, O. Brandt^{59a}, F. Braren⁴⁴, U. Bratzler¹⁶¹, B. Brau¹⁰⁰, J.E. Brau¹²⁷, W.D. Breaden Madden⁵⁵, K. Brendlinger⁴⁴, A.J. Brennan¹⁰², L. Brenner⁴⁴, R. Brenner¹⁶⁹, S. Bressler¹⁷⁷, B. Brickwedde⁹⁷, D.L. Briglin²¹, D. Britton⁵⁵, D. Britzger^{59b}, I. Brock²⁴, R. Brock¹⁰⁴, G. Brooijmans³⁸, T. Brooks⁹¹, W.K. Brooks^{144b}, E. Brost¹¹⁹, J.H. Broughton²¹, P.A. Bruckman de Renstrom⁸², D. Bruncko^{28b}, A. Bruni^{23b}, G. Bruni^{23b}, L.S. Bruni¹¹⁸, S. Bruno^{71a,71b}, B.H. Brunt³¹, M. Bruschi^{23b}, N. Bruscino¹³⁵, P. Bryant³⁶, L. Bryngemark⁴⁴, T. Buanes¹⁷, Q. Buat³⁵, P. Buchholz¹⁴⁸, A.G. Buckley⁵⁵, I.A. Budagov⁷⁷, F. Buehrer⁵⁰, M.K. Bugge¹³⁰, O. Bulekov¹¹⁰, D. Bullock⁸, T.J. Burch¹¹⁹, S. Burdin⁸⁸, C.D. Burgard¹¹⁸, A.M. Burger⁵, B. Burghgrave¹¹⁹, K. Burka⁸², S. Burke¹⁴¹, I. Burmeister⁴⁵, J.T.P. Burr¹³¹, D. Büscher⁵⁰, V. Büscher⁹⁷, E. Buschmann⁵¹, P. Bussey⁵⁵, J.M. Butler²⁵, C.M. Buttar⁵⁵, J.M. Butterworth⁹², P. Butti³⁵, W. Buttinger³⁵, A. Buzatu¹⁵⁵, A.R. Buzykaev^{120b,120a}, G. Cabras^{23b,23a}, S. Cabrera Urbán¹⁷¹, D. Caforio¹³⁸, H. Cai¹⁷⁰, V.M.M. Cairo², O. Cakir^{4a}, N. Calace⁵², P. Calafiura¹⁸, A. Calandri⁹⁹, G. Calderini¹³², P. Calfayan⁶³, G. Callea^{40b,40a}, L.P. Caloba^{78b}, S. Calvente Lopez⁹⁶, D. Calvet³⁷, S. Calvet³⁷, T.P. Calvet¹⁵², M. Calvetti^{69a,69b}, R. Camacho Toro¹³², S. Camarda³⁵, P. Camarri^{71a,71b}, D. Cameron¹³⁰, R. Caminal Armadans¹⁰⁰, C. Camincher³⁵, S. Campana³⁵, M. Campanelli⁹², A. Camplani³⁹, A. Campoverde¹⁴⁸, V. Canale^{67a,67b}, M. Cano Bret^{58c}, J. Cantero¹²⁵, T. Cao¹⁵⁸, Y. Cao¹⁷⁰, M.D.M. Capeans Garrido³⁵, I. Caprini^{27b}, M. Caprini^{27b}, M. Capua^{40b,40a}, R.M. Carbone³⁸, R. Cardarelli^{71a}, F.C. Cardillo⁵⁰, I. Carli¹³⁹, T. Carli³⁵, G. Carlino^{67a}, B.T. Carlson¹³⁵, L. Carminati^{66a,66b}, R.M.D. Carney^{43a,43b}, S. Caron¹¹⁷, E. Carquin^{144b}, S. Carrá^{66a,66b}, G.D. Carrillo-Montoya³⁵, D. Casadei^{32b}, M.P. Casado^{14,f}, A.F. Casha¹⁶⁴, M. Casolino¹⁴, D.W. Casper¹⁶⁸, R. Castelijn¹¹⁸, F.L. Castillo¹⁷¹, V. Castillo Gimenez¹⁷¹, N.F. Castro^{136a,136e}, A. Catinaccio³⁵, J.R. Catmore¹³⁰, A. Cattai³⁵, J. Caudron²⁴, V. Cavaliere²⁹, E. Cavallaro¹⁴, D. Cavalli^{66a}, M. Cavalli-Sforza¹⁴, V. Cavasinni^{69a,69b}, E. Celebi^{12b}, F. Ceradini^{72a,72b}, L. Cerdà Alberich¹⁷¹, A.S. Cerqueira^{78a}, A. Cerri¹⁵³, L. Cerrito^{71a,71b}, F. Cerutti¹⁸, A. Cervelli^{23b,23a}, S.A. Cetin^{12b}, A. Chafaq^{34a}, D. Chakraborty¹¹⁹, S.K. Chan⁵⁷, W.S. Chan¹¹⁸, Y.L. Chan^{61a}, J.D. Chapman³¹, D.G. Charlton²¹, C.C. Chau³³, C.A. Chavez Barajas¹⁵³, S. Che¹²², A. Chegwidden¹⁰⁴, S. Chekanov⁶, S.V. Chekulaev^{165a}, G.A. Chelkov^{77,ar}, M.A. Chelstowska³⁵, C. Chen^{58a}, C.H. Chen⁷⁶, H. Chen²⁹, J. Chen^{58a}, J. Chen³⁸, S. Chen¹³³, S.J. Chen^{15c}, X. Chen^{15b,aq}, Y. Chen⁸⁰, Y-H. Chen⁴⁴, H.C. Cheng¹⁰³, H.J. Cheng^{15d}, A. Cheplakov⁷⁷, E. Cheremushkina¹⁴⁰, R. Cherkaoui El Moursli^{34e}, E. Cheu⁷, K. Cheung⁶², T.J.A. Chevaléria¹⁴², L. Chevalier¹⁴², V. Chiarella⁴⁹, G. Chiarelli^{69a}, G. Chiodini^{65a}, A.S. Chisholm³⁵, A. Chitan^{27b}, I. Chiu¹⁶⁰, Y.H. Chiu¹⁷³, M.V. Chizhov⁷⁷, K. Choi⁶³, A.R. Chomont¹²⁸, S. Chouridou¹⁵⁹, Y.S. Chow¹¹⁸, V. Christodoulou⁹², M.C. Chu^{61a}, J. Chudoba¹³⁷, A.J. Chuinard¹⁰¹, J.J. Chwastowski⁸², L. Chytka¹²⁶, D. Cinca⁴⁵, V. Cindro⁸⁹, I.A. Cioara²⁴, A. Ciocio¹⁸, F. Cirotto^{67a,67b}, Z.H. Citron¹⁷⁷, M. Citterio^{66a}, A. Clark⁵², M.R. Clark³⁸, P.J. Clark⁴⁸, C. Clement^{43a,43b}, Y. Coadou⁹⁹, M. Cobal^{64a,64c}, A. Coccaro^{53b,53a}, J. Cochran⁷⁶, A.E.C. Coimbra¹⁷⁷, L. Colasurdo¹¹⁷, B. Cole³⁸, A.P. Colijn¹¹⁸, J. Collot⁵⁶, P. Conde Muñoz^{136a,136b}, E. Coniavitis⁵⁰, S.H. Connell^{32b}, I.A. Connelly⁹⁸, S. Constantinescu^{27b}, F. Conventi^{67a,at}, A.M. Cooper-Sarkar¹³¹, F. Cormier¹⁷², K.J.R. Cormier¹⁶⁴, M. Corradi^{70a,70b}, E.E. Corrigan⁹⁴, F. Corriveau^{101,ac}, A. Cortes-Gonzalez³⁵, M.J. Costa¹⁷¹, D. Costanzo¹⁴⁶, G. Cottin³¹, G. Cowan⁹¹, B.E. Cox⁹⁸, J. Crane⁹⁸, K. Cranmer¹²¹, S.J. Crawley⁵⁵, R.A. Creager¹³³, G. Cree³³, S. Crépé-Renaudin⁵⁶, F. Crescioli¹³², M. Cristinziani²⁴, V. Croft¹²¹,

G. Crosetti^{40b,40a}, A. Cueto⁹⁶, T. Cuhadar Donszelmann¹⁴⁶, A.R. Cukierman¹⁵⁰, J. Cúth⁹⁷,
 S. Czekierda⁸², P. Czodrowski³⁵, M.J. Da Cunha Sargedas De Sousa^{58b,136b}, C. Da Via⁹⁸,
 W. Dabrowski^{81a}, T. Dado^{28a,x}, S. Dahbi^{34e}, T. Dai¹⁰³, F. Dallaire¹⁰⁷, C. Dallapiccola¹⁰⁰, M. Dam³⁹,
 G. D'amen^{23b,23a}, J. Damp⁹⁷, J.R. Dandoy¹³³, M.F. Daneri³⁰, N.P. Dang^{178,j}, N.D Dann⁹⁸,
 M. Dannerger¹⁷², V. Dao³⁵, G. Darbo^{53b}, S. Darmora⁸, O. Dartsi⁵, A. Dattagupta¹²⁷, T. Daubney⁴⁴,
 S. D'Auria⁵⁵, W. Davey²⁴, C. David⁴⁴, T. Davidek¹³⁹, D.R. Davis⁴⁷, E. Dawe¹⁰², I. Dawson¹⁴⁶, K. De⁸,
 R. De Asmundis^{67a}, A. De Benedetti¹²⁴, M. De Beurs¹¹⁸, S. De Castro^{23b,23a}, S. De Cecco^{70a,70b},
 N. De Groot¹¹⁷, P. de Jong¹¹⁸, H. De la Torre¹⁰⁴, F. De Lorenzi⁷⁶, A. De Maria^{51,s}, D. De Pedis^{70a},
 A. De Salvo^{70a}, U. De Sanctis^{71a,71b}, A. De Santo¹⁵³, K. De Vasconcelos Corga⁹⁹,
 J.B. De Vivie De Regie¹²⁸, C. Debenedetti¹⁴³, D.V. Dedovich⁷⁷, N. Dehghanian³, M. Del Gaudio^{40b,40a},
 J. Del Peso⁹⁶, Y. Delabat Diaz⁴⁴, D. Delgove¹²⁸, F. Deliot¹⁴², C.M. Delitzsch⁷, M. Della Pietra^{67a,67b},
 D. Della Volpe⁵², A. Dell'Acqua³⁵, L. Dell'Asta²⁵, M. Delmastro⁵, C. Delporte¹²⁸, P.A. Delsart⁵⁶,
 D.A. DeMarco¹⁶⁴, S. Demers¹⁸⁰, M. Demichev⁷⁷, S.P. Denisov¹⁴⁰, D. Denysiuk¹¹⁸, L. D'Eramo¹³²,
 D. Derendarz⁸², J.E. Derkaoui^{34d}, F. Derue¹³², P. Dervan⁸⁸, K. Desch²⁴, C. Deterre⁴⁴, K. Dette¹⁶⁴,
 M.R. Devesa³⁰, P.O. Deviveiros³⁵, A. Dewhurst¹⁴¹, S. Dhaliwal²⁶, F.A. Di Bello⁵², A. Di Ciaccio^{71a,71b},
 L. Di Ciaccio⁵, W.K. Di Clemente¹³³, C. Di Donato^{67a,67b}, A. Di Girolamo³⁵, B. Di Micco^{72a,72b},
 R. Di Nardo¹⁰⁰, K.F. Di Petrillo⁵⁷, A. Di Simone⁵⁰, R. Di Sipio¹⁶⁴, D. Di Valentino³³, C. Diaconu⁹⁹,
 M. Diamond¹⁶⁴, F.A. Dias³⁹, T. Dias Do Vale^{136a}, M.A. Diaz^{144a}, J. Dickinson¹⁸, E.B. Diehl¹⁰³,
 J. Dietrich¹⁹, S. Díez Cornell⁴⁴, A. Dimitrievska¹⁸, J. Dingfelder²⁴, F. Dittus³⁵, F. Djama⁹⁹,
 T. Djobava^{156b}, J.I. Djuvsland^{59a}, M.A.B. Do Vale^{78c}, M. Dobre^{27b}, D. Dodsworth²⁶, C. Doglioni⁹⁴,
 J. Dolejsi¹³⁹, Z. Dolezal¹³⁹, M. Donadelli^{78d}, J. Donini³⁷, A. D'onofrio⁹⁰, M. D'Onofrio⁸⁸, J. Dopke¹⁴¹,
 A. Doria^{67a}, M.T. Dova⁸⁶, A.T. Doyle⁵⁵, E. Drechsler⁵¹, E. Dreyer¹⁴⁹, T. Dreyer⁵¹, Y. Du^{58b},
 J. Duarte-Campderros¹⁵⁸, F. Dubinin¹⁰⁸, M. Dubovsky^{28a}, A. Dubreuil⁵², E. Duchovni¹⁷⁷,
 G. Duckeck¹¹², A. Ducourthial¹³², O.A. Ducu^{107,w}, D. Duda¹¹³, A. Dudarev³⁵, A.C. Dudder⁹⁷,
 E.M. Duffield¹⁸, L. Duflot¹²⁸, M. Dührssen³⁵, C. Dülsen¹⁷⁹, M. Dumancic¹⁷⁷, A.E. Dumitriu^{27b,d},
 A.K. Duncan⁵⁵, M. Dunford^{59a}, A. Duperrin⁹⁹, H. Duran Yildiz^{4a}, M. Düren⁵⁴, A. Durglishvili^{156b},
 D. Duschinger⁴⁶, B. Dutta⁴⁴, D. Duvnjak¹, M. Dyndal⁴⁴, S. Dysch⁹⁸, B.S. Dziedzic⁸², C. Eckardt⁴⁴,
 K.M. Ecker¹¹³, R.C. Edgar¹⁰³, T. Eifert³⁵, G. Eigen¹⁷, K. Einsweiler¹⁸, T. Ekelof¹⁶⁹, M. El Kacimi^{34c},
 R. El Kosseifi⁹⁹, V. Ellajosyula⁹⁹, M. Ellert¹⁶⁹, F. Ellinghaus¹⁷⁹, A.A. Elliot⁹⁰, N. Ellis³⁵,
 J. Elmsheuser²⁹, M. Elsing³⁵, D. Emeliyanov¹⁴¹, Y. Enari¹⁶⁰, J.S. Ennis¹⁷⁵, M.B. Epland⁴⁷,
 J. Erdmann⁴⁵, A. Ereditato²⁰, S. Errede¹⁷⁰, M. Escalier¹²⁸, C. Escobar¹⁷¹, O. Estrada Pastor¹⁷¹,
 A.I. Etienne¹⁴², E. Etzion¹⁵⁸, H. Evans⁶³, A. Ezhilov¹³⁴, M. Ezzi^{34e}, F. Fabbri⁵⁵, L. Fabbri^{23b,23a},
 V. Fabiani¹¹⁷, G. Facini⁹², R.M. Faisca Rodrigues Pereira^{136a}, R.M. Fakhrutdinov¹⁴⁰, S. Falciano^{70a},
 P.J. Falke⁵, S. Falke⁵, J. Faltova¹³⁹, Y. Fang^{15a}, M. Fanti^{66a,66b}, A. Farbin⁸, A. Farilla^{72a},
 E.M. Farina^{68a,68b}, T. Farooque¹⁰⁴, S. Farrell¹⁸, S.M. Farrington¹⁷⁵, P. Farthouat³⁵, F. Fassi^{34e},
 P. Fassnacht³⁵, D. Fassouliotis⁹, M. Fucci Giannelli⁴⁸, A. Favareto^{53b,53a}, W.J. Fawcett⁵², L. Fayard¹²⁸,
 O.L. Fedin^{134,o}, W. Fedorko¹⁷², M. Feickert⁴¹, S. Feigl¹³⁰, L. Feligioni⁹⁹, C. Feng^{58b}, E.J. Feng³⁵,
 M. Feng⁴⁷, M.J. Fenton⁵⁵, A.B. Fenyuk¹⁴⁰, L. Feremenga⁸, J. Ferrando⁴⁴, A. Ferrari¹⁶⁹, P. Ferrari¹¹⁸,
 R. Ferrari^{68a}, D.E. Ferreira de Lima^{59b}, A. Ferrer¹⁷¹, D. Ferrere⁵², C. Ferretti¹⁰³, F. Fiedler⁹⁷,
 A. Filipčić⁸⁹, F. Filthaut¹¹⁷, K.D. Finelli²⁵, M.C.N. Fiolhais^{136a,136c,a}, L. Fiorini¹⁷¹, C. Fischer¹⁴,
 W.C. Fisher¹⁰⁴, N. Flaschel⁴⁴, I. Fleck¹⁴⁸, P. Fleischmann¹⁰³, R.R.M. Fletcher¹³³, T. Flick¹⁷⁹,
 B.M. Flierl¹¹², L.M. Flores¹³³, L.R. Flores Castillo^{61a}, N. Fomin¹⁷, G.T. Forcolin⁹⁸, A. Formica¹⁴²,
 F.A. Förster¹⁴, A.C. Forti⁹⁸, A.G. Foster²¹, D. Fournier¹²⁸, H. Fox⁸⁷, S. Fracchia¹⁴⁶, P. Francavilla^{69a,69b},
 M. Franchini^{23b,23a}, S. Franchino^{59a}, D. Francis³⁵, L. Franconi¹³⁰, M. Franklin⁵⁷, M. Frate¹⁶⁸,
 M. Fraternali^{68a,68b}, D. Freeborn⁹², S.M. Fressard-Batraneanu³⁵, B. Freund¹⁰⁷, W.S. Freund^{78b},
 D. Froidevaux³⁵, J.A. Frost¹³¹, C. Fukunaga¹⁶¹, E. Fullana Torregrosa¹⁷¹, T. Fusayasu¹¹⁴, J. Fuster¹⁷¹,
 O. Gabizon¹⁵⁷, A. Gabrielli^{23b,23a}, A. Gabrielli¹⁸, G.P. Gach^{81a}, S. Gadatsch⁵², P. Gadow¹¹³,

G. Gagliardi^{53b,53a}, L.G. Gagnon¹⁰⁷, C. Galea^{27b}, B. Galhardo^{136a,136c}, E.J. Gallas¹³¹, B.J. Gallop¹⁴¹,
 P. Gallus¹³⁸, G. Galster³⁹, R. Gamboa Goni⁹⁰, K.K. Gan¹²², S. Ganguly¹⁷⁷, J. Gao^{58a}, Y. Gao⁸⁸,
 Y.S. Gao^{150,1}, C. García¹⁷¹, J.E. García Navarro¹⁷¹, J.A. García Pascual^{15a}, M. Garcia-Sciveres¹⁸,
 R.W. Gardner³⁶, N. Garelli¹⁵⁰, V. Garonne¹³⁰, K. Gasnikova⁴⁴, A. Gaudiello^{53b,53a}, G. Gaudio^{68a},
 I.L. Gavrilenco¹⁰⁸, A. Gavrilyuk¹⁰⁹, C. Gay¹⁷², G. Gaycken²⁴, E.N. Gazis¹⁰, C.N.P. Gee¹⁴¹, J. Geisen⁵¹,
 M. Geisen⁹⁷, M.P. Geisler^{59a}, K. Gellerstedt^{43a,43b}, C. Gemme^{53b}, M.H. Genest⁵⁶, C. Geng¹⁰³,
 S. Gentile^{70a,70b}, S. George⁹¹, D. Gerbaudo¹⁴, G. Gessner⁴⁵, S. Ghasemi¹⁴⁸, M. Ghasemi Bostanabad¹⁷³,
 M. Ghneimat²⁴, B. Giacobbe^{23b}, S. Giagu^{70a,70b}, N. Giangiacomi^{23b,23a}, P. Giannetti^{69a},
 A. Giannini^{67a,67b}, S.M. Gibson⁹¹, M. Gignac¹⁴³, D. Gillberg³³, G. Gilles¹⁷⁹, D.M. Gingrich^{3,as},
 M.P. Giordani^{64a,64c}, F.M. Giorgi^{23b}, P.F. Giraud¹⁴², P. Giromini⁵⁷, G. Giugliarelli^{64a,64c}, D. Giugni^{66a},
 F. Juli¹³¹, M. Giulini^{59b}, S. Gkaitatzis¹⁵⁹, I. Gkialas^{9,i}, E.L. Gkougkousis¹⁴, P. Gkountoumis¹⁰,
 L.K. Gladilin¹¹¹, C. Glasman⁹⁶, J. Glatzer¹⁴, P.C.F. Glaysher⁴⁴, A. Glazov⁴⁴, M. Goblirsch-Kolb²⁶,
 J. Godlewski⁸², S. Goldfarb¹⁰², T. Golling⁵², D. Golubkov¹⁴⁰, A. Gomes^{136a,136b,136d},
 R. Goncalves Gama^{78a}, R. Gonçalo^{136a}, G. Gonella⁵⁰, L. Gonella²¹, A. Gongadze⁷⁷, F. Gonnella²¹,
 J.L. Gonski⁵⁷, S. González de la Hoz¹⁷¹, S. Gonzalez-Sevilla⁵², L. Goossens³⁵, P.A. Gorbounov¹⁰⁹,
 H.A. Gordon²⁹, B. Gorini³⁵, E. Gorini^{65a,65b}, A. Gorišek⁸⁹, A.T. Goshaw⁴⁷, C. Gössling⁴⁵,
 M.I. Gostkin⁷⁷, C.A. Gottardo²⁴, C.R. Goudet¹²⁸, D. Goujdami^{34c}, A.G. Goussiou¹⁴⁵, N. Govender^{32b,b},
 C. Goy⁵, E. Gozani¹⁵⁷, I. Grabowska-Bold^{81a}, P.O.J. Gradin¹⁶⁹, E.C. Graham⁸⁸, J. Gramling¹⁶⁸,
 E. Gramstad¹³⁰, S. Grancagnolo¹⁹, V. Gratchev¹³⁴, P.M. Gravila^{27f}, F.G. Gravili^{65a,65b}, C. Gray⁵⁵,
 H.M. Gray¹⁸, Z.D. Greenwood^{93,ai}, C. Grefe²⁴, K. Gregersen⁹², I.M. Gregor⁴⁴, P. Grenier¹⁵⁰,
 K. Grevtsov⁴⁴, J. Griffiths⁸, A.A. Grillo¹⁴³, K. Grimm¹⁵⁰, S. Grinstein^{14,y}, Ph. Gris³⁷, J.-F. Grivaz¹²⁸,
 S. Groh⁹⁷, E. Gross¹⁷⁷, J. Grosse-Knetter⁵¹, G.C. Grossi⁹³, Z.J. Grout⁹², C. Grud¹⁰³, A. Grummer¹¹⁶,
 L. Guan¹⁰³, W. Guan¹⁷⁸, J. Guenther³⁵, A. Guerguichon¹²⁸, F. Guescini^{165a}, D. Guest¹⁶⁸, R. Gugel⁵⁰,
 B. Gui¹²², T. Guillemin⁵, S. Guindon³⁵, U. Gul⁵⁵, C. Gumpert³⁵, J. Guo^{58c}, W. Guo¹⁰³, Y. Guo^{58a,r},
 Z. Guo⁹⁹, R. Gupta⁴¹, S. Gurbuz^{12c}, G. Gustavino¹²⁴, B.J. Gutelman¹⁵⁷, P. Gutierrez¹²⁴, C. Gutschow⁹²,
 C. Guyot¹⁴², M.P. Guzik^{81a}, C. Gwenlan¹³¹, C.B. Gwilliam⁸⁸, A. Haas¹²¹, C. Haber¹⁸, H.K. Hadavand⁸,
 N. Haddad^{34e}, A. Hadef^{58a}, S. Hageböck²⁴, M. Hagihara¹⁶⁶, H. Hakobyan^{181,*}, M. Haleem¹⁷⁴,
 J. Haley¹²⁵, G. Halladjian¹⁰⁴, G.D. Hallewell⁹⁹, K. Hamacher¹⁷⁹, P. Hamal¹²⁶, K. Hamano¹⁷³,
 A. Hamilton^{32a}, G.N. Hamity¹⁴⁶, K. Han^{58a,ah}, L. Han^{58a}, S. Han^{15d}, K. Hanagaki^{79,u}, M. Hance¹⁴³,
 D.M. Handl¹¹², B. Haney¹³³, R. Hankache¹³², P. Hanke^{59a}, E. Hansen⁹⁴, J.B. Hansen³⁹, J.D. Hansen³⁹,
 M.C. Hansen²⁴, P.H. Hansen³⁹, K. Hara¹⁶⁶, A.S. Hard¹⁷⁸, T. Harenberg¹⁷⁹, S. Harkusha¹⁰⁵,
 P.F. Harrison¹⁷⁵, N.M. Hartmann¹¹², Y. Hasegawa¹⁴⁷, A. Hasib⁴⁸, S. Hassani¹⁴², S. Haug²⁰,
 R. Hauser¹⁰⁴, L. Hauswald⁴⁶, L.B. Havener³⁸, M. Havranek¹³⁸, C.M. Hawkes²¹, R.J. Hawkings³⁵,
 D. Hayden¹⁰⁴, C. Hayes¹⁵², C.P. Hays¹³¹, J.M. Hays⁹⁰, H.S. Hayward⁸⁸, S.J. Haywood¹⁴¹, M.P. Heath⁴⁸,
 V. Hedberg⁹⁴, L. Heelan⁸, S. Heer²⁴, K.K. Heidegger⁵⁰, J. Heilman³³, S. Heim⁴⁴, T. Heim¹⁸,
 B. Heinemann^{44,an}, J.J. Heinrich¹¹², L. Heinrich¹²¹, C. Heinz⁵⁴, J. Hejbal¹³⁷, L. Helary³⁵, A. Held¹⁷²,
 S. Hellesund¹³⁰, S. Hellman^{43a,43b}, C. Helsens³⁵, R.C.W. Henderson⁸⁷, Y. Heng¹⁷⁸, S. Henkelmann¹⁷²,
 A.M. Henriques Correia³⁵, G.H. Herbert¹⁹, H. Herde²⁶, V. Herget¹⁷⁴, Y. Hernández Jiménez^{32c},
 H. Herr⁹⁷, M.G. Herrmann¹¹², G. Herten⁵⁰, R. Hertenberger¹¹², L. Hervas³⁵, T.C. Herwig¹³³,
 G.G. Hesketh⁹², N.P. Hessey^{165a}, J.W. Hetherly⁴¹, S. Higashino⁷⁹, E. Higón-Rodriguez¹⁷¹,
 K. Hildebrand³⁶, E. Hill¹⁷³, J.C. Hill³¹, K.K. Hill²⁹, K.H. Hiller⁴⁴, S.J. Hillier²¹, M. Hils⁴⁶,
 I. Hinchliffe¹⁸, M. Hirose¹²⁹, D. Hirschbuehl¹⁷⁹, B. Hiti⁸⁹, O. Hladik¹³⁷, D.R. Hlaluku^{32c}, X. Hoad⁴⁸,
 J. Hobbs¹⁵², N. Hod^{165a}, M.C. Hodgkinson¹⁴⁶, A. Hoecker³⁵, M.R. Hoeferkamp¹¹⁶, F. Hoenig¹¹²,
 D. Hohn²⁴, D. Hohov¹²⁸, T.R. Holmes³⁶, M. Holzbock¹¹², M. Homann⁴⁵, S. Honda¹⁶⁶, T. Honda⁷⁹,
 T.M. Hong¹³⁵, A. Hönle¹¹³, B.H. Hooberman¹⁷⁰, W.H. Hopkins¹²⁷, Y. Horii¹¹⁵, P. Horn⁴⁶,
 A.J. Horton¹⁴⁹, L.A. Horyn³⁶, J-Y. Hostachy⁵⁶, A. Hostiuc¹⁴⁵, S. Hou¹⁵⁵, A. Hoummada^{34a},
 J. Howarth⁹⁸, J. Hoya⁸⁶, M. Hrabovsky¹²⁶, J. Hrdinka³⁵, I. Hristova¹⁹, J. Hrvnac¹²⁸, A. Hrynevich¹⁰⁶,

T. Hryna'ova⁵, P.J. Hsu⁶², S.-C. Hsu¹⁴⁵, Q. Hu²⁹, S. Hu^{58c}, Y. Huang^{15a}, Z. Hubacek¹³⁸, F. Hubaut⁹⁹, M. Huebner²⁴, F. Huegging²⁴, T.B. Huffman¹³¹, E.W. Hughes³⁸, M. Huhtinen³⁵, R.F.H. Hunter³³, P. Huo¹⁵², A.M. Hupe³³, N. Huseynov^{77,ae}, J. Huston¹⁰⁴, J. Huth⁵⁷, R. Hyneman¹⁰³, G. Iacobucci⁵², G. Iakovidis²⁹, I. Ibragimov¹⁴⁸, L. Iconomidou-Fayard¹²⁸, Z. Idrissi^{34e}, P. Iengo³⁵, R. Ignazzi³⁹, O. Igonkina^{118,aa}, R. Iguchi¹⁶⁰, T. Iizawa⁵², Y. Ikegami⁷⁹, M. Ikeno⁷⁹, D. Iliadis¹⁵⁹, N. Ilic¹⁵⁰, F. Iltzsche⁴⁶, G. Introzzi^{68a,68b}, M. Iodice^{72a}, K. Iordanidou³⁸, V. Ippolito^{70a,70b}, M.F. Isacson¹⁶⁹, N. Ishijima¹²⁹, M. Ishino¹⁶⁰, M. Ishitsuka¹⁶², W. Islam¹²⁵, C. Issever¹³¹, S. Istin^{12c,am}, F. Ito¹⁶⁶, J.M. Iturbe Ponce^{61a}, R. Iuppa^{73a,73b}, A. Ivina¹⁷⁷, H. Iwasaki⁷⁹, J.M. Izen⁴², V. Izzo^{67a}, P. Jacka¹³⁷, P. Jackson¹, R.M. Jacobs²⁴, V. Jain², G. Jäkel¹⁷⁹, K.B. Jakobi⁹⁷, K. Jakobs⁵⁰, S. Jakobsen⁷⁴, T. Jakoubek¹³⁷, D.O. Jamin¹²⁵, D.K. Jana⁹³, R. Jansky⁵², J. Janssen²⁴, M. Janus⁵¹, P.A. Janus^{81a}, G. Jarlskog⁹⁴, N. Javadov^{77,ae}, T. Javůrek⁵⁰, M. Javurkova⁵⁰, F. Jeanneau¹⁴², L. Jeanty¹⁸, J. Jejelava^{156a,af}, A. Jelinskas¹⁷⁵, P. Jenni^{50,c}, J. Jeong⁴⁴, S. Jézéquel⁵, H. Ji¹⁷⁸, J. Jia¹⁵², H. Jiang⁷⁶, Y. Jiang^{58a}, Z. Jiang^{150,p}, S. Jiggins⁵⁰, F.A. Jimenez Morales³⁷, J. Jimenez Pena¹⁷¹, S. Jin^{15c}, A. Jinaru^{27b}, O. Jinnouchi¹⁶², H. Jivan^{32c}, P. Johansson¹⁴⁶, K.A. Johns⁷, C.A. Johnson⁶³, W.J. Johnson¹⁴⁵, K. Jon-And^{43a,43b}, R.W.L. Jones⁸⁷, S.D. Jones¹⁵³, S. Jones⁷, T.J. Jones⁸⁸, J. Jongmanns^{59a}, P.M. Jorge^{136a,136b}, J. Jovicevic^{165a}, X. Ju¹⁷⁸, J.J. Junggeburth¹¹³, A. Juste Rozas^{14,y}, A. Kaczmarska⁸², M. Kado¹²⁸, H. Kagan¹²², M. Kagan¹⁵⁰, T. Kaji¹⁷⁶, E. Kajomovitz¹⁵⁷, C.W. Kalderon⁹⁴, A. Kaluza⁹⁷, S. Kama⁴¹, A. Kamenshchikov¹⁴⁰, L. Kanjir⁸⁹, Y. Kano¹⁶⁰, V.A. Kantserov¹¹⁰, J. Kanzaki⁷⁹, B. Kaplan¹²¹, L.S. Kaplan¹⁷⁸, D. Kar^{32c}, M.J. Kareem^{165b}, E. Karentzos¹⁰, S.N. Karpov⁷⁷, Z.M. Karpova⁷⁷, V. Kartvelishvili⁸⁷, A.N. Karyukhin¹⁴⁰, K. Kasahara¹⁶⁶, L. Kashif¹⁷⁸, R.D. Kass¹²², A. Kastanas¹⁵¹, Y. Kataoka¹⁶⁰, C. Kato¹⁶⁰, J. Katzy⁴⁴, K. Kawade⁸⁰, K. Kawagoe⁸⁵, T. Kawamoto¹⁶⁰, G. Kawamura⁵¹, E.F. Kay⁸⁸, V.F. Kazanin^{120b,120a}, R. Keeler¹⁷³, R. Kehoe⁴¹, J.S. Keller³³, E. Kellermann⁹⁴, J.J. Kempster²¹, J. Kendrick²¹, O. Kepka¹³⁷, S. Kersten¹⁷⁹, B.P. Kerševan⁸⁹, R.A. Keyes¹⁰¹, M. Khader¹⁷⁰, F. Khalil-Zada¹³, A. Khanov¹²⁵, A.G. Kharlamov^{120b,120a}, T. Kharlamova^{120b,120a}, A. Khodinov¹⁶³, T.J. Khoo⁵², E. Khramov⁷⁷, J. Khubua^{156b}, S. Kido⁸⁰, M. Kiehn⁵², C.R. Kilby⁹¹, S.H. Kim¹⁶⁶, Y.K. Kim³⁶, N. Kimura^{64a,64c}, O.M. Kind¹⁹, B.T. King⁸⁸, D. Kirchmeier⁴⁶, J. Kirk¹⁴¹, A.E. Kiryunin¹¹³, T. Kishimoto¹⁶⁰, D. Kisielewska^{81a}, V. Kitali⁴⁴, O. Kiverny⁵, E. Kladiva^{28b}, T. Klapdor-Kleingrothaus⁵⁰, M.H. Klein¹⁰³, M. Klein⁸⁸, U. Klein⁸⁸, K. Kleinknecht⁹⁷, P. Klimek¹¹⁹, A. Klimentov²⁹, R. Klingenberg^{45,*}, T. Klingl²⁴, T. Klioutchnikova³⁵, F.F. Klitzner¹¹², P. Kluit¹¹⁸, S. Kluth¹¹³, E. Kneringer⁷⁴, E.B.F.G. Knoops⁹⁹, A. Knue⁵⁰, A. Kobayashi¹⁶⁰, D. Kobayashi⁸⁵, T. Kobayashi¹⁶⁰, M. Kobel⁴⁶, M. Kocian¹⁵⁰, P. Kodys¹³⁹, T. Koffas³³, E. Koffeman¹¹⁸, N.M. Köhler¹¹³, T. Koi¹⁵⁰, M. Kolb^{59b}, I. Koletsou⁵, T. Kondo⁷⁹, N. Kondrashova^{58c}, K. Köneke⁵⁰, A.C. König¹¹⁷, T. Kono⁷⁹, R. Konoplich^{121,aj}, V. Konstantinides⁹², N. Konstantinidis⁹², B. Konya⁹⁴, R. Kopeliansky⁶³, S. Koperny^{81a}, K. Korcyl⁸², K. Kordas¹⁵⁹, A. Korn⁹², I. Korolkov¹⁴, E.V. Korolkova¹⁴⁶, O. Kortner¹¹³, S. Kortner¹¹³, T. Kosek¹³⁹, V.V. Kostyukhin²⁴, A. Kotwal⁴⁷, A. Koulouris¹⁰, A. Kourkoumeli-Charalampidi^{68a,68b}, C. Kourkoumelis⁹, E. Kourlitis¹⁴⁶, V. Kouskoura²⁹, A.B. Kowalewska⁸², R. Kowalewski¹⁷³, T.Z. Kowalski^{81a}, C. Kozakai¹⁶⁰, W. Kozanecki¹⁴², A.S. Kozhin¹⁴⁰, V.A. Kramarenko¹¹¹, G. Kramberger⁸⁹, D. Krasnoperovtsev¹¹⁰, M.W. Krasny¹³², A. Krasznahorkay³⁵, D. Krauss¹¹³, J.A. Kremer^{81a}, J. Kretzschmar⁸⁸, P. Krieger¹⁶⁴, K. Krizka¹⁸, K. Kroeninger⁴⁵, H. Kroha¹¹³, J. Kroll¹³⁷, J. Kroll¹³³, J. Krstic¹⁶, U. Kruchonak⁷⁷, H. Krüger²⁴, N. Krumnack⁷⁶, M.C. Kruse⁴⁷, T. Kubota¹⁰², S. Kuday^{4b}, J.T. Kuechler¹⁷⁹, S. Kuehn³⁵, A. Kugel^{59a}, F. Kuger¹⁷⁴, T. Kuhl⁴⁴, V. Kukhtin⁷⁷, R. Kukla⁹⁹, Y. Kulchitsky¹⁰⁵, S. Kuleshov^{144b}, Y.P. Kulinich¹⁷⁰, M. Kuna⁵⁶, T. Kunigo⁸³, A. Kupco¹³⁷, T. Kupfer⁴⁵, O. Kuprash¹⁵⁸, H. Kurashige⁸⁰, L.L. Kurchaninov^{165a}, Y.A. Kurochkin¹⁰⁵, M.G. Kurth^{15d}, E.S. Kuwertz¹⁷³, M. Kuze¹⁶², J. Kvita¹²⁶, T. Kwan¹⁰¹, A. La Rosa¹¹³, J.L. La Rosa Navarro^{78d}, L. La Rotonda^{40b,40a}, F. La Ruffa^{40b,40a}, C. Lacasta¹⁷¹, F. Lacava^{70a,70b}, J. Lacey⁴⁴, D.P.J. Lack⁹⁸, H. Lacker¹⁹, D. Lacour¹³², E. Ladygin⁷⁷, R. Lafaye⁵, B. Laforge¹³², T. Lagouri^{32c}, S. Lai⁵¹, S. Lammers⁶³, W. Lampl⁷, E. Lançon²⁹,

U. Landgraf⁵⁰, M.P.J. Landon⁹⁰, M.C. Lanfermann⁵², V.S. Lang⁴⁴, J.C. Lange¹⁴, R.J. Langenberg³⁵,
 A.J. Lankford¹⁶⁸, F. Lanni²⁹, K. Lantzsch²⁴, A. Lanza^{68a}, A. Lapertosa^{53b,53a}, S. Laplace¹³²,
 J.F. Laporte¹⁴², T. Lari^{66a}, F. Lasagni Manghi^{23b,23a}, M. Lassnig³⁵, T.S. Lau^{61a}, A. Laudrain¹²⁸,
 M. Lavorgna^{67a,67b}, A.T. Law¹⁴³, P. Laycock⁸⁸, M. Lazzaroni^{66a,66b}, B. Le¹⁰², O. Le Dertz¹³²,
 E. Le Guirriec⁹⁹, E.P. Le Quilleuc¹⁴², M. LeBlanc⁷, T. LeCompte⁶, F. Ledroit-Guillon⁵⁶, C.A. Lee²⁹,
 G.R. Lee¹⁴⁴, L. Lee⁵⁷, S.C. Lee¹⁵⁵, B. Lefebvre¹⁰¹, M. Lefebvre¹⁷³, F. Legger¹¹², C. Leggett¹⁸,
 N. Lehmann¹⁷⁹, G. Lehmann Miotto³⁵, W.A. Leight⁴⁴, A. Leisos^{159,v}, M.A.L. Leite^{78d}, R. Leitner¹³⁹,
 D. Lellouch¹⁷⁷, B. Lemmer⁵¹, K.J.C. Leney⁹², T. Lenz²⁴, B. Lenzi³⁵, R. Leone⁷, S. Leone^{69a},
 C. Leonidopoulos⁴⁸, G. Lerner¹⁵³, C. Leroy¹⁰⁷, R. Les¹⁶⁴, A.A.J. Lesage¹⁴², C.G. Lester³¹,
 M. Levchenko¹³⁴, J. Levêque⁵, D. Levin¹⁰³, L.J. Levinson¹⁷⁷, D. Lewis⁹⁰, B. Li¹⁰³, C-Q. Li^{58a}, H. Li^{58b},
 L. Li^{58c}, Q. Li^{15d}, Q.Y. Li^{58a}, S. Li^{58d,58c}, X. Li^{58c}, Y. Li¹⁴⁸, Z. Liang^{15a}, B. Liberti^{71a}, A. Liblong¹⁶⁴,
 K. Lie^{61c}, S. Liem¹¹⁸, A. Limosani¹⁵⁴, C.Y. Lin³¹, K. Lin¹⁰⁴, T.H. Lin⁹⁷, R.A. Linck⁶³, B.E. Lindquist¹⁵²,
 A.L. Lioni⁵², E. Lipelles¹³³, A. Lipniacka¹⁷, M. Lisovyi^{59b}, T.M. Liss^{170,ap}, A. Lister¹⁷², A.M. Litke¹⁴³,
 J.D. Little⁸, B. Liu⁷⁶, B.L. Liu⁶, H.B. Liu²⁹, H. Liu¹⁰³, J.B. Liu^{58a}, J.K.K. Liu¹³¹, K. Liu¹³², M. Liu^{58a},
 P. Liu¹⁸, Y. Liu^{15a}, Y.L. Liu^{58a}, Y.W. Liu^{58a}, M. Livan^{68a,68b}, A. Lleres⁵⁶, J. Llorente Merino^{15a},
 S.L. Lloyd⁹⁰, C.Y. Lo^{61b}, F. Lo Sterzo⁴¹, E.M. Lobodzinska⁴⁴, P. Loch⁷, A. Loesle⁵⁰, K.M. Loew²⁶,
 T. Lohse¹⁹, K. Lohwasser¹⁴⁶, M. Lokajicek¹³⁷, B.A. Long²⁵, J.D. Long¹⁷⁰, R.E. Long⁸⁷, L. Longo^{65a,65b},
 K.A.Looper¹²², J.A. Lopez^{144b}, I. Lopez Paz¹⁴, A. Lopez Solis¹⁴⁶, J. Lorenz¹¹², N. Lorenzo Martinez⁵,
 M. Losada²², P.J. Lösel¹¹², X. Lou⁴⁴, X. Lou^{15a}, A. Lounis¹²⁸, J. Love⁶, P.A. Love⁸⁷,
 J.J. Lozano Bahilo¹⁷¹, H. Lu^{61a}, M. Lu^{58a}, N. Lu¹⁰³, Y.J. Lu⁶², H.J. Lubatti¹⁴⁵, C. Luci^{70a,70b},
 A. Lucotte⁵⁶, C. Luedtke⁵⁰, F. Luehring⁶³, I. Luise¹³², W. Lukas⁷⁴, L. Luminari^{70a}, B. Lund-Jensen¹⁵¹,
 M.S. Lutz¹⁰⁰, P.M. Luzi¹³², D. Lynn²⁹, R. Lysak¹³⁷, E. Lytken⁹⁴, F. Lyu^{15a}, V. Lyubushkin⁷⁷, H. Ma²⁹,
 L.L. Ma^{58b}, Y. Ma^{58b}, G. Maccarrone⁴⁹, A. Macchiolo¹¹³, C.M. Macdonald¹⁴⁶,
 J. Machado Miguens^{133,136b}, D. Madaffari¹⁷¹, R. Madar³⁷, W.F. Mader⁴⁶, A. Madsen⁴⁴, N. Madysa⁴⁶,
 J. Maeda⁸⁰, K. Maekawa¹⁶⁰, S. Maeland¹⁷, T. Maeno²⁹, A.S. Maevskiy¹¹¹, V. Magerl⁵⁰,
 C. Maidantchik^{78b}, T. Maier¹¹², A. Maio^{136a,136b,136d}, O. Majersky^{28a}, S. Majewski¹²⁷, Y. Makida⁷⁹,
 N. Makovec¹²⁸, B. Malaescu¹³², Pa. Malecki⁸², V.P. Maleev¹³⁴, F. Malek⁵⁶, U. Mallik⁷⁵, D. Malon⁶,
 C. Malone³¹, S. Maltezos¹⁰, S. Malyukov³⁵, J. Mamuzic¹⁷¹, G. Mancini⁴⁹, I. Mandic⁸⁹, J. Maneira^{136a},
 L. Manhaes de Andrade Filho^{78a}, J. Manjarres Ramos⁴⁶, K.H. Mankinen⁹⁴, A. Mann¹¹², A. Manousos⁷⁴,
 B. Mansoulie¹⁴², J.D. Mansour^{15a}, M. Mantoani⁵¹, S. Manzoni^{66a,66b}, G. Marceca³⁰, L. March⁵²,
 L. Marchese¹³¹, G. Marchiori¹³², M. Marcisovsky¹³⁷, C.A. Marin Tobon³⁵, M. Marjanovic³⁷,
 D.E. Marley¹⁰³, F. Marroquim^{78b}, Z. Marshall¹⁸, M.U.F Martensson¹⁶⁹, S. Marti-Garcia¹⁷¹,
 C.B. Martin¹²², T.A. Martin¹⁷⁵, V.J. Martin⁴⁸, B. Martin dit Latour¹⁷, M. Martinez^{14,y},
 V.I. Martinez Outschoorn¹⁰⁰, S. Martin-Haugh¹⁴¹, V.S. Martoiu^{27b}, A.C. Martyniuk⁹², A. Marzin³⁵,
 L. Masetti⁹⁷, T. Mashimo¹⁶⁰, R. Mashinistov¹⁰⁸, J. Masik⁹⁸, A.L. Maslennikov^{120b,120a}, L.H. Mason¹⁰²,
 L. Massa^{71a,71b}, P. Massarotti^{67a,67b}, P. Mastrandrea⁵, A. Mastroberardino^{40b,40a}, T. Masubuchi¹⁶⁰,
 P. Mättig¹⁷⁹, J. Maurer^{27b}, B. Maček⁸⁹, S.J. Maxfield⁸⁸, D.A. Maximov^{120b,120a}, R. Mazini¹⁵⁵,
 I. Maznas¹⁵⁹, S.M. Mazza¹⁴³, N.C. Mc Fadden¹¹⁶, G. Mc Goldrick¹⁶⁴, S.P. Mc Kee¹⁰³, A. McCarn¹⁰³,
 T.G. McCarthy¹¹³, L.I. McClymont⁹², E.F. McDonald¹⁰², J.A. McFayden³⁵, G. Mchedlidze⁵¹,
 M.A. McKay⁴¹, K.D. McLean¹⁷³, S.J. McMahon¹⁴¹, P.C. McNamara¹⁰², C.J. McNicol¹⁷⁵,
 R.A. McPherson^{173,ac}, J.E. Mdhuli^{32c}, Z.A. Meadows¹⁰⁰, S. Meehan¹⁴⁵, T.M. Megy⁵⁰, S. Mehlhase¹¹²,
 A. Mehta⁸⁸, T. Meideck⁵⁶, B. Meirose⁴², D. Melini^{171,g}, B.R. Mellado Garcia^{32c}, J.D. Mellenthin⁵¹,
 M. Melo^{28a}, F. Meloni⁴⁴, A. Melzer²⁴, S.B. Menary⁹⁸, E.D. Mendes Gouveia^{136a}, L. Meng⁸⁸,
 X.T. Meng¹⁰³, A. Mengarelli^{23b,23a}, S. Menke¹¹³, E. Meoni^{40b,40a}, S. Mergelmeyer¹⁹, C. Merlassino²⁰,
 P. Mermod⁵², L. Merola^{67a,67b}, C. Meroni^{66a}, F.S. Merritt³⁶, A. Messina^{70a,70b}, J. Metcalf⁶,
 A.S. Mete¹⁶⁸, C. Meyer¹³³, J. Meyer¹⁵⁷, J-P. Meyer¹⁴², H. Meyer Zu Theenhausen^{59a}, F. Miano¹⁵³,
 R.P. Middleton¹⁴¹, L. Mijovic⁴⁸, G. Mikenberg¹⁷⁷, M. Mikestikova¹³⁷, M. Mikuž⁸⁹, M. Milesi¹⁰²,

A. Milic¹⁶⁴, D.A. Millar⁹⁰, D.W. Miller³⁶, A. Milov¹⁷⁷, D.A. Milstead^{43a,43b}, A.A. Minaenko¹⁴⁰,
 M. Miñano Moya¹⁷¹, I.A. Minashvili^{156b}, A.I. Mincer¹²¹, B. Mindur^{81a}, M. Mineev⁷⁷, Y. Minegishi¹⁶⁰,
 Y. Ming¹⁷⁸, L.M. Mir¹⁴, A. Mirta^{65a,65b}, K.P. Mistry¹³³, T. Mitani¹⁷⁶, J. Mitrevski¹¹², V.A. Mitsou¹⁷¹,
 A. Miucci²⁰, P.S. Miyagawa¹⁴⁶, A. Mizukami⁷⁹, J.U. Mjörnmark⁹⁴, T. Mkrtchyan¹⁸¹, M. Mlynarikova¹³⁹,
 T. Moa^{43a,43b}, K. Mochizuki¹⁰⁷, P. Mogg⁵⁰, S. Mohapatra³⁸, S. Molander^{43a,43b}, R. Moles-Valls²⁴,
 M.C. Mondragon¹⁰⁴, K. Mönig⁴⁴, J. Monk³⁹, E. Monnier⁹⁹, A. Montalbano¹⁴⁹, J. Montejo Berlingen³⁵,
 F. Monticelli⁸⁶, S. Monzani^{66a}, R.W. Moore³, N. Morange¹²⁸, D. Moreno²², M. Moreno Llácer³⁵,
 P. Morettini^{53b}, M. Morgenstern¹¹⁸, S. Morgenstern⁴⁶, D. Mori¹⁴⁹, T. Mori¹⁶⁰, M. Morii⁵⁷,
 M. Morinaga¹⁷⁶, V. Morisbak¹³⁰, A.K. Morley³⁵, G. Mornacchi³⁵, A.P. Morris⁹², J.D. Morris⁹⁰,
 L. Morvaj¹⁵², P. Moschovakos¹⁰, M. Mosidze^{156b}, H.J. Moss¹⁴⁶, J. Moss^{150,m}, K. Motohashi¹⁶²,
 R. Mount¹⁵⁰, E. Mountricha³⁵, E.J.W. Moyse¹⁰⁰, S. Muanza⁹⁹, F. Mueller¹¹³, J. Mueller¹³⁵,
 R.S.P. Mueller¹¹², D. Muenstermann⁸⁷, P. Mullen⁵⁵, G.A. Mullier²⁰, F.J. Munoz Sanchez⁹⁸, P. Murin^{28b},
 W.J. Murray^{175,141}, A. Murrone^{66a,66b}, M. Muškinja⁸⁹, C. Mwewa^{32a}, A.G. Myagkov^{140,ak}, J. Myers¹²⁷,
 M. Myska¹³⁸, B.P. Nachman¹⁸, O. Nackenhorst⁴⁵, K. Nagai¹³¹, K. Nagano⁷⁹, Y. Nagasaka⁶⁰,
 K. Nagata¹⁶⁶, M. Nagel⁵⁰, E. Nagy⁹⁹, A.M. Nairz³⁵, Y. Nakahama¹¹⁵, K. Nakamura⁷⁹, T. Nakamura¹⁶⁰,
 I. Nakano¹²³, H. Nanjo¹²⁹, F. Napolitano^{59a}, R.F. Naranjo Garcia⁴⁴, R. Narayan¹¹, D.I. Narrias Villar^{59a},
 I. Naryshkin¹³⁴, T. Naumann⁴⁴, G. Navarro²², R. Nayyar⁷, H.A. Neal¹⁰³, P.Y. Nechaeva¹⁰⁸, T.J. Neep¹⁴²,
 A. Negri^{68a,68b}, M. Negrini^{23b}, S. Nektarijevic¹¹⁷, C. Nellist⁵¹, M.E. Nelson¹³¹, S. Nemecek¹³⁷,
 P. Nemethy¹²¹, M. Nessi^{35,e}, M.S. Neubauer¹⁷⁰, M. Neumann¹⁷⁹, P.R. Newman²¹, T.Y. Ng^{61c}, Y.S. Ng¹⁹,
 H.D.N. Nguyen⁹⁹, T. Nguyen Manh¹⁰⁷, E. Nibigira³⁷, R.B. Nickerson¹³¹, R. Nicolaïdou¹⁴²,
 J. Nielsen¹⁴³, N. Nikiforou¹¹, V. Nikolaenko^{140,ak}, I. Nikolic-Audit¹³², K. Nikolopoulos²¹, P. Nilsson²⁹,
 Y. Ninomiya⁷⁹, A. Nisati^{70a}, N. Nishu^{58c}, R. Nisius¹¹³, I. Nitsche⁴⁵, T. Nitta¹⁷⁶, T. Nobe¹⁶⁰,
 Y. Noguchi⁸³, M. Nomachi¹²⁹, I. Nomidis¹³², M.A. Nomura²⁹, T. Nooney⁹⁰, M. Nordberg³⁵,
 N. Norjoharuddeen¹³¹, T. Novak⁸⁹, O. Novgorodova⁴⁶, R. Novotny¹³⁸, L. Nozka¹²⁶, K. Ntekas¹⁶⁸,
 E. Nurse⁹², F. Nuti¹⁰², F.G. Oakham^{33,as}, H. Oberlack¹¹³, T. Obermann²⁴, J. Ocariz¹³², A. Ochi⁸⁰,
 I. Ochoa³⁸, J.P. Ochoa-Ricoux^{144a}, K. O'Connor²⁶, S. Oda⁸⁵, S. Odaka⁷⁹, S. Oerdekk⁵¹, A. Oh⁹⁸,
 S.H. Oh⁴⁷, C.C. Ohm¹⁵¹, H. Oide^{53b,53a}, H. Okawa¹⁶⁶, Y. Okazaki⁸³, Y. Okumura¹⁶⁰, T. Okuyama⁷⁹,
 A. Olariu^{27b}, L.F. Oleiro Seabra^{136a}, S.A. Olivares Pino^{144a}, D. Oliveira Damazio²⁹, J.L. Oliver¹,
 M.J.R. Olsson³⁶, A. Olszewski⁸², J. Olszowska⁸², D.C. O'Neil¹⁴⁹, A. Onofre^{136a,136e}, K. Onogi¹¹⁵,
 P.U.E. Onyisi¹¹, H. Oppen¹³⁰, M.J. Oreglia³⁶, Y. Oren¹⁵⁸, D. Orestano^{72a,72b}, E.C. Orgill⁹⁸,
 N. Orlando^{61b}, A.A. O'Rourke⁴⁴, R.S. Orr¹⁶⁴, B. Osculati^{53b,53a,*}, V. O'Shea⁵⁵, R. Ospanov^{58a},
 G. Otero y Garzon³⁰, H. Otono⁸⁵, M. Ouchrif^{34d}, F. Ould-Saada¹³⁰, A. Ouraou¹⁴², Q. Ouyang^{15a},
 M. Owen⁵⁵, R.E. Owen²¹, V.E. Ozcan^{12c}, N. Ozturk⁸, J. Pacalt¹²⁶, H.A. Pacey³¹, K. Pachal¹⁴⁹,
 A. Pacheco Pages¹⁴, L. Pacheco Rodriguez¹⁴², C. Padilla Aranda¹⁴, S. Pagan Griso¹⁸, M. Paganini¹⁸⁰,
 G. Palacino⁶³, S. Palazzo^{40b,40a}, S. Palestini³⁵, M. Palka^{81b}, D. Pallin³⁷, I. Panagoulias¹⁰, C.E. Pandini³⁵,
 J.G. Panduro Vazquez⁹¹, P. Pani³⁵, G. Panizzo^{64a,64c}, L. Paolozzi⁵², T.D. Papadopoulou¹⁰,
 K. Papageorgiou^{9,i}, A. Paramonov⁶, D. Paredes Hernandez^{61b}, S.R. Paredes Saenz¹³¹, B. Parida^{58c},
 A.J. Parker⁸⁷, K.A. Parker⁴⁴, M.A. Parker³¹, F. Parodi^{53b,53a}, J.A. Parsons³⁸, U. Parzefall⁵⁰,
 V.R. Pascuzzi¹⁶⁴, J.M.P. Pasner¹⁴³, E. Pasqualucci^{70a}, S. Passaggio^{53b}, F. Pastore⁹¹, P. Pasuwan^{43a,43b},
 S. Pataria⁹⁷, J.R. Pater⁹⁸, A. Pathak^{178,j}, T. Pauly³⁵, B. Pearson¹¹³, M. Pedersen¹³⁰, L. Pedraza Diaz¹¹⁷,
 R. Pedro^{136a,136b}, S.V. Peleganchuk^{120b,120a}, O. Penc¹³⁷, C. Peng^{15d}, H. Peng^{58a}, B.S. Peralva^{78a},
 M.M. Perego¹⁴², A.P. Pereira Peixoto^{136a}, D.V. Perepelitsa²⁹, F. Peri¹⁹, L. Perini^{66a,66b}, H. Pernegger³⁵,
 S. Perrella^{67a,67b}, V.D. Peshekhanov^{77,*}, K. Peters⁴⁴, R.F.Y. Peters⁹⁸, B.A. Petersen³⁵, T.C. Petersen³⁹,
 E. Petit⁵⁶, A. Petridis¹, C. Petridou¹⁵⁹, P. Petroff¹²⁸, E. Petrolo^{70a}, M. Petrov¹³¹, F. Petrucci^{72a,72b},
 M. Pettee¹⁸⁰, N.E. Pettersson¹⁰⁰, A. Peyaud¹⁴², R. Pezoa^{144b}, T. Pham¹⁰², F.H. Phillips¹⁰⁴,
 P.W. Phillips¹⁴¹, G. Piacquadro¹⁵², E. Pianori¹⁸, A. Picazio¹⁰⁰, M.A. Pickering¹³¹, R. Piegaia³⁰,
 J.E. Pilcher³⁶, A.D. Pilkington⁹⁸, M. Pinamonti^{71a,71b}, J.L. Pinfold³, M. Pitt¹⁷⁷, M.-A. Pleier²⁹,

V. Pleskot¹³⁹, E. Plotnikova⁷⁷, D. Pluth⁷⁶, P. Podberezko^{120b,120a}, R. Poettgen⁹⁴, R. Poggi⁵²,
 L. Poggioli¹²⁸, I. Pogrebnyak¹⁰⁴, D. Pohl²⁴, I. Pokharej⁵¹, G. Polesello^{68a}, A. Poley⁴⁴,
 A. Policicchio^{70a,70b}, R. Polifka³⁵, A. Polini^{23b}, C.S. Pollard⁴⁴, V. Polychronakos²⁹, D. Ponomarenko¹¹⁰,
 L. Pontecorvo^{70a}, G.A. Popeneciu^{27d}, D.M. Portillo Quintero¹³², S. Pospisil¹³⁸, K. Potamianos⁴⁴,
 I.N. Potrap⁷⁷, C.J. Potter³¹, H. Potti¹¹, T. Poulsen⁹⁴, J. Poveda³⁵, T.D. Powell¹⁴⁶,
 M.E. Pozo Astigarraga³⁵, P. Pralavorio⁹⁹, S. Prell⁷⁶, D. Price⁹⁸, M. Primavera^{65a}, S. Prince¹⁰¹,
 N. Proklova¹¹⁰, K. Prokofiev^{61c}, F. Prokoshin^{144b}, S. Protopopescu²⁹, J. Proudfoot⁶, M. Przybycien^{81a},
 A. Puri¹⁷⁰, P. Puzo¹²⁸, J. Qian¹⁰³, Y. Qin⁹⁸, A. Quadt⁵¹, M. Queitsch-Maitland⁴⁴, A. Qureshi¹,
 P. Rados¹⁰², F. Ragusa^{66a,66b}, G. Rahal⁹⁵, J.A. Raine⁹⁸, S. Rajagopalan²⁹, A. Ramirez Morales⁹⁰,
 T. Rashid¹²⁸, S. Raspopov⁵, M.G. Ratti^{66a,66b}, D.M. Rauch⁴⁴, F. Rauscher¹¹², S. Rave⁹⁷, B. Ravina¹⁴⁶,
 I. Ravinovich¹⁷⁷, J.H. Rawling⁹⁸, M. Raymond³⁵, A.L. Read¹³⁰, N.P. Readloff⁵⁶, M. Reale^{65a,65b},
 D.M. Rebuzzi^{68a,68b}, A. Redelbach¹⁷⁴, G. Redlinger²⁹, R. Reece¹⁴³, R.G. Reed^{32c}, K. Reeves⁴²,
 L. Rehnisch¹⁹, J. Reichert¹³³, A. Reiss⁹⁷, C. Rembser³⁵, H. Ren^{15d}, M. Rescigno^{70a}, S. Resconi^{66a},
 E.D. Ressegue¹³³, S. Rettie¹⁷², E. Reynolds²¹, O.L. Rezanova^{120b,120a}, P. Reznicek¹³⁹, E. Ricci^{73a,73b},
 R. Richter¹¹³, S. Richter⁹², E. Richter-Was^{81b}, O. Ricken²⁴, M. Ridel¹³², P. Rieck¹¹³, C.J. Riegel¹⁷⁹,
 O. Rifki⁴⁴, M. Rijssenbeek¹⁵², A. Rimoldi^{68a,68b}, M. Rimoldi²⁰, L. Rinaldi^{23b}, G. Ripellino¹⁵¹,
 B. Ristic⁸⁷, E. Ritsch³⁵, I. Riu¹⁴, J.C. Rivera Vergara^{144a}, F. Rizatdinova¹²⁵, E. Rizvi⁹⁰, C. Rizzi¹⁴,
 R.T. Roberts⁹⁸, S.H. Robertson^{101,ac}, A. Robichaud-Veronneau¹⁰¹, D. Robinson³¹, J.E.M. Robinson⁴⁴,
 A. Robson⁵⁵, E. Rocco⁹⁷, C. Roda^{69a,69b}, Y. Rodina⁹⁹, S. Rodriguez Bosca¹⁷¹, A. Rodriguez Perez¹⁴,
 D. Rodriguez Rodriguez¹⁷¹, A.M. Rodríguez Vera^{165b}, S. Roe³⁵, C.S. Rogan⁵⁷, O. Røhne¹³⁰,
 R. Röhrlig¹¹³, C.P.A. Roland⁶³, J. Roloff⁵⁷, A. Romaniouk¹¹⁰, M. Romano^{23b,23a}, N. Rompotis⁸⁸,
 M. Ronzani¹²¹, L. Roos¹³², S. Rosati^{70a}, K. Rosbach⁵⁰, P. Rose¹⁴³, N-A. Rosien⁵¹, E. Rossi⁴⁴,
 E. Rossi^{67a,67b}, L.P. Rossi^{53b}, L. Rossini^{66a,66b}, J.H.N. Rosten³¹, R. Rosten¹⁴, M. Rotaru^{27b},
 J. Rothberg¹⁴⁵, D. Rousseau¹²⁸, D. Roy^{32c}, A. Rozanova⁹⁹, Y. Rozen¹⁵⁷, X. Ruan^{32c}, F. Rubbo¹⁵⁰,
 F. Rühr⁵⁰, A. Ruiz-Martinez¹⁷¹, Z. Rurikova⁵⁰, N.A. Rusakovich⁷⁷, H.L. Russell¹⁰¹, J.P. Rutherford⁷,
 E.M. Rüttinger^{44,k}, Y.F. Ryabov¹³⁴, M. Rybar¹⁷⁰, G. Rybkin¹²⁸, S. Ryu⁶, A. Ryzhov¹⁴⁰, G.F. Rzechorz⁵¹,
 P. Sabatini⁵¹, G. Sabato¹¹⁸, S. Sacerdoti¹²⁸, H.F-W. Sadrozinski¹⁴³, R. Sadykov⁷⁷, F. Safai Tehrani^{70a},
 P. Saha¹¹⁹, M. Sahinsoy^{59a}, A. Sahu¹⁷⁹, M. Saimpert⁴⁴, M. Saito¹⁶⁰, T. Saito¹⁶⁰, H. Sakamoto¹⁶⁰,
 A. Sakharov^{121,aj}, D. Salamani⁵², G. Salamanna^{72a,72b}, J.E. Salazar Loyola^{144b}, D. Salek¹¹⁸,
 P.H. Sales De Bruin¹⁶⁹, D. Salihagic¹¹³, A. Salnikov¹⁵⁰, J. Salt¹⁷¹, D. Salvatore^{40b,40a}, F. Salvatore¹⁵³,
 A. Salvucci^{61a,61b,61c}, A. Salzburger³⁵, J. Samarati³⁵, D. Sammel⁵⁰, D. Sampsonidis¹⁵⁹,
 D. Sampsonidou¹⁵⁹, J. Sánchez¹⁷¹, A. Sanchez Pineda^{64a,64c}, H. Sandaker¹³⁰, C.O. Sander⁴⁴,
 M. Sandhoff¹⁷⁹, C. Sandoval²², D.P.C. Sankey¹⁴¹, M. Sannino^{53b,53a}, Y. Sano¹¹⁵, A. Sansoni⁴⁹,
 C. Santoni³⁷, H. Santos^{136a}, I. Santoyo Castillo¹⁵³, A. Sapronov⁷⁷, J.G. Saraiva^{136a,136d}, O. Sasaki⁷⁹,
 K. Sato¹⁶⁶, E. Sauvan⁵, P. Savard^{164,as}, N. Savic¹¹³, R. Sawada¹⁶⁰, C. Sawyer¹⁴¹, L. Sawyer^{93,ai},
 C. Sbarra^{23b}, A. Sbrizzi^{23b,23a}, T. Scanlon⁹², J. Schaarschmidt¹⁴⁵, P. Schacht¹¹³, B.M. Schachtner¹¹²,
 D. Schaefer³⁶, L. Schaefer¹³³, J. Schaeffer⁹⁷, S. Schaepe³⁵, U. Schäfer⁹⁷, A.C. Schaffer¹²⁸, D. Schaile¹¹²,
 R.D. Schamberger¹⁵², N. Scharmberg⁹⁸, V.A. Schegelsky¹³⁴, D. Scheirich¹³⁹, F. Schenck¹⁹,
 M. Schernau¹⁶⁸, C. Schiavi^{53b,53a}, S. Schier¹⁴³, L.K. Schildgen²⁴, Z.M. Schillaci²⁶, E.J. Schioppa³⁵,
 M. Schioppa^{40b,40a}, K.E. Schleicher⁵⁰, S. Schlenker³⁵, K.R. Schmidt-Sommerfeld¹¹³, K. Schmieden³⁵,
 C. Schmitt⁹⁷, S. Schmitt⁴⁴, S. Schmitz⁹⁷, U. Schnoor⁵⁰, L. Schoeffel¹⁴², A. Schoening^{59b}, E. Schopf²⁴,
 M. Schott⁹⁷, J.F.P. Schouwenberg¹¹⁷, J. Schovancova³⁵, S. Schramm⁵², A. Schulte⁹⁷,
 H-C. Schultz-Coulon^{59a}, M. Schumacher⁵⁰, B.A. Schumm¹⁴³, Ph. Schune¹⁴², A. Schwartzman¹⁵⁰,
 T.A. Schwarz¹⁰³, H. Schweiger⁹⁸, Ph. Schwemling¹⁴², R. Schwienhorst¹⁰⁴, A. Sciandra²⁴, G. Sciolla²⁶,
 M. Scornajenghi^{40b,40a}, F. Scuri^{69a}, F. Scutti¹⁰², L.M. Scyboz¹¹³, J. Searcy¹⁰³, C.D. Sebastiani^{70a,70b},
 P. Seema²⁴, S.C. Seidel¹¹⁶, A. Seiden¹⁴³, T. Seiss³⁶, J.M. Seixas^{78b}, G. Sekhniaidze^{67a}, K. Sekhon¹⁰³,
 S.J. Sekula⁴¹, N. Semprini-Cesari^{23b,23a}, S. Sen⁴⁷, S. Senkin³⁷, C. Serfon¹³⁰, L. Serin¹²⁸, L. Serkin^{64a,64b},

M. Sessa^{72a,72b}, H. Severini¹²⁴, F. Sforza¹⁶⁷, A. Sfyrla⁵², E. Shabalina⁵¹, J.D. Shahinian¹⁴³,
 N.W. Shaikh^{43a,43b}, L.Y. Shan^{15a}, R. Shang¹⁷⁰, J.T. Shank²⁵, M. Shapiro¹⁸, A.S. Sharma¹, A. Sharma¹³¹,
 P.B. Shatalov¹⁰⁹, K. Shaw¹⁵³, S.M. Shaw⁹⁸, A. Shcherbakova¹³⁴, Y. Shen¹²⁴, N. Sherafati³³,
 A.D. Sherman²⁵, P. Sherwood⁹², L. Shi^{155,ao}, S. Shimizu⁸⁰, C.O. Shimmin¹⁸⁰, M. Shimojima¹¹⁴,
 I.P.J. Shipsey¹³¹, S. Shirabe⁸⁵, M. Shiyakova⁷⁷, J. Shlomi¹⁷⁷, A. Shmeleva¹⁰⁸, D. Shoaleh Saadi¹⁰⁷,
 M.J. Shochet³⁶, S. Shojaii¹⁰², D.R. Shope¹²⁴, S. Shrestha¹²², E. Shulgá¹¹⁰, P. Sicho¹³⁷, A.M. Sickles¹⁷⁰,
 P.E. Sidebo¹⁵¹, E. Sideras Haddad^{32c}, O. Sidiropoulou¹⁷⁴, A. Sidoti^{23b,23a}, F. Siegert⁴⁶, Dj. Sijacki¹⁶,
 J. Silva^{136a}, M. Silva Jr.¹⁷⁸, M.V. Silva Oliveira^{78a}, S.B. Silverstein^{43a}, L. Simic⁷⁷, S. Simion¹²⁸,
 E. Simioni⁹⁷, M. Simon⁹⁷, R. Simoniello⁹⁷, P. Sinervo¹⁶⁴, N.B. Sinev¹²⁷, M. Sioli^{23b,23a}, G. Siragusa¹⁷⁴,
 I. Siral¹⁰³, S. Yu. Sivoklokov¹¹¹, J. Sjölin^{43a,43b}, M.B. Skinner⁸⁷, P. Skubic¹²⁴, M. Slater²¹, T. Slavicek¹³⁸,
 M. Slawinska⁸², K. Sliwa¹⁶⁷, R. Slovac¹³⁹, V. Smakhtin¹⁷⁷, B.H. Smart⁵, J. Smiesko^{28a}, N. Smirnov¹¹⁰,
 S. Yu. Smirnov¹¹⁰, Y. Smirnov¹¹⁰, L.N. Smirnova¹¹¹, O. Smirnova⁹⁴, J.W. Smith⁵¹, M.N.K. Smith³⁸,
 R.W. Smith³⁸, M. Smizanska⁸⁷, K. Smolek¹³⁸, A. Smykiewicz⁸², A.A. Snesarev¹⁰⁸, I.M. Snyder¹²⁷,
 S. Snyder²⁹, R. Sobie^{173,ac}, A.M. Soffa¹⁶⁸, A. Soffer¹⁵⁸, A. Søgaard⁴⁸, D.A. Soh¹⁵⁵, G. Sokhrannyi⁸⁹,
 C.A. Solans Sanchez³⁵, M. Solar¹³⁸, E.Yu. Soldatov¹¹⁰, U. Soldevila¹⁷¹, A.A. Solodkov¹⁴⁰,
 A. Soloshenko⁷⁷, O.V. Solovyanov¹⁴⁰, V. Solovyev¹³⁴, P. Sommer¹⁴⁶, H. Son¹⁶⁷, W. Song¹⁴¹,
 A. Sopczak¹³⁸, F. Sopkova^{28b}, D. Sosa^{59b}, C.L. Sotiropoulou^{69a,69b}, S. Sottocornola^{68a,68b},
 R. Soualah^{64a,64c,h}, A.M. Soukharev^{120b,120a}, D. South⁴⁴, B.C. Sowden⁹¹, S. Spagnolo^{65a,65b},
 M. Spalla¹¹³, M. Spangenberg¹⁷⁵, F. Spanò⁹¹, D. Sperlich¹⁹, F. Spettel¹¹³, T.M. Spieker^{59a}, R. Spighi^{23b},
 G. Spigo³⁵, L.A. Spiller¹⁰², D.P. Spiteri⁵⁵, M. Spousta¹³⁹, A. Stabile^{66a,66b}, R. Stamen^{59a}, S. Stamm¹⁹,
 E. Stanecka⁸², R.W. Stanek⁶, C. Stanescu^{72a}, B. Stanislaus¹³¹, M.M. Stanitzki⁴⁴, B. Staff¹¹⁸,
 S. Stapnes¹³⁰, E.A. Starchenko¹⁴⁰, G.H. Stark³⁶, J. Stark⁵⁶, S.H Stark³⁹, P. Staroba¹³⁷, P. Starovoitov^{59a},
 S. Stärz³⁵, R. Staszewski⁸², M. Stegler⁴⁴, P. Steinberg²⁹, B. Stelzer¹⁴⁹, H.J. Stelzer³⁵,
 O. Stelzer-Chilton^{165a}, H. Stenzel⁵⁴, T.J. Stevenson⁹⁰, G.A. Stewart⁵⁵, M.C. Stockton¹²⁷, G. Stoicea^{27b},
 P. Stolte⁵¹, S. Stonjek¹¹³, A. Straessner⁴⁶, J. Strandberg¹⁵¹, S. Strandberg^{43a,43b}, M. Strauss¹²⁴,
 P. Strizenec^{28b}, R. Ströhmer¹⁷⁴, D.M. Strom¹²⁷, R. Stroynowski⁴¹, A. Strubig⁴⁸, S.A. Stucci²⁹,
 B. Stugu¹⁷, J. Stupak¹²⁴, N.A. Styles⁴⁴, D. Su¹⁵⁰, J. Su¹³⁵, S. Suchek^{59a}, Y. Sugaya¹²⁹, M. Suk¹³⁸,
 V.V. Sulin¹⁰⁸, D.M.S. Sultan⁵², S. Sultansoy^{4c}, T. Sumida⁸³, S. Sun¹⁰³, X. Sun³, K. Suruliz¹⁵³,
 C.J.E. Suster¹⁵⁴, M.R. Sutton¹⁵³, S. Suzuki⁷⁹, M. Svatos¹³⁷, M. Swiatlowski³⁶, S.P. Swift²,
 A. Sydorenko⁹⁷, I. Sykora^{28a}, T. Sykora¹³⁹, D. Ta⁹⁷, K. Tackmann^{44,z}, J. Taenzer¹⁵⁸, A. Taffard¹⁶⁸,
 R. Tafirout^{165a}, E. Tahirovic⁹⁰, N. Taiblum¹⁵⁸, H. Takai²⁹, R. Takashima⁸⁴, E.H. Takasugi¹¹³,
 K. Takeda⁸⁰, T. Takeshita¹⁴⁷, Y. Takubo⁷⁹, M. Talby⁹⁹, A.A. Talyshев^{120b,120a}, J. Tanaka¹⁶⁰,
 M. Tanaka¹⁶², R. Tanaka¹²⁸, R. Tanioka⁸⁰, B.B. Tannenwald¹²², S. Tapia Araya^{144b}, S. Tapprogge⁹⁷,
 A. Tarek Abouelfadl Mohamed¹³², S. Tarem¹⁵⁷, G. Tarna^{27b,d}, G.F. Tartarelli^{66a}, P. Tas¹³⁹,
 M. Tasevsky¹³⁷, T. Tashiro⁸³, E. Tassi^{40b,40a}, A. Tavares Delgado^{136a,136b}, Y. Tayalati^{34e}, A.C. Taylor¹¹⁶,
 A.J. Taylor⁴⁸, G.N. Taylor¹⁰², P.T.E. Taylor¹⁰², W. Taylor^{165b}, A.S. Tee⁸⁷, P. Teixeira-Dias⁹¹,
 H. Ten Kate³⁵, P.K. Teng¹⁵⁵, J.J. Teoh¹¹⁸, F. Tepel¹⁷⁹, S. Terada⁷⁹, K. Terashi¹⁶⁰, J. Terron⁹⁶, S. Terzo¹⁴,
 M. Testa⁴⁹, R.J. Teuscher^{164,ac}, S.J. Thais¹⁸⁰, T. Theveneaux-Pelzer⁴⁴, F. Thiele³⁹, D.W. Thomas⁹¹,
 J.P. Thomas²¹, A.S. Thompson⁵⁵, P.D. Thompson²¹, L.A. Thomsen¹⁸⁰, E. Thomson¹³³, Y. Tian³⁸,
 R.E. Ticse Torres⁵¹, V.O. Tikhomirov^{108,al}, Yu.A. Tikhonov^{120b,120a}, S. Timoshenko¹¹⁰, P. Tipton¹⁸⁰,
 S. Tisserant⁹⁹, K. Todome¹⁶², S. Todorova-Nova⁵, S. Todt⁴⁶, J. Tojo⁸⁵, S. Tokár^{28a}, K. Tokushuku⁷⁹,
 E. Tolley¹²², K.G. Tomiwa^{32c}, M. Tomoto¹¹⁵, L. Tompkins^{150,p}, K. Toms¹¹⁶, B. Tong⁵⁷, P. Tornambe⁵⁰,
 E. Torrence¹²⁷, H. Torres⁴⁶, E. Torró Pastor¹⁴⁵, C. Tosciri¹³¹, J. Toth^{99,ab}, F. Touchard⁹⁹, D.R. Tovey¹⁴⁶,
 C.J. Treado¹²¹, T. Trefzger¹⁷⁴, F. Tresoldi¹⁵³, A. Tricoli²⁹, I.M. Trigger^{165a}, S. Trincaz-Duvold¹³²,
 M.F. Tripiana¹⁴, W. Trischuk¹⁶⁴, B. Trocmé⁵⁶, A. Trofymov¹²⁸, C. Troncon^{66a}, M. Trovatelli¹⁷³,
 F. Trovato¹⁵³, L. Truong^{32b}, M. Trzebinski⁸², A. Trzupek⁸², F. Tsai⁴⁴, J.C-L. Tseng¹³¹,
 P.V. Tsiareshka¹⁰⁵, N. Tsirintanis⁹, V. Tsiskaridze¹⁵², E.G. Tskhadadze^{156a}, I.I. Tsukerman¹⁰⁹,

V. Tsulaia¹⁸, S. Tsuno⁷⁹, D. Tsybychev¹⁵², Y. Tu^{61b}, A. Tudorache^{27b}, V. Tudorache^{27b}, T.T. Tulbure^{27a}, A.N. Tuna⁵⁷, S. Turchikhin⁷⁷, D. Turgeman¹⁷⁷, I. Turk Cakir^{4b,t}, R. Turra^{66a}, P.M. Tuts³⁸, E. Tzovara⁹⁷, G. Ucchielli^{23b,23a}, I. Ueda⁷⁹, M. Ughetto^{43a,43b}, F. Ukegawa¹⁶⁶, G. Unal³⁵, A. Undrus²⁹, G. Unel¹⁶⁸, F.C. Ungaro¹⁰², Y. Unno⁷⁹, K. Uno¹⁶⁰, J. Urban^{28b}, P. Urquijo¹⁰², P. Urrejola⁹⁷, G. Usai⁸, J. Usui⁷⁹, L. Vacavant⁹⁹, V. Vacek¹³⁸, B. Vachon¹⁰¹, K.O.H. Vadla¹³⁰, A. Vaidya⁹², C. Valderanis¹¹², E. Valdes Santurio^{43a,43b}, M. Valente⁵², S. Valentineti^{23b,23a}, A. Valero¹⁷¹, L. Valéry⁴⁴, R.A. Vallance²¹, A. Vallier⁵, J.A. Valls Ferrer¹⁷¹, T.R. Van Daalen¹⁴, W. Van Den Wollenberg¹¹⁸, H. Van der Graaf¹¹⁸, P. Van Gemmeren⁶, J. Van Nieuwkoop¹⁴⁹, I. Van Vulpen¹¹⁸, M. Vanadia^{71a,71b}, W. Vandelli³⁵, A. Vaniachine¹⁶³, P. Vankov¹¹⁸, R. Vari^{70a}, E.W. Varnes⁷, C. Varni^{53b,53a}, T. Varol⁴¹, D. Varouchas¹²⁸, K.E. Varvell¹⁵⁴, G.A. Vasquez^{144b}, J.G. Vasquez¹⁸⁰, F. Vazeille³⁷, D. Vazquez Furelos¹⁴, T. Vazquez Schroeder¹⁰¹, J. Veatch⁵¹, V. Vecchio^{72a,72b}, L.M. Veloce¹⁶⁴, F. Veloso^{136a,136c}, S. Veneziano^{70a}, A. Ventura^{65a,65b}, M. Venturi¹⁷³, N. Venturi³⁵, V. Vercesi^{68a}, M. Verducci^{72a,72b}, C.M. Vergel Infante⁷⁶, W. Verkerke¹¹⁸, A.T. Vermeulen¹¹⁸, J.C. Vermeulen¹¹⁸, M.C. Vetterli^{149,as}, N. Viaux Maira^{144b}, M. Vicente Barreto Pinto⁵², I. Vichou^{170,*}, T. Vickey¹⁴⁶, O.E. Vickey Boeriu¹⁴⁶, G.H.A. Viehhäuser¹³¹, S. Viel¹⁸, L. Vigani¹³¹, M. Villa^{23b,23a}, M. Villaplana Perez^{66a,66b}, E. Vilucchi⁴⁹, M.G. Vincter³³, V.B. Vinogradov⁷⁷, A. Vishwakarma⁴⁴, C. Vittori^{23b,23a}, I. Vivarelli¹⁵³, S. Vlachos¹⁰, M. Vogel¹⁷⁹, P. Vokac¹³⁸, G. Volpi¹⁴, S.E. von Buddenbrock^{32c}, E. Von Toerne²⁴, V. Vorobel¹³⁹, K. Vorobev¹¹⁰, M. Vos¹⁷¹, J.H. Vossebeld⁸⁸, N. Vranjes¹⁶, M. Vranjes Milosavljevic¹⁶, V. Vrba¹³⁸, M. Vreeswijk¹¹⁸, T. Šfiligoj⁸⁹, R. Vuillermet³⁵, I. Vukotic³⁶, T. Ženiš^{28a}, L. Živković¹⁶, P. Wagner²⁴, W. Wagner¹⁷⁹, J. Wagner-Kuhr¹¹², H. Wahlberg⁸⁶, S. Wahrmund⁴⁶, K. Wakamiya⁸⁰, V.M. Walbrecht¹¹³, J. Walder⁸⁷, R. Walker¹¹², S.D. Walker⁹¹, W. Walkowiak¹⁴⁸, V. Wallangen^{43a,43b}, A.M. Wang⁵⁷, C. Wang^{58b,d}, F. Wang¹⁷⁸, H. Wang¹⁸, H. Wang³, J. Wang¹⁵⁴, J. Wang^{59b}, P. Wang⁴¹, Q. Wang¹²⁴, R.-J. Wang¹³², R. Wang^{58a}, R. Wang⁶, S.M. Wang¹⁵⁵, W.T. Wang^{58a}, W. Wang^{15c,ad}, W.X. Wang^{58a,ad}, Y. Wang^{58a}, Z. Wang^{58c}, C. Wanotayaroj⁴⁴, A. Warburton¹⁰¹, C.P. Ward³¹, D.R. Wardrope⁹², A. Washbrook⁴⁸, P.M. Watkins²¹, A.T. Watson²¹, M.F. Watson²¹, G. Watts¹⁴⁵, S. Watts⁹⁸, B.M. Waugh⁹², A.F. Webb¹¹, S. Webb⁹⁷, C. Weber¹⁸⁰, M.S. Weber²⁰, S.A. Weber³³, S.M. Weber^{59a}, A.R. Weidberg¹³¹, B. Weinert⁶³, J. Weingarten⁵¹, M. Weirich⁹⁷, C. Weiser⁵⁰, P.S. Wells³⁵, T. Wenaus²⁹, T. Wengler³⁵, S. Wenig³⁵, N. Wermes²⁴, M.D. Werner⁷⁶, P. Werner³⁵, M. Wessels^{59a}, T.D. Weston²⁰, K. Whalen¹²⁷, N.L. Whallon¹⁴⁵, A.M. Wharton⁸⁷, A.S. White¹⁰³, A. White⁸, M.J. White¹, R. White^{144b}, D. Whiteson¹⁶⁸, B.W. Whitmore⁸⁷, F.J. Wickens¹⁴¹, W. Wiedenmann¹⁷⁸, M. Wielers¹⁴¹, C. Wiglesworth³⁹, L.A.M. Wiik-Fuchs⁵⁰, A. Wildauer¹¹³, F. Wilk⁹⁸, H.G. Wilkens³⁵, L.J. Wilkins⁹¹, H.H. Williams¹³³, S. Williams³¹, C. Willis¹⁰⁴, S. Willocq¹⁰⁰, J.A. Wilson²¹, I. Wingerter-Seez⁵, E. Winkels¹⁵³, F. Winklmeier¹²⁷, O.J. Winston¹⁵³, B.T. Winter²⁴, M. Wittgen¹⁵⁰, M. Wobisch⁹³, A. Wolf⁹⁷, T.M.H. Wolf¹¹⁸, R. Wolff⁹⁹, M.W. Wolter⁸², H. Wolters^{136a,136c}, V.W.S. Wong¹⁷², N.L. Woods¹⁴³, S.D. Worm²¹, B.K. Wosiek⁸², K.W. Woźniak⁸², K. Wraith⁵⁵, M. Wu³⁶, S.L. Wu¹⁷⁸, X. Wu⁵², Y. Wu^{58a}, T.R. Wyatt⁹⁸, B.M. Wynne⁴⁸, S. Xella³⁹, Z. Xi¹⁰³, L. Xia¹⁷⁵, D. Xu^{15a}, H. Xu^{58a}, L. Xu²⁹, T. Xu¹⁴², W. Xu¹⁰³, B. Yabsley¹⁵⁴, S. Yacoob^{32a}, K. Yajima¹²⁹, D.P. Yallup⁹², D. Yamaguchi¹⁶², Y. Yamaguchi¹⁶², A. Yamamoto⁷⁹, T. Yamanaka¹⁶⁰, F. Yamane⁸⁰, M. Yamatani¹⁶⁰, T. Yamazaki¹⁶⁰, Y. Yamazaki⁸⁰, Z. Yan²⁵, H.J. Yang^{58c,58d}, H.T. Yang¹⁸, S. Yang⁷⁵, Y. Yang¹⁶⁰, Z. Yang¹⁷, W-M. Yao¹⁸, Y.C. Yap⁴⁴, Y. Yasu⁷⁹, E. Yatsenko^{58c,58d}, J. Ye⁴¹, S. Ye²⁹, I. Yeletskikh⁷⁷, E. Yigitbasi²⁵, E. Yildirim⁹⁷, K. Yorita¹⁷⁶, K. Yoshihara¹³³, C.J.S. Young³⁵, C. Young¹⁵⁰, J. Yu⁸, J. Yu⁷⁶, X. Yue^{59a}, S.P.Y. Yuen²⁴, B. Zabinski⁸², G. Zacharis¹⁰, E. Zaffaroni⁵², R. Zaidan¹⁴, A.M. Zaitsev^{140,ak}, N. Zakharchuk⁴⁴, J. Zalieckas¹⁷, S. Zambito⁵⁷, D. Zanzi³⁵, D.R. Zaripovas⁵⁵, S.V. Zeißner⁴⁵, C. Zeitnitz¹⁷⁹, G. Zemaityte¹³¹, J.C. Zeng¹⁷⁰, Q. Zeng¹⁵⁰, O. Zenin¹⁴⁰, D. Zerwas¹²⁸, M. Zgubič¹³¹, D.F. Zhang^{58b}, D. Zhang¹⁰³, F. Zhang¹⁷⁸, G. Zhang^{58a}, H. Zhang^{15c}, J. Zhang⁶, L. Zhang^{15c}, L. Zhang^{58a}, M. Zhang¹⁷⁰, P. Zhang^{15c}, R. Zhang^{58a}, R. Zhang²⁴, X. Zhang^{58b}, Y. Zhang^{15d}, Z. Zhang¹²⁸, X. Zhao⁴¹, Y. Zhao^{58b,128,ah}, Z. Zhao^{58a}, A. Zhemchugov⁷⁷, Z. Zheng¹⁰³, B. Zhou¹⁰³, C. Zhou¹⁷⁸, L. Zhou⁴¹,

M.S. Zhou^{15d}, M. Zhou¹⁵², N. Zhou^{58c}, Y. Zhou⁷, C.G. Zhu^{58b}, H.L. Zhu^{58a}, H. Zhu^{15a}, J. Zhu¹⁰³, Y. Zhu^{58a}, X. Zhuang^{15a}, K. Zhukov¹⁰⁸, V. Zhulanov^{120b,120a}, A. Zibell¹⁷⁴, D. Ziemska⁶³, N.I. Zimine⁷⁷, S. Zimmermann⁵⁰, Z. Zinonos¹¹³, M. Zinser⁹⁷, M. Ziolkowski¹⁴⁸, G. Zobernig¹⁷⁸, A. Zoccoli^{23b,23a}, K. Zoch⁵¹, T.G. Zorbas¹⁴⁶, R. Zou³⁶, M. Zur Nedden¹⁹, L. Zwalinski³⁵.

¹Department of Physics, University of Adelaide, Adelaide; Australia.

²Physics Department, SUNY Albany, Albany NY; United States of America.

³Department of Physics, University of Alberta, Edmonton AB; Canada.

^{4(a)}Department of Physics, Ankara University, Ankara;^(b)Istanbul Aydin University, Istanbul;^(c)Division of Physics, TOBB University of Economics and Technology, Ankara; Turkey.

⁵LAPP, Université Grenoble Alpes, Université Savoie Mont Blanc, CNRS/IN2P3, Annecy; France.

⁶High Energy Physics Division, Argonne National Laboratory, Argonne IL; United States of America.

⁷Department of Physics, University of Arizona, Tucson AZ; United States of America.

⁸Department of Physics, University of Texas at Arlington, Arlington TX; United States of America.

⁹Physics Department, National and Kapodistrian University of Athens, Athens; Greece.

¹⁰Physics Department, National Technical University of Athens, Zografou; Greece.

¹¹Department of Physics, University of Texas at Austin, Austin TX; United States of America.

^{12(a)}Bahcesehir University, Faculty of Engineering and Natural Sciences, Istanbul;^(b)Istanbul Bilgi University, Faculty of Engineering and Natural Sciences, Istanbul;^(c)Department of Physics, Bogazici University, Istanbul;^(d)Department of Physics Engineering, Gaziantep University, Gaziantep; Turkey.

¹³Institute of Physics, Azerbaijan Academy of Sciences, Baku; Azerbaijan.

¹⁴Institut de Física d'Altes Energies (IFAE), Barcelona Institute of Science and Technology, Barcelona; Spain.

^{15(a)}Institute of High Energy Physics, Chinese Academy of Sciences, Beijing;^(b)Physics Department, Tsinghua University, Beijing;^(c)Department of Physics, Nanjing University, Nanjing;^(d)University of Chinese Academy of Science (UCAS), Beijing; China.

¹⁶Institute of Physics, University of Belgrade, Belgrade; Serbia.

¹⁷Department for Physics and Technology, University of Bergen, Bergen; Norway.

¹⁸Physics Division, Lawrence Berkeley National Laboratory and University of California, Berkeley CA; United States of America.

¹⁹Institut für Physik, Humboldt Universität zu Berlin, Berlin; Germany.

²⁰Albert Einstein Center for Fundamental Physics and Laboratory for High Energy Physics, University of Bern, Bern; Switzerland.

²¹School of Physics and Astronomy, University of Birmingham, Birmingham; United Kingdom.

²²Centro de Investigaciones, Universidad Antonio Nariño, Bogota; Colombia.

^{23(a)}Dipartimento di Fisica e Astronomia, Università di Bologna, Bologna;^(b)INFN Sezione di Bologna; Italy.

²⁴Physikalisches Institut, Universität Bonn, Bonn; Germany.

²⁵Department of Physics, Boston University, Boston MA; United States of America.

²⁶Department of Physics, Brandeis University, Waltham MA; United States of America.

^{27(a)}Transilvania University of Brasov, Brasov;^(b)Horia Hulubei National Institute of Physics and Nuclear Engineering, Bucharest;^(c)Department of Physics, Alexandru Ioan Cuza University of Iasi, Iasi;^(d)National Institute for Research and Development of Isotopic and Molecular Technologies, Physics Department, Cluj-Napoca;^(e)University Politehnica Bucharest, Bucharest;^(f)West University in Timisoara, Timisoara; Romania.

^{28(a)}Faculty of Mathematics, Physics and Informatics, Comenius University, Bratislava;^(b)Department of Subnuclear Physics, Institute of Experimental Physics of the Slovak Academy of Sciences, Kosice;

Slovak Republic.

²⁹Physics Department, Brookhaven National Laboratory, Upton NY; United States of America.

³⁰Departamento de Física, Universidad de Buenos Aires, Buenos Aires; Argentina.

³¹Cavendish Laboratory, University of Cambridge, Cambridge; United Kingdom.

^{32(a)}Department of Physics, University of Cape Town, Cape Town;^(b)Department of Mechanical Engineering Science, University of Johannesburg, Johannesburg;^(c)School of Physics, University of the Witwatersrand, Johannesburg; South Africa.

³³Department of Physics, Carleton University, Ottawa ON; Canada.

^{34(a)}Faculté des Sciences Ain Chock, Réseau Universitaire de Physique des Hautes Energies - Université Hassan II, Casablanca;^(b)Centre National de l'Energie des Sciences Techniques Nucleaires (CNESTEN), Rabat;^(c)Faculté des Sciences Semlalia, Université Cadi Ayyad, LPHEA-Marrakech;^(d)Faculté des Sciences, Université Mohamed Premier and LPTPM, Oujda;^(e)Faculté des sciences, Université Mohammed V, Rabat; Morocco.

³⁵CERN, Geneva; Switzerland.

³⁶Enrico Fermi Institute, University of Chicago, Chicago IL; United States of America.

³⁷LPC, Université Clermont Auvergne, CNRS/IN2P3, Clermont-Ferrand; France.

³⁸Nevis Laboratory, Columbia University, Irvington NY; United States of America.

³⁹Niels Bohr Institute, University of Copenhagen, Copenhagen; Denmark.

^{40(a)}Dipartimento di Fisica, Università della Calabria, Rende;^(b)INFN Gruppo Collegato di Cosenza, Laboratori Nazionali di Frascati; Italy.

⁴¹Physics Department, Southern Methodist University, Dallas TX; United States of America.

⁴²Physics Department, University of Texas at Dallas, Richardson TX; United States of America.

^{43(a)}Department of Physics, Stockholm University;^(b)Oskar Klein Centre, Stockholm; Sweden.

⁴⁴Deutsches Elektronen-Synchrotron DESY, Hamburg and Zeuthen; Germany.

⁴⁵Lehrstuhl für Experimentelle Physik IV, Technische Universität Dortmund, Dortmund; Germany.

⁴⁶Institut für Kern- und Teilchenphysik, Technische Universität Dresden, Dresden; Germany.

⁴⁷Department of Physics, Duke University, Durham NC; United States of America.

⁴⁸SUPA - School of Physics and Astronomy, University of Edinburgh, Edinburgh; United Kingdom.

⁴⁹INFN e Laboratori Nazionali di Frascati, Frascati; Italy.

⁵⁰Physikalischs Institut, Albert-Ludwigs-Universität Freiburg, Freiburg; Germany.

⁵¹II. Physikalischs Institut, Georg-August-Universität Göttingen, Göttingen; Germany.

⁵²Département de Physique Nucléaire et Corpusculaire, Université de Genève, Genève; Switzerland.

^{53(a)}Dipartimento di Fisica, Università di Genova, Genova;^(b)INFN Sezione di Genova; Italy.

⁵⁴II. Physikalischs Institut, Justus-Liebig-Universität Giessen, Giessen; Germany.

⁵⁵SUPA - School of Physics and Astronomy, University of Glasgow, Glasgow; United Kingdom.

⁵⁶LPSC, Université Grenoble Alpes, CNRS/IN2P3, Grenoble INP, Grenoble; France.

⁵⁷Laboratory for Particle Physics and Cosmology, Harvard University, Cambridge MA; United States of America.

^{58(a)}Department of Modern Physics and State Key Laboratory of Particle Detection and Electronics, University of Science and Technology of China, Hefei;^(b)Institute of Frontier and Interdisciplinary Science and Key Laboratory of Particle Physics and Particle Irradiation (MOE), Shandong University, Qingdao;^(c)School of Physics and Astronomy, Shanghai Jiao Tong University, KLPPAC-MoE, SKLPPC, Shanghai;^(d)Tsung-Dao Lee Institute, Shanghai; China.

^{59(a)}Kirchhoff-Institut für Physik, Ruprecht-Karls-Universität Heidelberg, Heidelberg;^(b)Physikalischs Institut, Ruprecht-Karls-Universität Heidelberg, Heidelberg; Germany.

⁶⁰Faculty of Applied Information Science, Hiroshima Institute of Technology, Hiroshima; Japan.

^{61(a)}Department of Physics, Chinese University of Hong Kong, Shatin, N.T., Hong Kong;^(b)Department

of Physics, University of Hong Kong, Hong Kong;^(c)Department of Physics and Institute for Advanced Study, Hong Kong University of Science and Technology, Clear Water Bay, Kowloon, Hong Kong; China.

⁶²Department of Physics, National Tsing Hua University, Hsinchu; Taiwan.

⁶³Department of Physics, Indiana University, Bloomington IN; United States of America.

^{64(a)}INFN Gruppo Collegato di Udine, Sezione di Trieste, Udine;^(b)ICTP, Trieste;^(c)Dipartimento di Chimica, Fisica e Ambiente, Università di Udine, Udine; Italy.

^{65(a)}INFN Sezione di Lecce;^(b)Dipartimento di Matematica e Fisica, Università del Salento, Lecce; Italy.

^{66(a)}INFN Sezione di Milano;^(b)Dipartimento di Fisica, Università di Milano, Milano; Italy.

^{67(a)}INFN Sezione di Napoli;^(b)Dipartimento di Fisica, Università di Napoli, Napoli; Italy.

^{68(a)}INFN Sezione di Pavia;^(b)Dipartimento di Fisica, Università di Pavia, Pavia; Italy.

^{69(a)}INFN Sezione di Pisa;^(b)Dipartimento di Fisica E. Fermi, Università di Pisa, Pisa; Italy.

^{70(a)}INFN Sezione di Roma;^(b)Dipartimento di Fisica, Sapienza Università di Roma, Roma; Italy.

^{71(a)}INFN Sezione di Roma Tor Vergata;^(b)Dipartimento di Fisica, Università di Roma Tor Vergata, Roma; Italy.

^{72(a)}INFN Sezione di Roma Tre;^(b)Dipartimento di Matematica e Fisica, Università Roma Tre, Roma; Italy.

^{73(a)}INFN-TIFPA;^(b)Università degli Studi di Trento, Trento; Italy.

⁷⁴Institut für Astro- und Teilchenphysik, Leopold-Franzens-Universität, Innsbruck; Austria.

⁷⁵University of Iowa, Iowa City IA; United States of America.

⁷⁶Department of Physics and Astronomy, Iowa State University, Ames IA; United States of America.

⁷⁷Joint Institute for Nuclear Research, Dubna; Russia.

^{78(a)}Departamento de Engenharia Elétrica, Universidade Federal de Juiz de Fora (UFJF), Juiz de Fora;^(b)Universidade Federal do Rio De Janeiro COPPE/EE/IF, Rio de Janeiro;^(c)Universidade Federal de São João del Rei (UFSJ), São João del Rei;^(d)Instituto de Física, Universidade de São Paulo, São Paulo; Brazil.

⁷⁹KEK, High Energy Accelerator Research Organization, Tsukuba; Japan.

⁸⁰Graduate School of Science, Kobe University, Kobe; Japan.

^{81(a)}AGH University of Science and Technology, Faculty of Physics and Applied Computer Science, Krakow;^(b)Marian Smoluchowski Institute of Physics, Jagiellonian University, Krakow; Poland.

⁸²Institute of Nuclear Physics Polish Academy of Sciences, Krakow; Poland.

⁸³Faculty of Science, Kyoto University, Kyoto; Japan.

⁸⁴Kyoto University of Education, Kyoto; Japan.

⁸⁵Research Center for Advanced Particle Physics and Department of Physics, Kyushu University, Fukuoka ; Japan.

⁸⁶Instituto de Física La Plata, Universidad Nacional de La Plata and CONICET, La Plata; Argentina.

⁸⁷Physics Department, Lancaster University, Lancaster; United Kingdom.

⁸⁸Oliver Lodge Laboratory, University of Liverpool, Liverpool; United Kingdom.

⁸⁹Department of Experimental Particle Physics, Jožef Stefan Institute and Department of Physics, University of Ljubljana, Ljubljana; Slovenia.

⁹⁰School of Physics and Astronomy, Queen Mary University of London, London; United Kingdom.

⁹¹Department of Physics, Royal Holloway University of London, Egham; United Kingdom.

⁹²Department of Physics and Astronomy, University College London, London; United Kingdom.

⁹³Louisiana Tech University, Ruston LA; United States of America.

⁹⁴Fysiska institutionen, Lunds universitet, Lund; Sweden.

⁹⁵Centre de Calcul de l’Institut National de Physique Nucléaire et de Physique des Particules (IN2P3), Villeurbanne; France.

- ⁹⁶Departamento de Física Teórica C-15 and CIAFF, Universidad Autónoma de Madrid, Madrid; Spain.
- ⁹⁷Institut für Physik, Universität Mainz, Mainz; Germany.
- ⁹⁸School of Physics and Astronomy, University of Manchester, Manchester; United Kingdom.
- ⁹⁹CPPM, Aix-Marseille Université, CNRS/IN2P3, Marseille; France.
- ¹⁰⁰Department of Physics, University of Massachusetts, Amherst MA; United States of America.
- ¹⁰¹Department of Physics, McGill University, Montreal QC; Canada.
- ¹⁰²School of Physics, University of Melbourne, Victoria; Australia.
- ¹⁰³Department of Physics, University of Michigan, Ann Arbor MI; United States of America.
- ¹⁰⁴Department of Physics and Astronomy, Michigan State University, East Lansing MI; United States of America.
- ¹⁰⁵B.I. Stepanov Institute of Physics, National Academy of Sciences of Belarus, Minsk; Belarus.
- ¹⁰⁶Research Institute for Nuclear Problems of Byelorussian State University, Minsk; Belarus.
- ¹⁰⁷Group of Particle Physics, University of Montreal, Montreal QC; Canada.
- ¹⁰⁸P.N. Lebedev Physical Institute of the Russian Academy of Sciences, Moscow; Russia.
- ¹⁰⁹Institute for Theoretical and Experimental Physics (ITEP), Moscow; Russia.
- ¹¹⁰National Research Nuclear University MEPhI, Moscow; Russia.
- ¹¹¹D.V. Skobeltsyn Institute of Nuclear Physics, M.V. Lomonosov Moscow State University, Moscow; Russia.
- ¹¹²Fakultät für Physik, Ludwig-Maximilians-Universität München, München; Germany.
- ¹¹³Max-Planck-Institut für Physik (Werner-Heisenberg-Institut), München; Germany.
- ¹¹⁴Nagasaki Institute of Applied Science, Nagasaki; Japan.
- ¹¹⁵Graduate School of Science and Kobayashi-Maskawa Institute, Nagoya University, Nagoya; Japan.
- ¹¹⁶Department of Physics and Astronomy, University of New Mexico, Albuquerque NM; United States of America.
- ¹¹⁷Institute for Mathematics, Astrophysics and Particle Physics, Radboud University Nijmegen/Nikhef, Nijmegen; Netherlands.
- ¹¹⁸Nikhef National Institute for Subatomic Physics and University of Amsterdam, Amsterdam; Netherlands.
- ¹¹⁹Department of Physics, Northern Illinois University, DeKalb IL; United States of America.
- ¹²⁰(^a)Budker Institute of Nuclear Physics, SB RAS, Novosibirsk; (^b)Novosibirsk State University Novosibirsk; Russia.
- ¹²¹Department of Physics, New York University, New York NY; United States of America.
- ¹²²Ohio State University, Columbus OH; United States of America.
- ¹²³Faculty of Science, Okayama University, Okayama; Japan.
- ¹²⁴Homer L. Dodge Department of Physics and Astronomy, University of Oklahoma, Norman OK; United States of America.
- ¹²⁵Department of Physics, Oklahoma State University, Stillwater OK; United States of America.
- ¹²⁶Palacký University, RCPTM, Joint Laboratory of Optics, Olomouc; Czech Republic.
- ¹²⁷Center for High Energy Physics, University of Oregon, Eugene OR; United States of America.
- ¹²⁸LAL, Université Paris-Sud, CNRS/IN2P3, Université Paris-Saclay, Orsay; France.
- ¹²⁹Graduate School of Science, Osaka University, Osaka; Japan.
- ¹³⁰Department of Physics, University of Oslo, Oslo; Norway.
- ¹³¹Department of Physics, Oxford University, Oxford; United Kingdom.
- ¹³²LPNHE, Sorbonne Université, Paris Diderot Sorbonne Paris Cité, CNRS/IN2P3, Paris; France.
- ¹³³Department of Physics, University of Pennsylvania, Philadelphia PA; United States of America.
- ¹³⁴Konstantinov Nuclear Physics Institute of National Research Centre "Kurchatov Institute", PNPI, St. Petersburg; Russia.

- ¹³⁵Department of Physics and Astronomy, University of Pittsburgh, Pittsburgh PA; United States of America.
- ^{136(a)}Laboratório de Instrumentação e Física Experimental de Partículas - LIP;^(b)Departamento de Física, Faculdade de Ciências, Universidade de Lisboa, Lisboa;^(c)Departamento de Física, Universidade de Coimbra, Coimbra;^(d)Centro de Física Nuclear da Universidade de Lisboa, Lisboa;^(e)Departamento de Física, Universidade do Minho, Braga;^(f)Departamento de Física Teorica y del Cosmos, Universidad de Granada, Granada (Spain);^(g)Dep Física and CEFITEC of Faculdade de Ciências e Tecnologia, Universidade Nova de Lisboa, Caparica; Portugal.
- ¹³⁷Institute of Physics, Academy of Sciences of the Czech Republic, Prague; Czech Republic.
- ¹³⁸Czech Technical University in Prague, Prague; Czech Republic.
- ¹³⁹Charles University, Faculty of Mathematics and Physics, Prague; Czech Republic.
- ¹⁴⁰State Research Center Institute for High Energy Physics, NRC KI, Protvino; Russia.
- ¹⁴¹Particle Physics Department, Rutherford Appleton Laboratory, Didcot; United Kingdom.
- ¹⁴²IRFU, CEA, Université Paris-Saclay, Gif-sur-Yvette; France.
- ¹⁴³Santa Cruz Institute for Particle Physics, University of California Santa Cruz, Santa Cruz CA; United States of America.
- ^{144(a)}Departamento de Física, Pontificia Universidad Católica de Chile, Santiago;^(b)Departamento de Física, Universidad Técnica Federico Santa María, Valparaíso; Chile.
- ¹⁴⁵Department of Physics, University of Washington, Seattle WA; United States of America.
- ¹⁴⁶Department of Physics and Astronomy, University of Sheffield, Sheffield; United Kingdom.
- ¹⁴⁷Department of Physics, Shinshu University, Nagano; Japan.
- ¹⁴⁸Department Physik, Universität Siegen, Siegen; Germany.
- ¹⁴⁹Department of Physics, Simon Fraser University, Burnaby BC; Canada.
- ¹⁵⁰SLAC National Accelerator Laboratory, Stanford CA; United States of America.
- ¹⁵¹Physics Department, Royal Institute of Technology, Stockholm; Sweden.
- ¹⁵²Departments of Physics and Astronomy, Stony Brook University, Stony Brook NY; United States of America.
- ¹⁵³Department of Physics and Astronomy, University of Sussex, Brighton; United Kingdom.
- ¹⁵⁴School of Physics, University of Sydney, Sydney; Australia.
- ¹⁵⁵Institute of Physics, Academia Sinica, Taipei; Taiwan.
- ^{156(a)}E. Andronikashvili Institute of Physics, Iv. Javakhishvili Tbilisi State University, Tbilisi;^(b)High Energy Physics Institute, Tbilisi State University, Tbilisi; Georgia.
- ¹⁵⁷Department of Physics, Technion, Israel Institute of Technology, Haifa; Israel.
- ¹⁵⁸Raymond and Beverly Sackler School of Physics and Astronomy, Tel Aviv University, Tel Aviv; Israel.
- ¹⁵⁹Department of Physics, Aristotle University of Thessaloniki, Thessaloniki; Greece.
- ¹⁶⁰International Center for Elementary Particle Physics and Department of Physics, University of Tokyo, Tokyo; Japan.
- ¹⁶¹Graduate School of Science and Technology, Tokyo Metropolitan University, Tokyo; Japan.
- ¹⁶²Department of Physics, Tokyo Institute of Technology, Tokyo; Japan.
- ¹⁶³Tomsk State University, Tomsk; Russia.
- ¹⁶⁴Department of Physics, University of Toronto, Toronto ON; Canada.
- ^{165(a)}TRIUMF, Vancouver BC;^(b)Department of Physics and Astronomy, York University, Toronto ON; Canada.
- ¹⁶⁶Division of Physics and Tomonaga Center for the History of the Universe, Faculty of Pure and Applied Sciences, University of Tsukuba, Tsukuba; Japan.
- ¹⁶⁷Department of Physics and Astronomy, Tufts University, Medford MA; United States of America.
- ¹⁶⁸Department of Physics and Astronomy, University of California Irvine, Irvine CA; United States of

America.

¹⁶⁹Department of Physics and Astronomy, University of Uppsala, Uppsala; Sweden.

¹⁷⁰Department of Physics, University of Illinois, Urbana IL; United States of America.

¹⁷¹Instituto de Física Corpuscular (IFIC), Centro Mixto Universidad de Valencia - CSIC, Valencia; Spain.

¹⁷²Department of Physics, University of British Columbia, Vancouver BC; Canada.

¹⁷³Department of Physics and Astronomy, University of Victoria, Victoria BC; Canada.

¹⁷⁴Fakultät für Physik und Astronomie, Julius-Maximilians-Universität Würzburg, Würzburg; Germany.

¹⁷⁵Department of Physics, University of Warwick, Coventry; United Kingdom.

¹⁷⁶Waseda University, Tokyo; Japan.

¹⁷⁷Department of Particle Physics, Weizmann Institute of Science, Rehovot; Israel.

¹⁷⁸Department of Physics, University of Wisconsin, Madison WI; United States of America.

¹⁷⁹Fakultät für Mathematik und Naturwissenschaften, Fachgruppe Physik, Bergische Universität Wuppertal, Wuppertal; Germany.

¹⁸⁰Department of Physics, Yale University, New Haven CT; United States of America.

¹⁸¹Yerevan Physics Institute, Yerevan; Armenia.

^a Also at Borough of Manhattan Community College, City University of New York, NY; United States of America.

^b Also at Centre for High Performance Computing, CSIR Campus, Rosebank, Cape Town; South Africa.

^c Also at CERN, Geneva; Switzerland.

^d Also at CPPM, Aix-Marseille Université, CNRS/IN2P3, Marseille; France.

^e Also at Département de Physique Nucléaire et Corpusculaire, Université de Genève, Genève; Switzerland.

^f Also at Departament de Fisica de la Universitat Autonoma de Barcelona, Barcelona; Spain.

^g Also at Departamento de Física Teorica y del Cosmos, Universidad de Granada, Granada (Spain); Spain.

^h Also at Department of Applied Physics and Astronomy, University of Sharjah, Sharjah; United Arab Emirates.

ⁱ Also at Department of Financial and Management Engineering, University of the Aegean, Chios; Greece.

^j Also at Department of Physics and Astronomy, University of Louisville, Louisville, KY; United States of America.

^k Also at Department of Physics and Astronomy, University of Sheffield, Sheffield; United Kingdom.

^l Also at Department of Physics, California State University, Fresno CA; United States of America.

^m Also at Department of Physics, California State University, Sacramento CA; United States of America.

ⁿ Also at Department of Physics, King's College London, London; United Kingdom.

^o Also at Department of Physics, St. Petersburg State Polytechnical University, St. Petersburg; Russia.

^p Also at Department of Physics, Stanford University; United States of America.

^q Also at Department of Physics, University of Fribourg, Fribourg; Switzerland.

^r Also at Department of Physics, University of Michigan, Ann Arbor MI; United States of America.

^s Also at Dipartimento di Fisica E. Fermi, Università di Pisa, Pisa; Italy.

^t Also at Giresun University, Faculty of Engineering, Giresun; Turkey.

^u Also at Graduate School of Science, Osaka University, Osaka; Japan.

^v Also at Hellenic Open University, Patras; Greece.

^w Also at Horia Hulubei National Institute of Physics and Nuclear Engineering, Bucharest; Romania.

^x Also at II. Physikalisches Institut, Georg-August-Universität Göttingen, Göttingen; Germany.

^y Also at Institutio Catalana de Recerca i Estudis Avancats, ICREA, Barcelona; Spain.

^z Also at Institut für Experimentalphysik, Universität Hamburg, Hamburg; Germany.

- ^{aa} Also at Institute for Mathematics, Astrophysics and Particle Physics, Radboud University Nijmegen/Nikhef, Nijmegen; Netherlands.
- ^{ab} Also at Institute for Particle and Nuclear Physics, Wigner Research Centre for Physics, Budapest; Hungary.
- ^{ac} Also at Institute of Particle Physics (IPP); Canada.
- ^{ad} Also at Institute of Physics, Academia Sinica, Taipei; Taiwan.
- ^{ae} Also at Institute of Physics, Azerbaijan Academy of Sciences, Baku; Azerbaijan.
- ^{af} Also at Institute of Theoretical Physics, Ilia State University, Tbilisi; Georgia.
- ^{ag} Also at Istanbul University, Dept. of Physics, Istanbul; Turkey.
- ^{ah} Also at LAL, Université Paris-Sud, CNRS/IN2P3, Université Paris-Saclay, Orsay; France.
- ^{ai} Also at Louisiana Tech University, Ruston LA; United States of America.
- ^{aj} Also at Manhattan College, New York NY; United States of America.
- ^{ak} Also at Moscow Institute of Physics and Technology State University, Dolgoprudny; Russia.
- ^{al} Also at National Research Nuclear University MEPhI, Moscow; Russia.
- ^{am} Also at Near East University, Nicosia, North Cyprus, Mersin; Turkey.
- ^{an} Also at Physikalisches Institut, Albert-Ludwigs-Universität Freiburg, Freiburg; Germany.
- ^{ao} Also at School of Physics, Sun Yat-sen University, Guangzhou; China.
- ^{ap} Also at The City College of New York, New York NY; United States of America.
- ^{aq} Also at The Collaborative Innovation Center of Quantum Matter (CICQM), Beijing; China.
- ^{ar} Also at Tomsk State University, Tomsk, and Moscow Institute of Physics and Technology State University, Dolgoprudny; Russia.
- ^{as} Also at TRIUMF, Vancouver BC; Canada.
- ^{at} Also at Universita di Napoli Parthenope, Napoli; Italy.

* Deceased

Auxiliary material

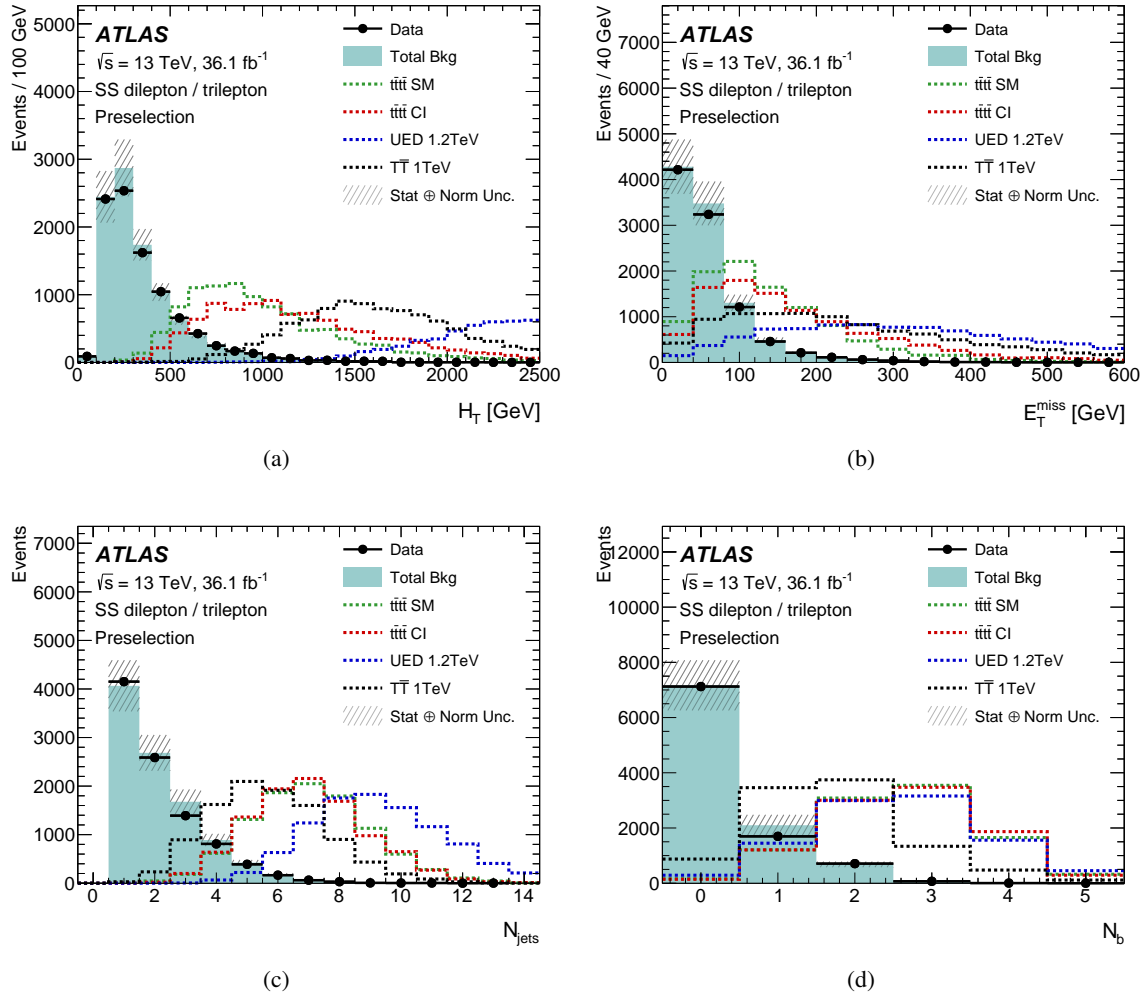


Figure 15: Signature of four typical BSM signals, compared with the expected total background distribution at the preselection level for H_T , E_T^{miss} , jet multiplicity and b -tagged jet multiplicity. The total uncertainty, shown as the hashed region, includes both statistical uncertainty and systematic uncertainty on the normalisation of each background source. Signal predictions are normalised to the total expected background.

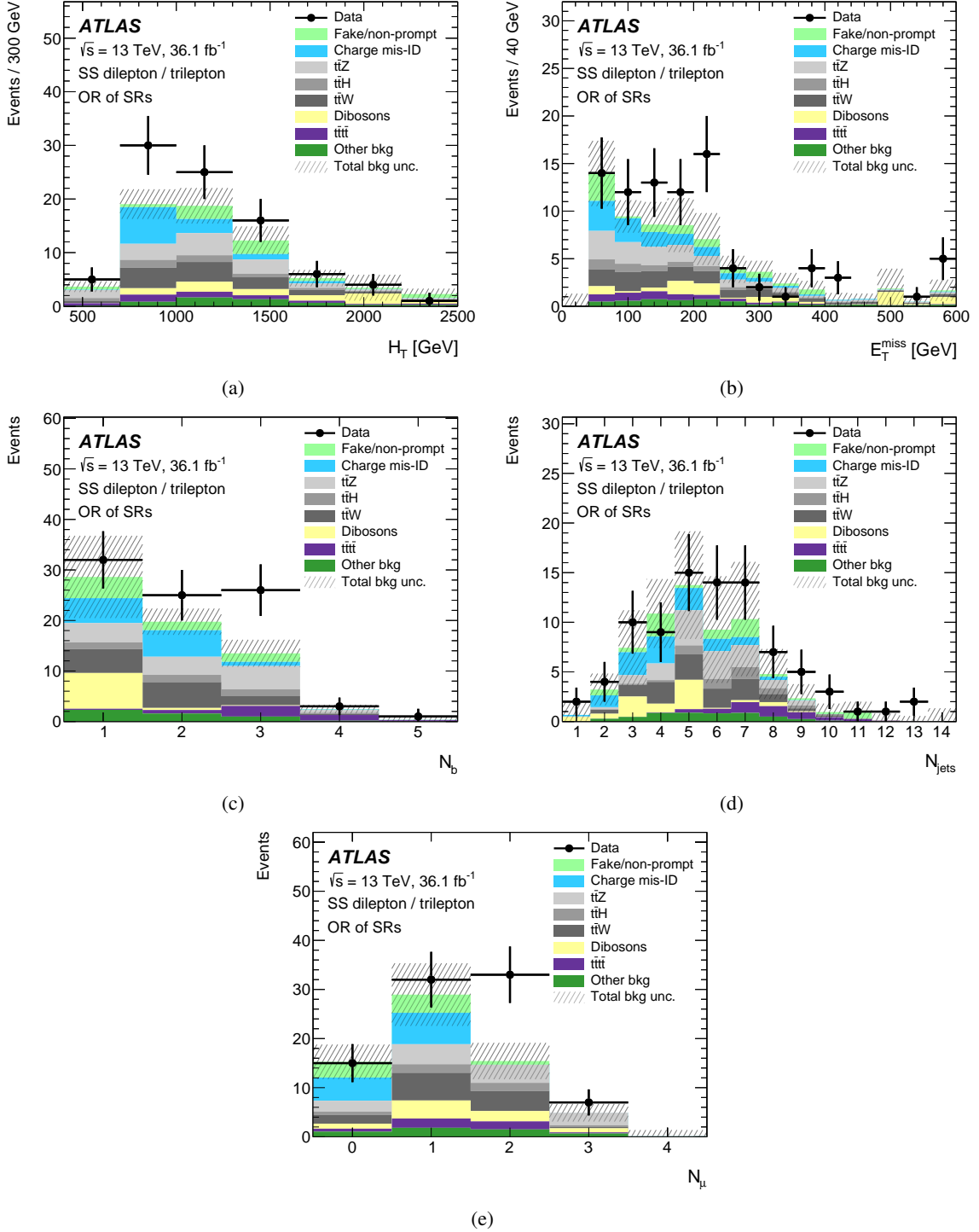


Figure 16: Distributions of (a) H_T , (b) E_T^{miss} , (c) b -tagged jet multiplicity, (d) jet multiplicity and (e) muon multiplicity in all the signal regions used in this analysis. The total uncertainty, shown as the hashed region, includes both statistical uncertainty and systematic uncertainty on the normalisation of each background source.

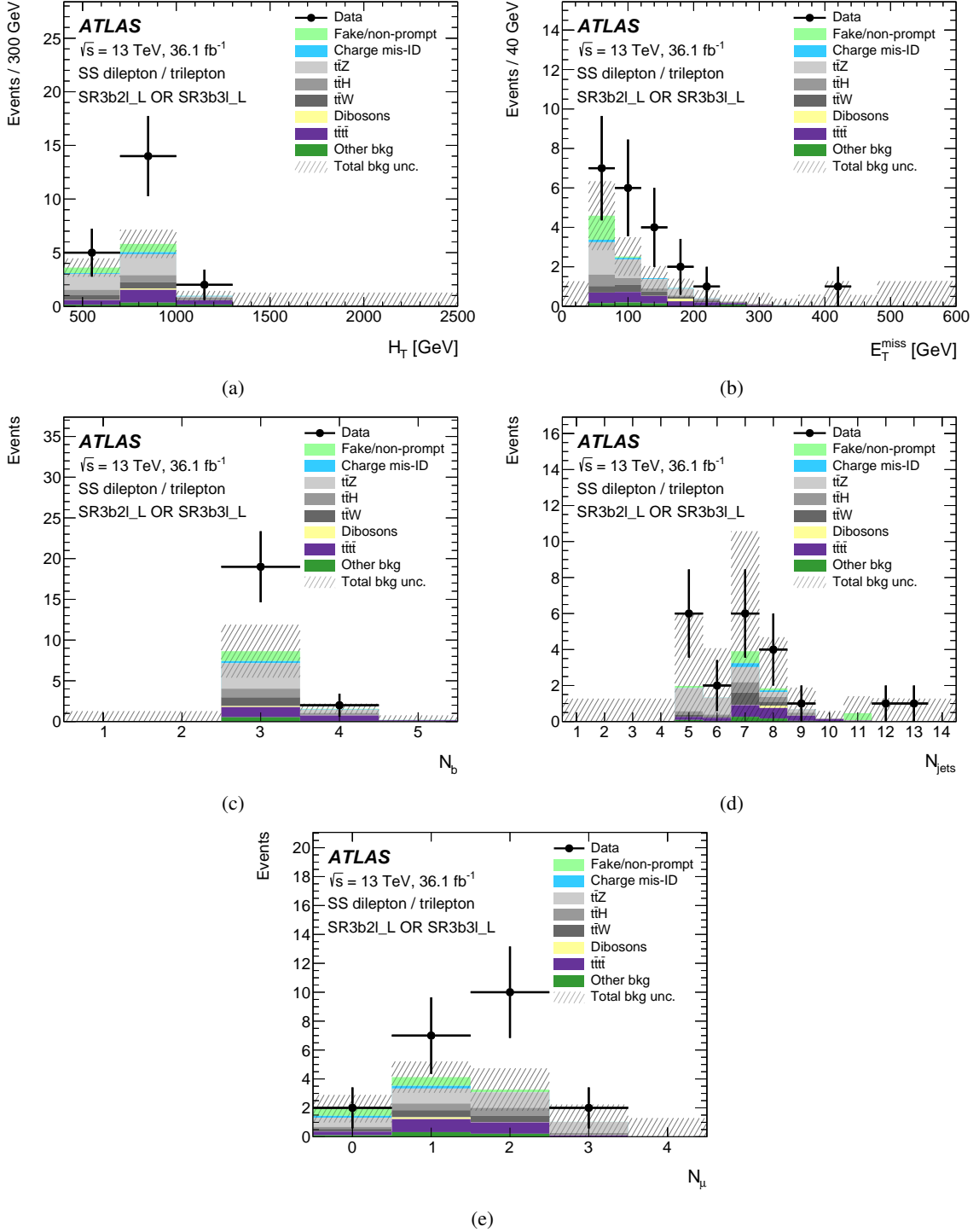


Figure 17: Distributions of (a) H_T , (b) E_T^{miss} , (c) b -tagged jet multiplicity, (d) jet multiplicity and (e) muon multiplicity for events with the SR3b2 ℓ _L or SR3b3 ℓ _L selections. The total uncertainty, shown as the hashed region, includes both statistical uncertainty and systematic uncertainty on the normalisation of each background source.